Università di Pisa

Dipartimento di Ingegneria dell'Informazione
Corso di Laurea Specialistica in Ingegneria Elettronica
Curriculum Microsistemi
Anno Accademico 2012/2013

Studies on discharges in Micro Pattern Gaseous Detectors

Towards a spark resistant THGEM detector

Candidato: **Cosimo Cantini**

Relatori:

Prof. Luca Fanucci

Ing. Rui De Oliveira

Questo elaborato è il risultato della mia attività come Technical Student al CERN fra Agosto 2011 e Settembre 2012.

MOTIVATIONS

This work has been developed during my stay at CERN, the European Organization for Nuclear Research, within the framework of the Technical Student Program, between August 2011 and September 2012. I worked in the fine pitch workshop, a fundamental facility at CERN which provides service to all the experiments and infrastructures, developing PCBs, flexible circuits and well established gaseous detectors (GEM, MICROMEGAS).

The MPE-EM fine pitch workshop, part of the Technology Department at CERN is even providing leading technology support for the development of various types of Micro Pattern Gas Detectors for the RD51 High Energy Physics community.

One of these devices is the Thick GEM, which offers the advantage of applying a more standard PCB technology for the assembly of particle gas multiplication chambers for physics research and also for industrial applications. Performance comparable to the more sophisticated GEM detectors can be obtained providing an intense qualification activity, aimed at fine adjusting the numerous fabrication parameters and adapting the process technology.

The problem afflicting any of MPGDs is the phenomenon of discharging which might be destructive in some highly energetic cases, at least being responsible of a slow ageing of the detector.

So far the solution to discharge has been cascading several gain elements reducing the gain of each one; this method, spreading the charges along their path, reduce effectively the likelihood of a discharge but introduce more material due to the multiple stages of amplification.

Our goal is developing a single stage THGEM detector which could withstand discharges, not reducing the gain, hence being still able to amplify low level ionizing particles while implementing some methodologies to reduce the damages due to discharge induced by high rate of particles' flux and/or highly ionizing particles.

This would pave the way to many applications in a wide range of rate of incoming particles; having THGEM detector high sensitivity to rare events, with low radioactive background, low energy threshold, and capable to cover large areas at low cost, make it the ideal detector for carrying out advanced research in the fields of neutrino, double-beta decay and dark-matter physics (1) (2).

On the other hand some groups have reported good behavior even in a high rate experimental environment, up to 1 MHz/mm^2 (3) making THGEM possibly suitable for a Digital Calorimeter (DHCAL).

There are several applications in various fields that employ for example GEM electrodes but do not require their very precise localization resolution and can tolerate the 0.4 mm thick insulator material of the THGEM (4). For these applications the THGEM may offer a very attractive alternative solution, at lower cost and better robustness (particle tracking at sub-mm resolutions, X-ray and neutron imaging, Ring Imaging Cherenkov detectors).

OUTLINE

This report follows the orderly temporal flow of what I had learnt at CERN since the beginning till the end. The first two chapters mainly concern theory of gas and gaseous detectors, while the last two chapters are about my activity within the workshop.

So the first chapter is intended to be a humble introduction to gases or at least to the main aspects of gas, related to discharge into gaseous detector: of course is not a complete view, but shows shortly the problem of interest and the minimum vocabulary to face it. Moreover the I-V characteristic of the gas is introduced; the load line method, which makes the most of said characteristic, seems to be not commonly taken in account while designing gaseous detector. This work shows the importance of such a chart and the need of deeper electrical studies on different gases, in order to extract their *I-V* behavior.

The second chapter is about detectors; here I wrote down the basics of gaseous detectors, the working principle, the main features, problems and some details on technology. Micro Pattern Gaseous Detectors are introduced and specifically GEM, MICROMEGAS and THGEM, currently among the most reliable gaseous detectors. However they suffer from the effects of electrical discharges and many efforts have been made over decades trying to find new structures, geometries and materials which possibly make the detectors more resistant once irradiated with high flux/highly ionizing particles.

The third one is a review of the first part of my lab activity: it describes the test bench set up to study discharges between simple structures, which are actually models of the bigger detector. The idea behind this approach is to reduce the complexity of the whole phenomenon, in order to focus directly on a single point to point discharge. Once understood that repetitive discharges modify the electrical behavior of the system, we tried implementing these findings on prototypes of THGEMs, made and then tested in the workshop. Results of these tests are reported and compared.

Eventually the last chapter reports the efforts made in defining technological process for 3 new standard dimensions ($10\ cm\ x\ 10\ cm$) THGEM elements; the experience made with the tests described in chapter 3 suggests that in order to increase the endurance of THGEM detectors against discharges new materials and even new structures have to be tested. Here is documented the attempt to build such structures: one obtained dividing into sector the electrodes of the gain element, the second suggested by the equivalent model of MICROMEGAS (a spark resistant detector), the last made using a different substrates (epoxy glue by Krempel group) instead of the common FR4 (glass fiber reinforced epoxy glue).

The results obtained were material for my presentation at the R&D51 Collaboration Meeting in June 2012 at CERN; the findings of this study have increased the knowledge of the mechanism of discharges damages in MPGDs and the solutions provided will be possibly implemented in large scale production in the next future.

ACKNOLEDGMENTS

My deepest gratitude goes to Rui De Oliveira and Fabio Formenti, my supervisors at CERN, for having introduced me from scratch, day after day with patient and willingness, into the complicated world of gaseous detectors. They offered me the priceless opportunity to gain technical skills in a unique environment, moreover I got introduced by them even to the scientific community where I learnt the importance of communication between groups working for a common and big goal.

I offer my heartfelt thanks to Prof. Luca Fanucci who has been supporting me in this experience since the beginning, giving me his precious tips and patiently helping me even during hard periods.

Then it is a pleasure name Prof. Rino Castaldi; without his inestimable lessons on HEP in September 2010 I would not even ever thought about CERN and now my life would be at least different, surely worse. Thank you for your help during this year and for your constant wise presence.

The building 102, where the TE-MPE-EM fine pitch workshop takes place, has to be mentioned as the physical place where I grow up; really magic people are working there and daily carrying forward all the stunning complex steps required to build detectors and to develop PCBs. Their determination and constancy have shown me how hard is technology and achieving big goal a fact of good collaboration among people. Any of them has helped me a lot, teaching different aspects of machineries and technological steps and warmly welcoming me as one of them, even though my French is not good (yet!). Without them this work would not have been possible.

I would thank here all of them: Jonathan Scalet, Julien Burnens, Katia Jauregui, Olivier Pizzirusso, Antonio Teixeira, Alexis Rodrigues, Xavier Thery, Serge Ferry, Matthieu Robin, Alexandra Gris, Julie Veron, Bertrand Mehl, Cedric Callau, Ercan Budun, Jean-Baptiste Neyret, Benilde Martins, Julien Lollierou. A great team!

Working at CERN especially over the last year, which saw the discovery of a new boson, likely the long sought Higgs boson, has been an utterly fascinating experience and I shared time with many outstanding people which gave me new perspectives; if I had to mention them one by one this work would not be never long enough, but I would thank expressly Eraldo Oliveri, Yorito Yamaguchi, Elena Rocco for their availability, Michael Jonker and Rob Veenhof for interest shown and helpful tips, Luciano Periale for believing in me.

Special mention to the “magic lunch group”, a group of international smart colleagues firstly, which became soon close friends and to all the people I shared time, thoughts and experiences with: good luck!

I have to thank even Maurizio D’Angelo which provided an outstanding remote-control facility from Pisa, making possible what at first seemed not.

CHAPTER 1

CHAPTER 2

CHAPTER 3

CHAPTER 4

Chapter 1

1.1 Electrical Discharges

An *electrical discharge* results from the creation of a conducting path between two points of different electrical potential in the medium in which the points are immersed. If the supply of electrical charge is continuous, the discharge is permanent, otherwise it is temporary, and serves to equalize the potentials.

Usually, the medium is a gas, often the atmosphere, and the potential difference is a large one, from a few hundred volts to millions of volts. If the two points are separated by a vacuum, there can be no discharge. The transfer of matter between the two points is necessary, since only matter can carry electric charge. This matter is usually electrons.

However, ions can also carry charge, although they are more than 1000 times heavier, and sometimes are important carriers[(5), (6)].Where both electrons and ions are available, however, the electrons carry the majority of the current. Ions can be positively or negatively charged, usually positively, and carry small multiples of the electronic charge.

Electrical discharges have been studied since the middle of the 19th century, when vacuum pumps and sources of current electricity became available. After the fundamental studies of Ludwig Boltzmann and the invention of the Geiger-Muller counter in 1908, studies concerning motion of charges inside gases rose, preparing the field for new applications. Townsend, Loeb, Thomson are only some that contributed during the `30s in the development and arrangement of the complex study of gases, thanks even to the improvement of the available instrumentation, e.g. the possibility of generate and control electrical discharge through gases.

These laboratory discharges in partially-evacuated tubes are very familiar today, but there are also electrical discharges in nature, lightning being the primary example. All of them result from the high potentials of static charges.

Technology offers a wealth of examples, such as arc welding, the corona discharge on high-tension lines, fluorescent lamps, including their automatic starters, neon advertising signs, neon and argon glow lamps, mercury and sodium lamps, mercury-arc lamps for illumination and UV, carbon arc lights, vacuum tubes, including gas-filled rectifiers, Nixie numerical indicators and similar devices.

The two termini of a discharge are at different potentials. The higher, or positive, potential is at the *anode*, while the lower, or negative, potential is at the *cathode*. These *electrodes* are often conductors, but need not be. In a thunderstorm, a cloud electrode may simply be a region of excess charge distributed over a volume.

1.2 Gas: basic concepts

THE IDEAL GAS LAW

The medium is a gas predominantly composed of neutral molecules, which we usually treat as ideal. Then, the pressure *p* of the gas is simply related to its number density *n* by the ideal gas law:

$$p = nkT$$

where *T* is the absolute temperature, and *k* is Boltzmann's Constant, 1.38 x 10^{-16} erg/K.

If *T* is in K, and *n* is in cm^{-3}, then *p* is in $dyne/cm^2$. In technical work, gas pressure is measured in mmHg, and 760 mmHg is atmospheric pressure, 1.0123 x 10^6 $dyne/cm^3$, from which the conversion can be derived.

At one atmosphere and 273K, the number density in a gas is 3.22 x 10^{18} cm^{-3}, which is the same for all gases (Avogadro's Law). The gas is normally electrically neutral and contains neither ions nor electrons, so is a non-conductor.

The electrons, ions and neutral molecules are in incessant thermal motion, because their collisions are perfectly elastic. In equilibrium, the velocities are distributed according to the Maxwell distribution:

$$f(v) = \left(\frac{m}{2\pi kT}\right)^{3/2} e^{\left(-mv^2/2kT\right)} 4\pi v^2$$

which integrates to unity with respect to *dv*.

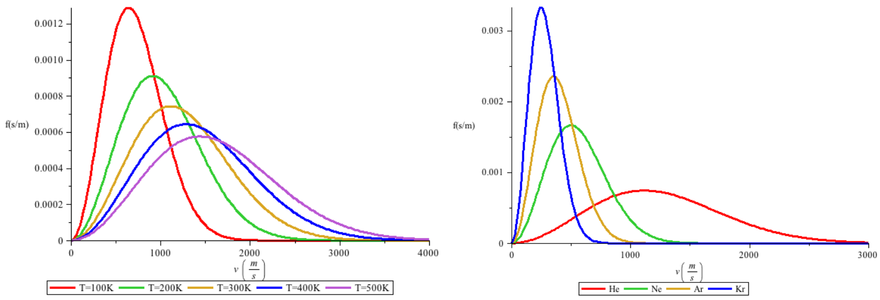

Pic. 1.1:distributions of speed for He atoms at various temperatures on the left and for the first 4 noble gases at room temperature on the right.

The electron temperature T_e is usually very different from the ion and neutral temperature T_n at low pressures, because the electrons receive more energy from the electric fields in a discharge and can exchange kinetic energy with the neutrals only with great difficulty, so they represent a reservoir of kinetic energy that is in very weak contact with the neutrals.

The much greater mass of the ions and neutrals also means that they move at much lower velocities. Speeds given to the electrons by electric fields are often very much greater than thermal speeds, especially near the cathode, where the electric field is very high. These electrons, naturally, do not have a Maxwellian distribution until they have lost most of their energy in inelastic collisions and ionization.

The average kinetic energy of a particle at temperature T is $\frac{3}{2}kT$. The *rms* velocity $\sqrt{3kT/m}$ is the velocity of a particle with the average energy. Approximately 60% of the particles have less energy, 40% more.

MOBILITY

Mobility is defined as the proportionality coefficient between the drift velocity of a charged particle and the field.

$$v_d = \mu E$$

The mobility of electrons is:

$$\mu_e = \frac{e}{m}\bar{\tau}[m^2/(V \cdot s)]$$

where e is the elementary charge, m is the electron mass and $\bar{\tau}$the average scattering time.

The mean energy of electrons is field-dependent; hence, $v_d$is not a strictly linear function of E and the mobility depends on the field strength.

However, the convenient linear relation with μ_e =const is used for theoretical analysis of various discharge processes. A reasonable effective value of $\mu_e$is chosen from numerical estimates (Gas Discharge Physics, Yuri P. Raizer). In some cases the nonlinearity of the function $v_d\ (E)$ causes well pronounced effects.

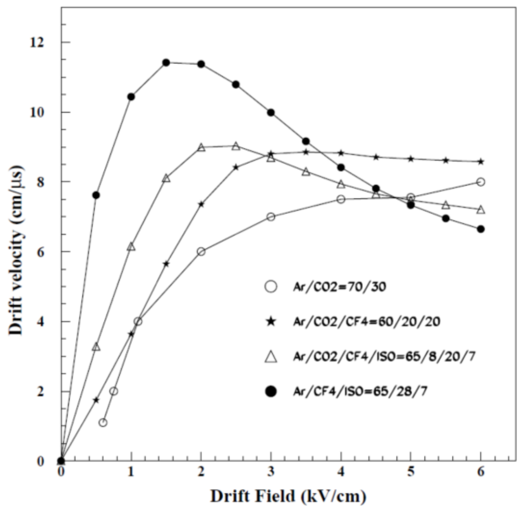

Pic. 1.2 electron drift velocity for different gas mixtures (7)

Normally, more than one source of scattering is present, for example both impurities and lattice phonons. It is normally a very good approximation to combine their influences using "Matthiessen's Rule" that is:

$$\mu^{-1} = \sum_i \mu_i^{-1}$$

CONDUCTIVITY IN WEAKLY AND STRONGLY IONIZED PLASMA

The mobility of massive ions are hundreds of times less than for light electrons. The contribution of ions to electric current is thus small, except in those rare cases when the ion densities n_+, n_- exceed by an appropriate number of times the electron densities n_e. The current density j and the conductivity σ in a plasma with $n_e \approx n_+$are:

$$j = -en_e v_d = en_e \mu_e E = \sigma E$$

$$\sigma = en_e \mu_e = \frac{e^2 n_e}{m} \bar{\tau}$$

The conductivity of a weakly ionized gas is mostly determined by the degree of ionization n_e/N.

The scattering of electrons by ions impedes their drift along the field as much as that by molecules. If ionization is not too weak, then electron-ion collisions become to be appreciable at ionizations greater than 10^{-3} and dominant at still higher degrees of ionization. In this case:

$$\bar{\tau}^{-1} \propto n_e$$

And the conductivity assumes the form:

$$\sigma = en_e \mu_e = \frac{e^2 n_e}{m} \bar{\tau} = \frac{e^2}{mv\sigma_{Coul}}$$

Where v is the velocity of random motion and $\sigma_{Coul}$is the cross section of electron-ion collisions dominated by Coulomb forces.

A BIT MORE ON THE MEAN FREE PATH

The mean free path *l* is determined by collisions hence it depends on the energy of the electrons or in general of the particle passing through matter. A simple expression of it is deduced by the Drude model, in which the microscopic behaviour of electrons in a solid may be treated classically and looks much like a pinball machine, with a sea of constantly jittering electrons bouncing and re-bouncing off heavier, relatively immobile positive ions:

$$l(E_{kin}) = v(E_{kin})\tau = \frac{hk}{2\pi m}\tau$$

Where $v$is the velocity and $\tau$is the mean time between two scattering events. The mean free part of the electrons in several elements is plotted in Pic. 1.3 as a function of energy.

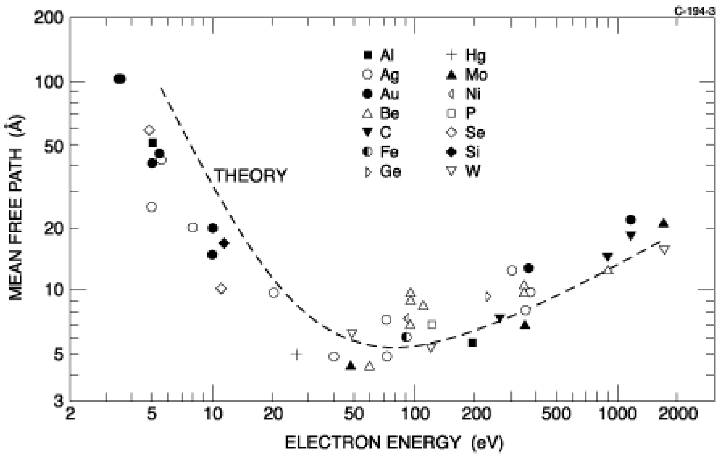

Pic. 1.3: The dashed curve shows a calculation of the mean free path independent of the material and the points are measured data from many elemental solids.

In kinetic theory, if the velocities of the particles have a Maxwell distribution, the following relationship applies:

$$l = \frac{kT}{\sqrt{2}\pi d^2 p}$$

where k is the Boltzmann constant in J/K, T is the temperature in K, p is pressure in Pascals, and d is the diameter of the gas particles in meters. So the mean free path l is inversely proportional to the pressure, (8) so pressure has a great effect on how an electron gains energy.

The molecules of the gas also have a mean free path, but since molecules are larger, their mean free path *l* is shorter than l_e. As an estimate, we can take l_e= 5.64*l*.

In Ne, the mean free path at 760 mmHg and 273K is 1.93 x 10^{-5} cm, while in air it is 9.6 x 10^{-6} cm. By "air" we mean the usual mixture of nitrogen and oxygen, and the values are an average.

Intense studies have been carried on over decades about drift and diffusion speed of electrons (9)into different media (gasses); usually in particle gaseous detectors a mixture of Ar and CO2 is used in different proportion, due to its feature of being inert with materials. Moreover CO2 is used as a quencher thanks to its fundamental property of adsorbing luminous radiation that might happen during a discharge, avoiding any other avalanche triggered by light.

1.3 Ionization Mechanisms

The energy loss of a charged particle in matter is essentially divided between two types of reaction: *excitation* and *ionization* in which a free electron and ion are created.

The *excitation* of an atom, *X*,

$$X + p \rightarrow X^* + p$$

where *p* is a charged particle, is a resonant reaction which requires the correct amount of energy to be transferred. While no free electrons or ions are created, the excited molecule or atom may participate in further reactions which do result in ionization.

For an ionization,

$$X + p \rightarrow X^+ + p + e^-$$

The ionization process has an energy threshold relatively high and since low energy transfers are more probable, the excitation reactions generally dominate.

The electrons and ions created by the incident radiation itself are known as primary ionization. In a number of these ionizations however a sufficiently large amount of energy is transferred to the electron such that this electron also creates ion-electron pairs; this latter ionization is known as secondary ionization. If their energy is high enough, the secondary ionization electrons may also ionize and so on, until the threshold for ionizing reactions is reached.

A second mechanism of ionization in gases is the Penning Effect. In certain atoms, metastable states are excited which, because of a large spin-parity difference, are unable to de-excite immediately to the ground state by the emission of a photon. In such atoms, a de-excitation may occur through a collision with a second atom resulting in the ionization of the latter. Common examples are molecular gases on noble gases and noble gases on noble gases, e.g.

$$Ne^* + Ar \rightarrow Ne + Ar^+ + e^-$$

A third important mechanism which occurs in noble gases is the formation of molecular ions. In this process, a positive gas ion interacts with a neutral atom of the same type to form a molecular atom, i.e.

$$He^+ + He \rightarrow He_2^+$$

RECOMBINATION AND ELECTRON ATTACHMENT

While the number of electron-ion pairs created is important for the efficiency and energy resolution of the detector, it is equally important that these pairs remain in a free state long enough to be collected. Two processes hinder this operation: recombination and electron attachment.

Where there is no electric field, ion-electron pairs will generally recombine under the force of their electric attraction, emitting a photon in the process:

$$X^+ + e^- \rightarrow X + hv$$

In general the rate of recombination will depend on the concentrations of the positive and negative ions so that,

$$dn = bn^+n^-dt$$

Where b is a constant dependent on the type of gas and $n^+$and $n^-$are the positive and negative ion concentration respectively.

Electrons attachment involves the capture of free electrons by electronegative atoms to form negative ions,

$$X + e^- \rightarrow X^- + hv$$

These are atoms which have an almost full outer electron shell so that the addition of an extra electron actually results in the release of energy. The negative ion formed is consequently stable. The energy released in this capture is known as the electron affinity. Clearly therefore the presence of any electronegative gases in the detector will severely diminish the efficiency of electron-ion collection by trapping the electrons before they can reach the electrodes.

1.4 The gas system

The term *gas discharge* originates (10)with the process of discharge of a capacitor into a circuit incorporating a gap between electrodes. If the voltage is sufficiently high, electric breakdown occurs in the gas and an ionized state is formed. The circuit is closed and the capacitor discharges.

Later the term discharge was applied to any flow of electric current through ionized gas and to any process of ionization of the gas by the applied electric field. As gases ionized to a sufficient degree emit light, it has become customary to say that a discharge *light up* or is *burning*.

A relatively simple experiment introduces us to several fundamental types of discharge. Two metal electrodes connected to a DC power supply are inserted into a glass tube; the tube can be evacuated and filled with various gases at different pressures. The quantities measured in the experiment are the voltage between the electrodes and the current in the circuit. This classical device served the study of discharge processes for 150 years and still remains useful.

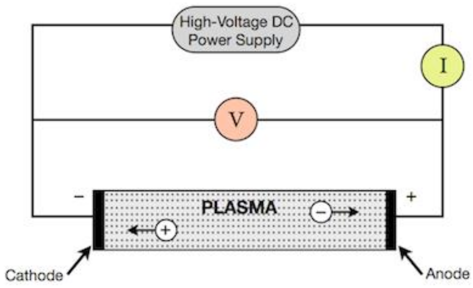

Pic. 1.4: typical gas discharge tube

If V is the difference in potential between the anode and cathode, and d is the distance between them, then the average potential gradient, or electric field, is V/d. The field E will be in V/cm. This average field will drive a positive ion in its direction, an electron in the opposite direction.

For a discharge to occur, there must usually be a source of electrons at the cathode, and the nature of this source controls the form of the discharge. Cosmic rays and natural radioactivity continually produce a small number of electrons and ions in all gases at the surface of the earth and this gives air a small conductivity.

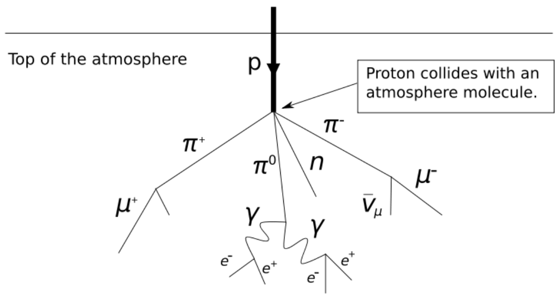

Pic. 1.5: cosmic rays produce continuously shower of particles

The electrons will migrate to the anode, the ions to the cathode and a small current will flow, on the order of $10^{-15}\ A$; this current has no visible effects and can be detected and measured only with difficulty, but is always present. Any charged body attracts charges of the opposite sign that sooner or later will neutralize its charge, though the usual reason for the loss of charge is conduction over the surface of the supports of the body, which is normally far greater than the small space current from the ions and electrons normally present in the air.

1.5 Main phenomena providing charges during a discharge

THE PHOTOELECTRIC EFFECT

More copious sources of electrons are necessary for a good discharge. One source is the photoelectric effect, when light of sufficiently short wavelength falls on a metal or semiconductor and liberates a *photoelectron*. Photons can also be absorbed by a molecule, which gives up an electron and becomes a positive ion.

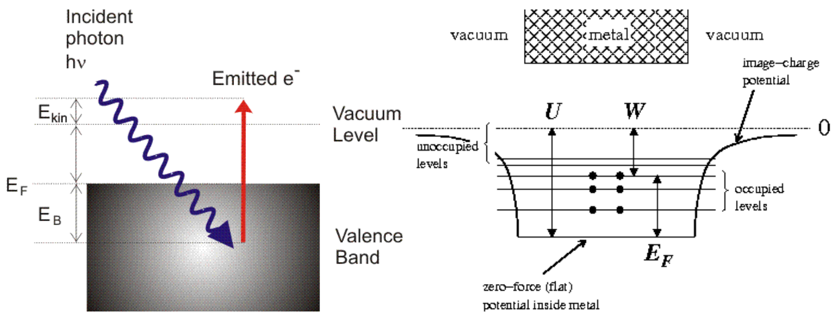

Pic. 1.6: emission of an electron from a metal by photon stimulation and energy bands.

The photon energy hν must be greater than the energy required to free the electron, the work function W.

The photo effect from the surface at $h\nu > eW$ is characterized by its quantum yield, that is the number of electrons per photon γ_{ν}.

THERMIONIC EMISSION

Thermionic emission, the emission of electrons by a heated body, can supply heavy currents. The body must be heated to incandescence and for efficient emission its work function must be low.

The current density J of a heated wire follows the Richardson's law:

$$J = A_G T^2 e^{-W/kT}$$

where A_G is a typical parameter for each material.

Tungsten has a work function of 4 eV and has long been used as an electron emitter, since it also has a high melting point. Alkali metals have a small work function, but cannot be used by themselves because of their low melting points.

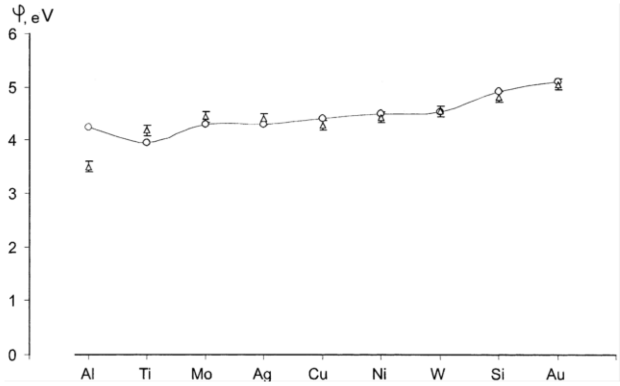

Pic. 1.7 : Work function for several elements (11).

FIELD ELECTRON EMISSION

The field that pulls the electrons away transforms the potential wall into a potential barrier of finite width; as a result, electrons can escape from the metal by tunneling.

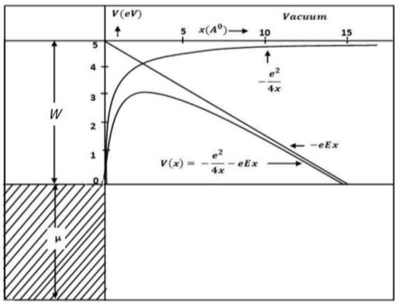

Pic. 1.8: lowering of the potential barrier induced by the applied field.

The result is a field electron emission and the emission current is given by the Fowler-Nordheim formula:

$$j_F = A(y) \frac{E}{W} e^{-B\frac{W^{3/2}}{E}\theta(y)}$$

Where E is the applied field, while A and θ are function of $y = e\sqrt{eE}/W$.

EMISSION OF SECONDARY ELECTRONS

Electrons striking a metal surface can knock loose *secondary electrons* readily, but this is of little use for discharges, since the electrons impact the anode, and secondary electrons would simply fall back into the anode, not contributing to the discharge current.

However, positive ions impinging the cathode can also create secondary electrons; although this is not an efficient process, it produces electrons at the right place and can support a discharge. It is characterized by a coefficient:

$$\gamma_i = \frac{electrons\ emitted\ at\ the\ cathode}{incident\ positive\ ions}$$

And we will analyze later its contribution in determining the current; though is extremely difficult to define a precise value for γ_i, since it depends strongly on the clearness and roughness of the surfaces, in addition to the material itself (12)**.**

In this work the capital relevance of the quality of the electrodes in defining the electrical behaviour of the system has been proven, so we think that the aging of a gaseous detector is related to the changings of this coefficient $\gamma_i$due to energetic and locally release of energy during discharges.

1.6 Electron-ion pair

Electrons already in the discharge, such as the random electrons produced by cosmic rays and radioactivity, can add to their number by ionizing gas molecules by collision. Each ionizing collision produces a new electron, and a positive ion that moves the other way, an *electron-ion pair*.

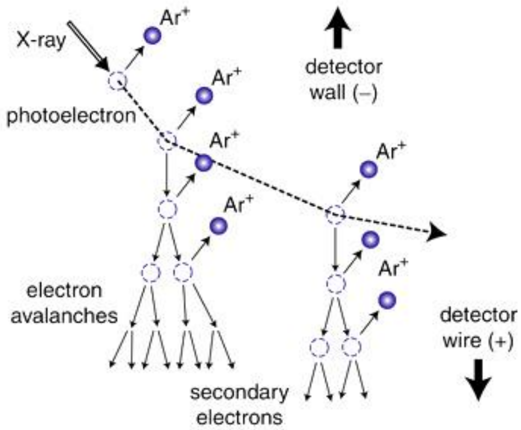

Pic. 1.9: Electron avalanche. Principle of detection of an X-ray photon. Incident X-rays ionize the Ar detector gas losing energy, then continue to ionize other Ar atoms. The resulting secondary electrons are accelerated toward the detector wire, gaining sufficient energy to ionize other Ar atoms, producing an electron avalanche.

An electron cannot ionize a neutral atom until he has acquired sufficient kinetic energy by being accelerated in an electric field; there are two ways this can be done. If the electron makes no collisions, even a small electric field will allow it to accumulate energy in a long-enough run. In this case, $E_{kin} = mv^2/2 = eEx$ where x is the distance travelled. Electron energies are often quoted in *electron-volts*, abbreviated eV, and such that the energy *U* in eV is given by $eU = eEx$, so that *U* is just the potential drop in the distance x.

On the other hand, if the probability of collision of the electron in a distance *dx* is dx/l_e, where l_e is called the electron *mean free path*, that is the average distance the electron travels between collisions, and l_e is much smaller than the distance *x*, then the speed of the electron is given by $v_d = \mu E$, where μ is the electron *mobility* in the gas. Then, the only way for the electron to accelerate is to find a larger field *E*.

The energy required to ionize neon, called the *ionization energy*, in the reaction Ne → $Ne^+ + e^-$, is 21.559 eV, and to knock two electrons off requires 41.07 eV. To raise a Ne atom to its first excited state requires 16.58 eV, which is called the *resonance energy*, of course, less than the ionization energy.

This gives an idea of the energy required to produce an ion pair. Since most collisions do not result in ionization, and there are many ways to fritter energy away uselessly, the average energy per ion pair produced is greater than the ionization potential.

	1st Ionization Potential (eV)	Effective Ionization Potential (eV)
He	24.5	27.8
Ar	15.7	26.4
Xe	12.1	20.8

To give an electron, between a collision and another (mean free path) sufficient energy to ionize Ne at one atmosphere, the field strength would have to be:

$$E = \frac{21.599}{5.64 \cdot (1.93 \times 10^{-5})} V/cm \cong 200.000\ V/cm$$

an extremely high field that would have some untoward effects. At 1 mmHg, the field would have to be 260 V/cm, a more tractable value.

The inert gases, which have a closed shell of electrons in the ground state, have very large resonance energies. For He, it is 19.81V, and for Ne, 16.62 eV. These levels are also *metastable*, which means that a transition to the ground state by radiation is difficult, and they may retain their excitation energy for an extended period, perhaps until they collide with a wall, or experience another collision with an electron or atom.

This makes *cumulative ionization* possible, where an atom can be ionized by multiple collisions in which the electrons have insufficient energy to ionize in a single collision. The energy of a metastable can be transferred to a different atom or molecule by a *collision of the second kind*.

1.7 Detection process – the case of an X-ray detector

The average number of electron-ion pairs, $\boldsymbol{n}$, produced by an X-ray is:

$$n = \frac{E}{e_i}$$

where $\boldsymbol{E}$ = incident X-ray energy (eV) and $\boldsymbol{e_i}$ = effective ionization potential of the detector gas (eV).

Consider a Cu-Kα X-ray, which has an energy of 8.04 keV. With Ar detector gas, $\boldsymbol{n}$ = 8040/26.4 = 304 primary electron-ion pairs.

This number is too small to detect by itself, but placing a potential across the gas from wire to tube wall will produce amplification. The electrons produced by the incoming X-ray are accelerated towards the anode wire by the detector voltage and can in turn ionize other Ar atoms producing another electron-ion pair and so on. The resulting *electron avalanche* is still proportional to the initial signal.

The chain of ionizations causes a momentary voltage across the detector producing a pulse. The amount of amplification produced by the gas depends on the amount of voltage applied to the detector. At very low voltages in the region of "under-saturation", the detector potential difference is too small to prevent recombination of electron-ion pairs formed by incident X-rays before they reach the collecting wire. At slightly higher voltages in the ionization chamber region, the potential is just sufficient to counter recombination so that the number of electron-ion pairs produced by X-rays equals the number reaching the anode wire; the resulting amplification (gain) is 1.

Further increases in the detector voltage produce the avalanche effect and significant amplifications. At voltages in the proportional counter region, the pulse height is proportional to the energy of the incident X-ray. Too high a voltage drives the detector out of the proportional region and into the Geiger region.

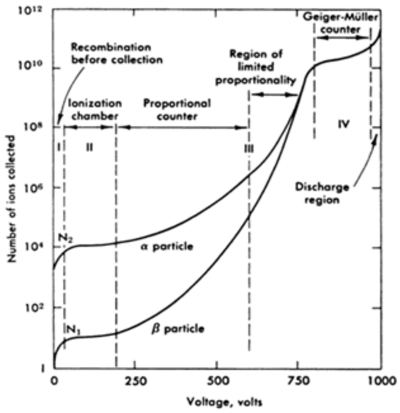

Pic. 1.10 Numbers of ions collected versus applied voltage in a single wire gas chamber

1.8 Townshend theory for the development of the avalanche

If an electron frees another by an ionizing collision, then these two can both free additional electrons, and so on. This creates an electron *avalanche*, which may send a burst of electrons toward the anode, leaving in their wake a cloud of slow positive ions that will make their way to the cathode. The result is a multiplication of the primary electrons.

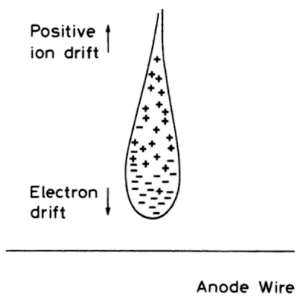

Pic. 1.11 Shape of an avalanche

Because of the greater mobility of the electrons, the avalanche has the form of a liquid drop with the electrons grouped near the head and the slower ions trailing behind, like shown in Pic. 1.11.

This does not start a sustained discharge, but merely increases the current that otherwise would be available. This type of discharge produces little light, so it is called a *dark* or *Townsend* discharge, after the man who studied them in detail first.

If l is the mean free path of the electron for a secondary ionizing collision, then $\alpha = 1/l$ is the probability of ionization per unit path length. This is better known as the *first Townsend coefficient* from the name of the first physicist who studied extensively discharges (13). The electrons added to the avalanche in a distance dx will be:

$$dn = \alpha n dx$$

proportional both to the number of electrons, and to the distance dx. Integrating, this yields the total number of electrons created in a path x

$$n = n_0 \exp(\alpha x)$$

Where n_0 is the number of primary electrons coming from the ionization process or due to background radioactivity and cosmic rays. The multiplication factor is then

$$M = n/n_0 = exp(\alpha x)$$

Physically the multiplication factor M is limited to about 10^8 after which breakdown occurs; this is known as the *Raether's limit*.

The number of electrons that arrive at the anode will be

$$n = n_0 exp(\alpha d)$$

where *d* is the distance from the cathode to the anode.

In general, α will be a function of the electric field E, but here we assume E is constant, so our equation holds exactly only for plane-parallel electrodes and in the absence of space-charge effects. The number of positive ions produced in the avalanche will be:

$$n - n_0$$

We assume that all return to the cathode, where they release:

$$\gamma_i (n - n_0)$$

new electrons, where γ_i is the factor which expresses the efficiency of the ions impinging the cathode in liberating electrons. This means that the net number of electrons leaving the cathode will be:

$$n_0 + \gamma_i (n - n_0)$$

and the number eventually reaching the anode will be:

$$n = (n_0 + \gamma_i (n - n_0)) \exp(\alpha d)$$

If we solve for n, we find that:

$$n = \frac{n_0 exp(\alpha d)}{1 - \gamma_i(\exp(\alpha d) - 1)}$$

If $\exp(\alpha d)$is much greater than 1, we have simply:

$$n = \frac{n_0 exp(\alpha d)}{1 - \gamma_i\big(\exp(\alpha d)\big)}$$

1.9 Transition to spark discharge

Having a look to the denominator, it vanishes for a precise condition:

$$\gamma_i\big(\exp(\alpha d)\big) = 1$$

That is the condition for the spark. Now the discharge produces its own electrons, without relying on cosmic rays or natural radioactivity, and becomes *self-maintained*. This is a significant event in the life of a discharge, and usually means that the discharge becomes evident through light or noise. The potential between anode and cathode at which this occurs is called the *sparking voltage* V_b, or *breakdown voltage*. Now the whole path between anode and cathode becomes conducting because of the electrons and ions distributed along it.

Unless something limits the current, such as the disappearance of the potential difference or the lack of current from the power supply, it increases rapidly and without bounds.

1.10 Paschen’s curves

These curves express the breakdown voltage of a gas as a function of *pd*, the product of the gas' pressure in the bulb by the distance between the electrodes.

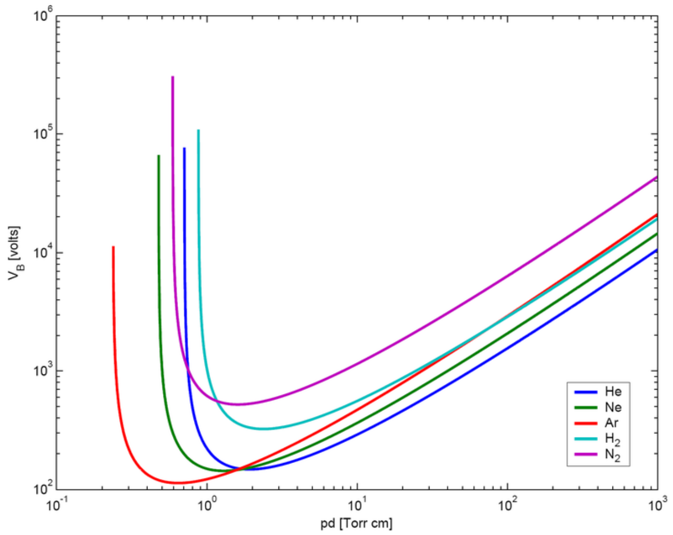

Pic. 1.12 Paschen's curve for several gasses(17)

The analytical expression of these curves is a consequence of the Townsend theory exposed in paragraph(1.8):

$$V_b = \frac{Bpd}{\log Apd - \log\left[\log\left(1 + {}^{1}/_{\gamma}\right)\right]}$$

Where $V_b$is the breakdown voltage in Volts, p is the pressure in Atmospheres or Bar, and d is the gap distance in meters. The constants A and B depend upon the composition of the gas while γ is a weak fuction of the electrodes' material (14).

gas	A $[Pa^{-1}m^{-1}]$	calculated A $[Pa^{-1}m^{-1}]$	B $[V Pa^{-1}m^{-1}]$	calculated B $[V Pa^{-1}m^{-1}]$
He	2.10	2.69	25.50	45.12
N_2 (air)	10.95	9.91	273.78	220.27
Ar	10.20	7.93	176.27	84.78

gas	electrode	γ	calculated γ
He	sodium - glass	0.263	0.236
N_2 (air)	platinum	0.025	0.035
Ar	tungsten	0.095	0.068

Pic. 1.13 Measured Vs calculated Townsend coefficients for several commonly used gas

For air at standard atmospheric pressure of 101*kPa*, A = 4.36×10^7 *V/(atm·m)* and B= 12.8 *V/(atm·m)* (15).

The typical shape of the curve shows a minimum value $V_{b,min}$, while the voltage tends to increase for high and low pressure either. Consistent drift from this behaviour has been observed for low pressure in small gap (<5 um) devices [(16), (17)]

By differentiating V_b with respect to pd and setting the derivative to zero, the minimum voltage can be found. This yields to:

$$V_{b,min} = B(pd)_{min}$$

Where:

$$(pd)_{min} = \frac{1}{A}e^{1+C}$$

And C is defined as:

$$C \triangleq \log\left[\log\left(1 + {}^{1}/_{\gamma}\right)\right]$$

and predicts the occurrence of a minimum breakdown voltage for pd = 7.5×10^{-6} m·atm. This is 327V in air at standard atmospheric pressure at a distance of 7.5 µm.

The analytical expression has been found in the case of a parallel plate electrodes configuration with theoretical considerations but it shows to be valid even in other configurations; the high voltage test performed on any Micro Pattern Gaseous Device to validate its quality just after production shows a good consistency between the values of voltage effectively observed at the onset of a discharge in air and the one predicted by the Paschen’s curve.

1.11 V-I characteristic of DC discharge

This work has introduced and demonstrated the importance of the voltage-current characteristic of the gas to explain the behaviour of a gaseous detector over its lifetime and the reasons of possible degradation due to defects induced by discharges and/or bad quality of the electrodes.

So far in literature, only the plot number of charges collected by the electrodes over applied voltage is referred when studies on gaseous detectors are approached but we believe that a new perspective on the gas, as we will have room to explain in the next chapters, might be useful in linking the gas system with the “external world”, that is the electronic front-end elected to pick up and elaborate the signal.

Since any electronic component is defined in terms of its V-I characteristic, maybe a comprehensive description of the system "gas + electronics" is possible if we stare at the gas under a different light or we bring it at the same level of an electronic component.

Then a V-I characteristic of the gas is required.

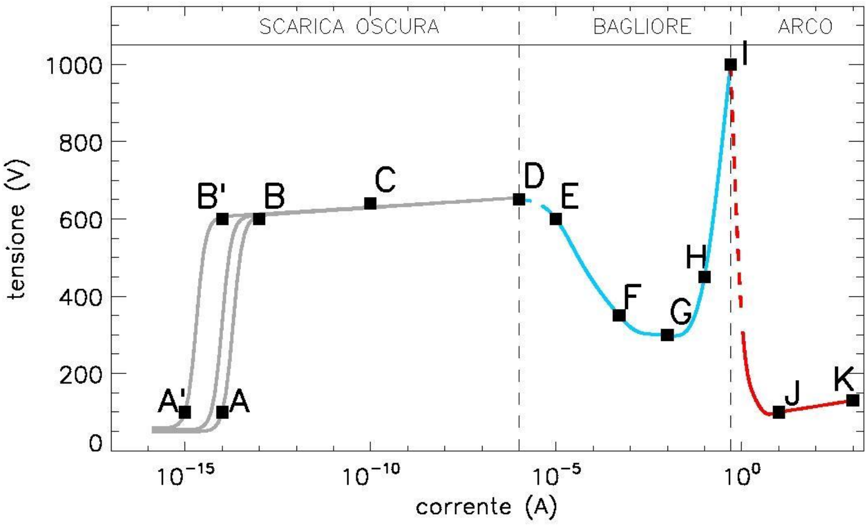

Pic. 1.14: Voltage-Current characteristic of Ne

The one shown here is related to a bulb 50 cm long, filled with Neon at 1 torr; actually is the only one available (18) showing some precise values, most of the characteristic being qualitative (19). We think that this lack of information is due to the extreme difficulty in experimentally extrapolating this characteristic over such a large range of current (note that the current is ranging from fA to kA).

The values of current and voltage depend on the gas, the gap between the electrodes, the pressure of the gas; then we will make some qualitative considerations, which might be not applicable to the systems we were working with in terms of exact values of current and voltage, but were definitely helpful in interpreting some effects observed in gaseous detectors.

A brief description of the different regions in the I-V characteristic is mandatory.

The first one up to point D, is called dark discharge zone ("scarica oscura") and is where the charges induced by cosmic rays are collected (A to B line) and detected as small pulses of current. From B to D is where Townsend avalanche takes place: charges generated by any ionizing phenomenon are "amplified".

From D the condition for a self-maintained discharge is established, as already explained quantitatively in paragraph (1.9). The discharge starts to be visible. As a reminder, this transition is highly influenced by the secondary emission coefficient of the cathode γ_i, hence secondary emission is a dominating phenomenon in the glow discharge region ("bagliore").

In the normal glow region (G) any increase of the current lead to an increase of the spot on the electrodes where the discharge impinges, so the voltage is almost independent from current.

But when the secondary emission involves up all the area of the cathode, then the voltage increases roughly linearly with the current.

The ion bombardment heats up the cathode surface, which becomes incandescent and begins to emit thermo-ionic electrons without reference to the number of ions coming in or the efficiency of the electron avalanche. Any spot that becomes hotter than its neighbour, tends to become even hotter as the extra thermionic electrons attract the positive ions to the spot.

The huge increase in the electrons flow due to the thermo ionic emission causes another transition to the final state of the discharge, the *arc*. It requires very little potential difference to support the arc, because the thermo ionic phenomenon is way more efficient then the secondary emission.

In any discharge, multiple processes compete at the electrodes and in the gas, so explanations and theories can become subjects of dispute. A theory usually takes into account only the principal process operating under the conditions of the problem, and this is often quite satisfactory. Sometimes different assumptions and mechanisms can lead to the same outcome, which further complicates things.

The reader should keep in mind that complete explanations are probably impossible in many cases, and we must be satisfied with qualitative or semi-quantitative results. Also, the variety of phenomena in discharges is very rich and depends on many factors, such as purity and surface preparation, that are difficult to quantify. The whole variety cannot be mentioned here, only what is typical under reasonable assumptions. There is great scope for thought and reasoning in this field, which makes it fascinating, along with the beauty of the phenomena.

EMISSION OF LIGHT

The emission of light is one of the principal characteristics of discharges. Light of a definite frequency is emitted when an excited atom falls to a lower energy level. If there is an electric dipole transition moment, then the transition is called *allowed*, and occurs in about $10^{-8} s$ if nothing intervenes. The collision frequency is about 10^{11} per second at atmospheric pressure, so usually the excitation energy is lost in a collision before it can be radiated.

At 1 mmHg, however, the collision frequency is comparable to the radiation lifetime, and radiation is a possibility. Radiation is always a competition between de-excitation processes. If the dipole transition moment is forced to be zero by symmetry considerations, then radiation may occur by other means, but the radiative lifetime for these is much longer, so they are not seen even at 1 mmHg pressure. These are *forbidden* transitions. They are not really forbidden, just improbable.

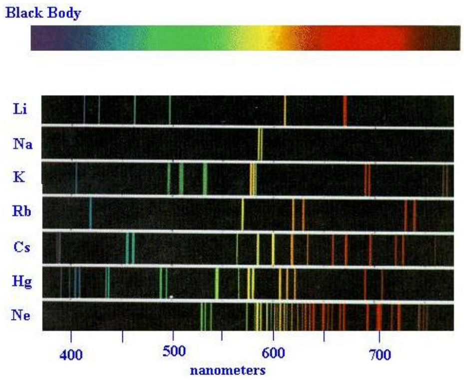

Pic. 1.15 Emission lines for several elements

At higher pressures, excited atoms are continually affected by collisions, which broaden the lines emitted. At still higher pressures, the atom states are spread and the radiation begins to assume the characteristics of black-body thermal radiation.

Since we had been working with discharges in air, here after the composition chart of air (20) and the emission lines.

Pic. 1.16 Composition of air and emission spectrum (21)

In dry air, the colour of produced light by lightning is dominated by the emission lines of nitrogen, yielding the spectrum with primarily blue emission lines.

Chapter 2

2.1 How a detector works

The job of a particle detector (22) is to record and visualize the explosions of particles that result from the collisions at accelerators. The information obtained on a particle's speed, mass, and electric charge help physicists to work out the identity of the particle.

Modern particle physics apparatus consists of layers of sub-detectors, each specializing in a particular type of particle or property. There are 3 main types of sub-detector:

- Tracking device – detects and reveals the path of a particle
- Calorimeter – stops, absorbs and measures the energy of a particle
- Particle identification detector – identifies the type of particle using various techniques

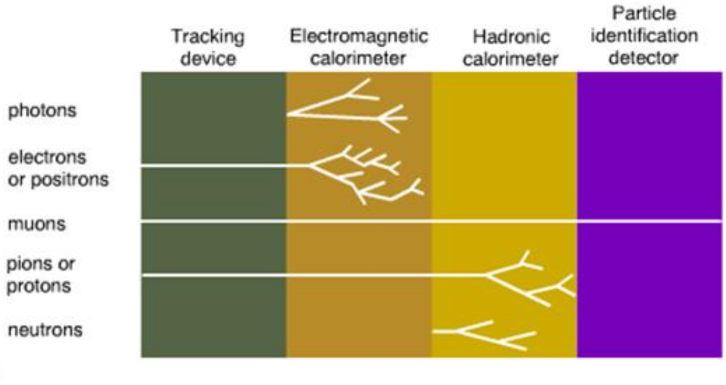

Pic. 2.1 schematic view of a modern detector

To help identify the particles produced in the collisions, the detector usually includes a magnetic field.

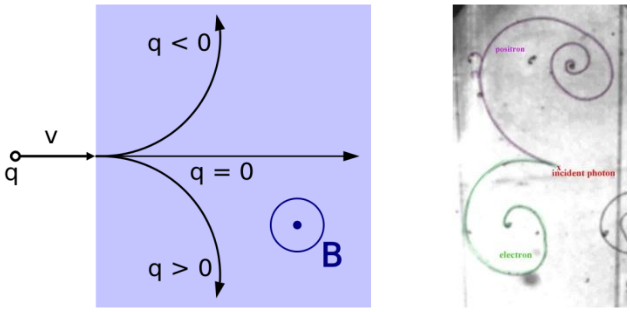

Pic. 2.2 track of a charged particle moving in a magnetic field and an electron positron couple in an early bubble chamber

A particle normally travels in a straight line, but in the presence of a magnetic field, its path is bent into a curve. In fact the force F acting on a particle of electric charge *q* with instantaneous velocity v, due to an external electric field E and magnetic field B, is given by the Lorentz law:

$$F = q(E + v \times B)$$

From the curvature of the path, it is possible to calculate the momentum of the particle which helps in identifying its type. Particles with very high momentum travel in almost straight lines, whereas those with low momentum move forward in tight spirals.

TRACKING DEVICES

Tracking devices reveal the paths of electrically charged particles through the trails they leave behind. When particles pass through suitable substances the interaction of the passing particle with the atoms of the substance itself can be revealed.

Most modern tracking devices do not make the tracks of particles directly visible. Instead, they produce tiny electrical signals that can be recorded as computer data. A computer program then reconstructs the patterns of tracks recorded by the detector, and displays them on a screen.

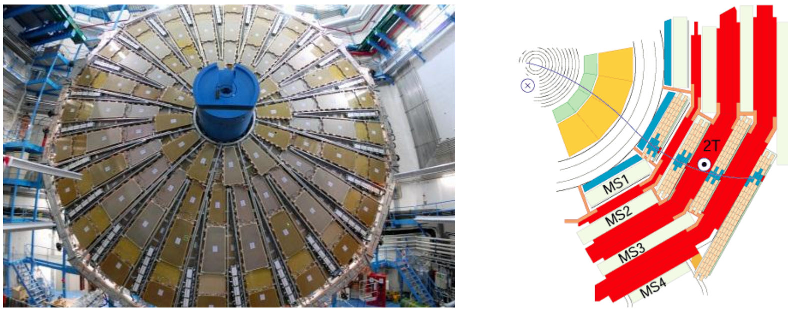

Pic. 2.3 A Toroidal LHC Apparatus (ATLAS) The end cap wheel equipped with Thin Gap Chambers and on the right a section of Compact Muon Solenoi; the returning joke for the magnetic field is equipped with muon chambers, made of different gaseous detectors.

Muon chambers are tracking devices used to detect muons. These particles interact very little with matter and can travel long distances through meters of dense material. Like a ghost walking through a wall, muons can pass through successive layers of a detector. The muon chambers usually make up the outermost layer (23). The present state-of-the-art of muon detection systems using gaseous detectors at the Large Hadron collider (LHC) is described in (24).

CALORIMETERS

A calorimeter measures the energy lost by a particle that goes through it. It is usually designed to entirely stop or 'absorb' most of the particles coming from a collision, forcing them to deposit all of their energy within the detector.

Calorimeters typically consist of layers of 'passive' or 'absorbing' high–density material (lead for instance) interleaved with layers of 'active' medium such as solid lead-glass or liquid argon.

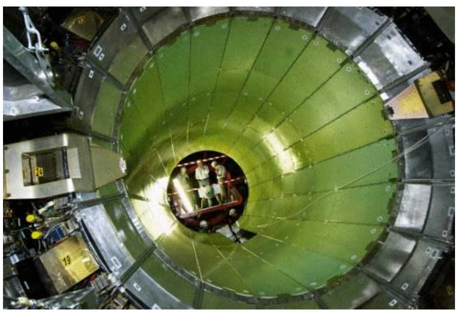

Pic. 2.4 The CMS lead tungstate crystal calorimeter

Electromagnetic calorimeters measure the energy of light particles – electrons and photons – as they interact with the electrically charged particles inside matter.

Hadronic calorimeters sample the energy of hadrons (particles containing quarks, such as protons and neutrons) as they interact with atomic nuclei.

Calorimeters can stop most known particles except muons and neutrinos.

PARTICLE IDENTIFICATION DETECTORS

Two methods of particle identification work by detecting radiation emitted by charged particles:

- Cherenkov radiation: this is light emitted when a charged particle travels faster than the speed of light through a given medium. The light is given off at a specific angle according to the velocity of the particle. Combined with a measurement of the momentum of the particle the velocity can be used to determine the mass and hence to identify the particle.
- Transition radiation: this radiation is produced by a fast charged particle as it crosses the boundary between two electrical insulators with different resistances to electric currents. The phenomenon is related to the energy of a particle and distinguishes different particle types.

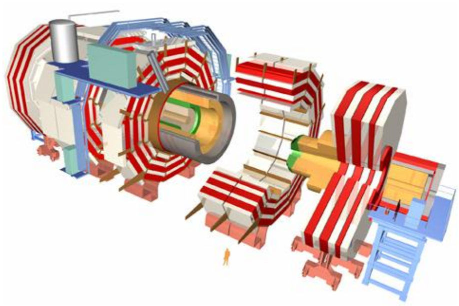

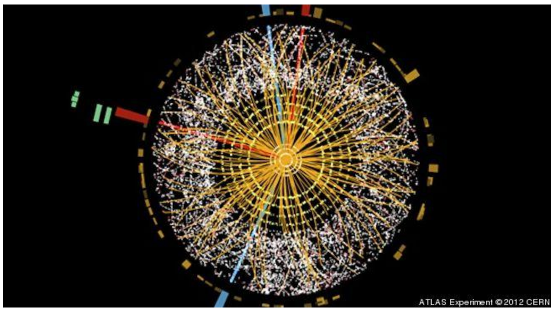

Pic. 2.5 CMS detector. Size: 21 m long, 15 m diameter. and Reconstruction of an event in the ATLAS experiment, searching for the Higgs boson.

DETECTOR'S PERFORMANCES

A detector is described in terms of its features:

- Energy resolution:

  the energy resolution of the system is defined as the ratio of the full-width at half-maximum (FWHM) of the full energy peak and the energy value at the full energy peak maximum.

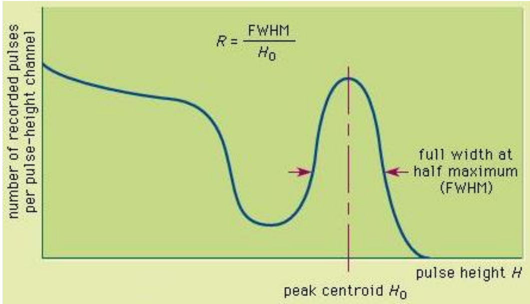

Pic. 2.6 Definition of Full Width at Half Maximum

- Time resolution:

  refers to the precision of a measurement with respect to time.
- Gain: defined as

$$G = \frac{N}{n}$$

  Where *N*= number of electrons reaching the anode pads, *n*= number of electrons produced by the ionization.
- Spatial resolution:

  is used in a double sense:

  a) the precision of localizing a track, or, more precisely, the square root of the variance of the conditional probability density function to get a signal x when a particle has crossed the detector at x'.

  b) the capability of a detector to separate the signals arising from two particles traversing the detector at close distance.
- Detecting efficiency:

  likelihood that the detector replies to a passing through particle.
- Response time:

  time needed to obtain the signal (from *ps* in scintillators to *μs* in a liquid medium).
- Dead time:

  for how long the detector is blind after a signal (from *ns* of scintillators to *ms* of Geiger counters).
- Stability over time:

  once calibrated the detector has to provide the same signal for the same particle impinging.
- Radiation tolerance:

  the detector has to be resistant to the harsh environment of a modern high energy physics experiment.

- Cost
- Power consumption

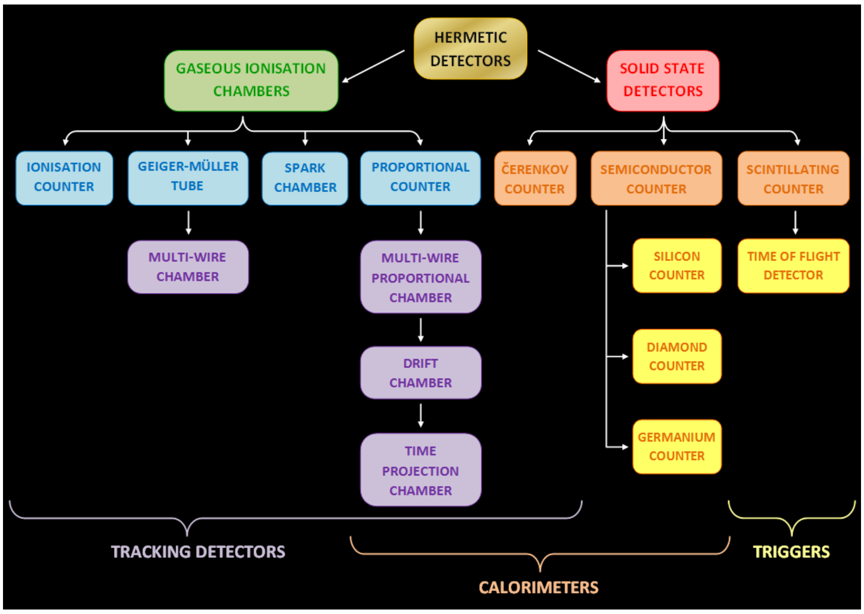

Pic. 2.7 Detectors: a classification.

2.2 Ionization detectors

Ionization detectors were the first electrical devices developed for radiation detection.

These instruments are based on the direct collection of the ionization electrons and ions produced in a gas by passing of a radiation.

During the first half of the century, three basic types of detector were developed: the ionization chamber, the proportional counter and the Geiger-Muller counter. Except for specific applications, these particular devices are not in widespread use anymore in nuclear and particle physics experiments. They are however still very much employed in laboratories as radiation monitors. Their basic design and structure have changed little since the late 1940's when the then newly-developed scintillation counter began taking the place of these instruments in nuclear research.

During the late 1960's, a renewed interest in gas ionization instruments was stimulated in the particle physics domain by the invention of the multi-wire proportional chamber by Georges Charpak who was then awarded with the Nobel Prize in 1992.

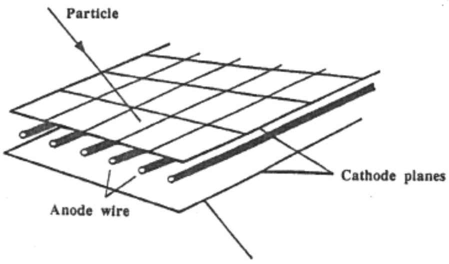

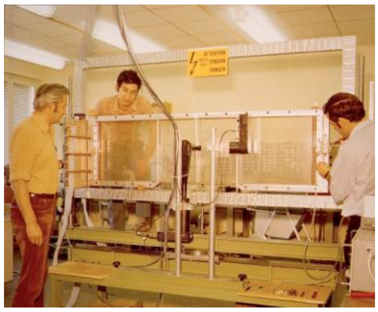

Pic. 2.8 MWPC and a large prototype at CERN on the right. Charpak and Sauli in the left of the photo.

This device was able to localize particle trajectories to less than a millimetre and was very quickly adopted in high energy experiments.

Stimulated by this success, the following years saw the development of the drift chamber and, somewhat later, the time projection chamber. These devices operate on the same basic principles as the simple proportional counter and they are still used extensively in high energy particle physics experiments.

A detailed report on how to reveal particle in gaseous medium (25).

2.3 Gaseous Ionization Detectors (26)

Because of the greater mobility of electrons and ions, a gas is the obvious medium to use for the collection of ionization from radiation.

Many ionization phenomena arise in gases and over years these have been studied and exploited in the detectors we will describe below. The three original devices,

- the ionization chamber,
- the proportional counter
- the Geiger-Muller counter,

serve as good illustration of the application of gas ionization phenomena on this class of instruments and will introduce the theory which Micro Pattern Gaseous detectors relies on: these latter devices are, at a first stage, nothing more than the former ones on scaled down dimensions.

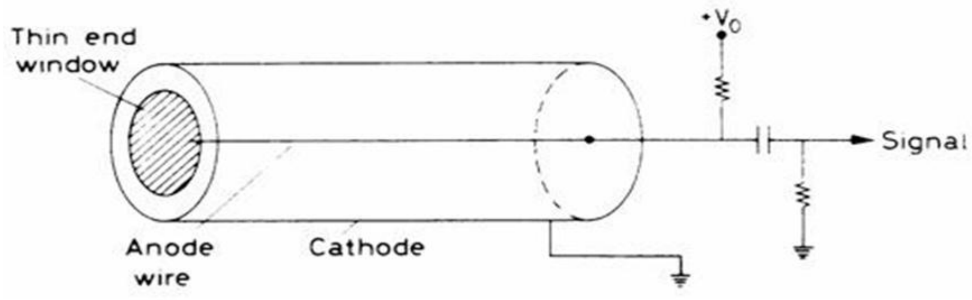

Pic. 2.9 Basic construction of a simple gas ionization detector

These three devices therefore are actually the same device working under different operating parameters, exploiting different phenomena.

The basic configuration (Pic 9) consists of a container, a cylinder, with conducting walls and a thin end window. The cylinder is filled with suitable gas, usually a noble gas such as argon. Along its axis is suspended a conducting wire to which a positive voltage relative to the walls is applied. A radial electric field

$$E = \frac{1}{r}\frac{V_0}{\ln b/a}$$

with r: radial distance from axis; b: inside radius of the cylinder; a: radius of central wire is thereby established.

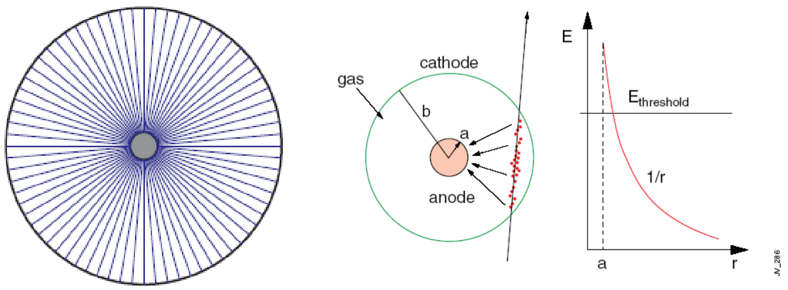

Pic. 2.10 Electrical field's configuration in a single wire chamber

If radiation now penetrates the cylinder, a certain number of electron-ion pairs will be created, either directly, if the radiation is a charged particle, or indirectly through secondary reactions if the radiation is neutral, as already explained in chapter 1.

The mean number of pairs created is proportional to the energy deposited in the counter. Under the action of the electric field, the electrons will be accelerated towards the anode and the ions toward the cathode where they are collected.

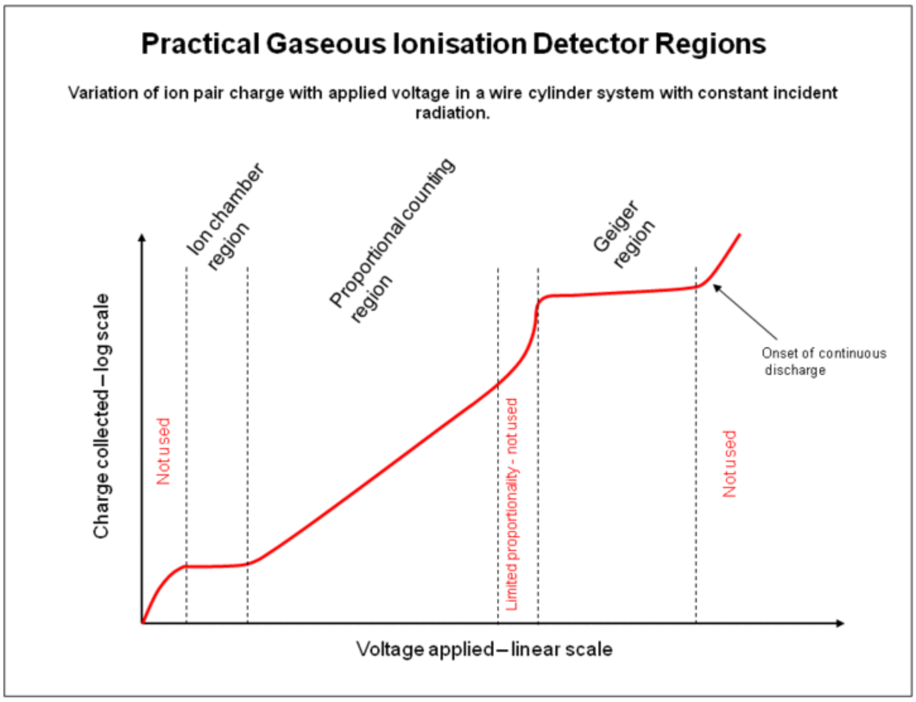

Pic. 2.11 Number of ions versus applied voltage in a single wire chamber

The current signal observed, however, depends on the field intensity. This is illustrated in pic 11 which plots the total charge collected as a function of V.

At zero voltage no charge is collected as the ion-electron pairs recombine under their own electrical attraction. As the voltage is raised the recombination forces overcome and the current begins to increase as more and more of the electron-ion pairs are collected before they can recombine. At some point all created pairs will be collected and further increases in voltage show no effect.

Each of the three detectors mentioned exploits one of the region in pic 11 to measure the total number of ion-pairs that are collected. The strength of the electric field between the electrodes and the type and pressure of the fill gas determines the detector's response to ionizing radiation.

Ionization Chamber

Ionization chambers operate at a low electric field strength, selected such that no gas multiplication takes place. The ion current is generated by the creation of "ion pairs" by the incoming radiation. The positive ions drift to the cathode whilst free electrons drift to the anode under the influence of the electric field.

The signal amplitude of course is very small and must be measured with an electrometer equipped with a low noise amplifier. This current is independent of the applied voltage if the device is being operated in the "ion chamber region".

Ion chambers are preferred for high radiation dose rates because they have no "dead time"; a phenomenon which affects the accuracy of the Geiger Muller tube at high dose rates.

PROPORTIONAL COUNTER

If we now increase the voltage beyond the ionization chamber region we find that the current increases again with the voltage. At this point, the electric field is strong enough to accelerate freed electrons to an energy where they are also capable of ionizing gas molecules in the cylinder. The electrons liberated in these secondary ionizations then accelerate to produce still more ionization and so on. This results in an ionization avalanche or cascade.

Since the electric field is stronger near the anode (pic 10 and equation), this avalanche occurs very quickly and almost entirely within a few radii of this wire. The chain of ionizations causes a momentary voltage across the detector producing a pulse.

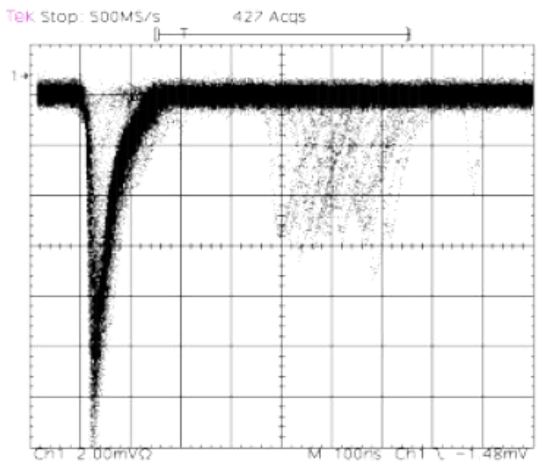

Pic. 2.12 Signals on the 50 μm diameter wire at 3100 V with 50 Ω load. Chamber is filled with DME (27).

The number of electron-ion pairs in the avalanche, however, is directly proportional to the number of primary electrons. What results then is a proportional amplification of the current, with a multiplication factor depending on the working voltage V. This factor can be as high as 10^7 so that the output signal is much larger than that from an ionization chamber, but still in proportion to the original ionization produced in the detector.

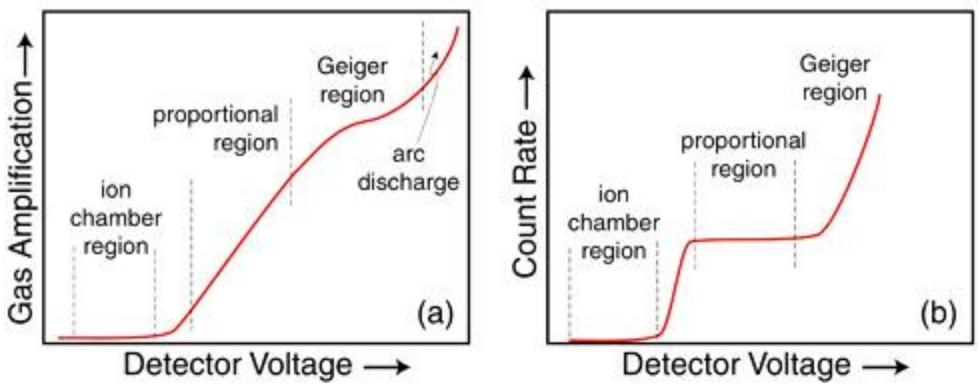

Pic. 2.13 The effect of increasing the applied anode voltage on (a) the gas amplification factor and (b) the observed count rate for a gas proportional counter (28).

This is the "proportional counting" region and proportional counters operate in this region.

The term "gas proportional detector" (GPD) is generally used in radiometric practice, and the property of being able to detect particle energy is particular useful when using flat arrays for Alpha and Beta particle detection and discrimination, such as in installed personnel monitoring equipment. The Wire chamber is a multi-electrode proportional counter, like any other gaseous detector.

GEIGER-MÜLLER TUBE

If the voltage is now increased beyond proportional region, the total amount of ionization created through multiplication becomes sufficiently large that the space charge created distorts the electric field about the anode. Proportionality thus begins to be lost. This is known as the region of limited proportionality.

Increasing V still higher, the energy becomes so large that a discharge occurs in the gas .

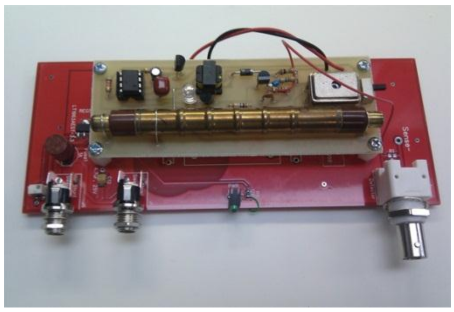

Pic. 2.14 A Geiger-Muller muon detector - ERGO Telescope Project (29)

What happens is that instead of a single localized avalanche at some point along the anode wire a chain reaction of many avalanches spread out along the entire length of the anode is triggered. These secondary avalanches are caused by UV photons of the previous avalanches.

The output current becomes completely saturated, giving the same amplitude regardless of the energy of the initial event. In order to stop the discharge, a quenching gas must be present (usually a mixture containing CO_2) in the medium to absorb the photons and drain their energy into other channels.

This is the "Geiger region" of operation.

The current pulses produced by the ionizing events are passed to processing electronics which can derive a visual display of count rate or radiation dose, and usually in the case of hand-held instruments, an audio device producing clicks. In general the working voltage of a Geiger counter is chosen to be in the middle of the plateau in order to minimize any variations due to voltage drift.

BREAKDOWN

Finally, if the voltage is increased still further a continuous breakdown occurs with or without radiation that will be stopped only if the power supply will be not able whether to maintain the voltage across the gap or provide the current to sustain the DC discharge. This region, of course, is to be avoided to prevent damage to the counter.

2.4 Micro Pattern Gaseous Detectors

In 1988, Anton Oed, at the Institut Laue-Langevin (ILL) introduced a novel concept in Grenoble: the micro-strip gas chamber (MSGC). Consisting of a set of tiny metal strips engraved on a thin insulating support, and alternatively connected as anodes and cathodes, the MSGC relies for its operation on the same processes of avalanche multiplication as the multi-wire devices.

The photolithography technology used for manufacturing, however, permits to reduce the electrode spacing by at least an order of magnitude, correspondingly improving the multi-hit capability.

Moreover, the fast collection of most positive ions by the nearby cathode strips reduces space charge build-up, and provides a largely increased rate capability.

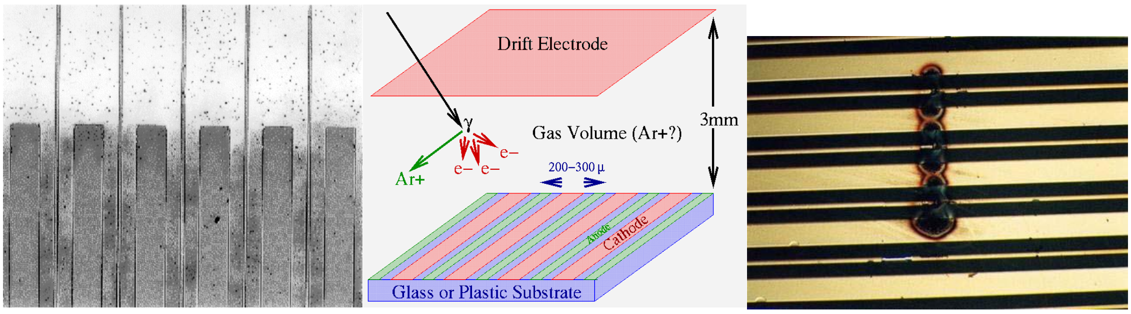

Pic. 2.15 MSGC: a photo, schematic view of the detector and effects of discharges in adjacent strips.

A substantial and successful development effort has been undertaken to improve the technology, with the development of supports preventing charge accumulations. Some problems persisted however, namely the slow degradation under sustained irradiation (aging) and the serious damages that can be produced by accidental discharges (30).

Advances in photo-lithography and micro-processing techniques in the chip industry during the past decade triggered a major transition in the field of gas detectors from wire structures to Micro-Pattern Gas Detector (MPGD) concepts, revolutionizing cell size limitations for many gas detector applications [(31), (32)].

They have in general higher reliability and can be produced at lower costs.

Anyway all of them make the most of the same phenomenon of ionization into a gas into a proportional mode, using though different configuration of the electric field which drives towards the read out pads the induced and then "amplified" charges.

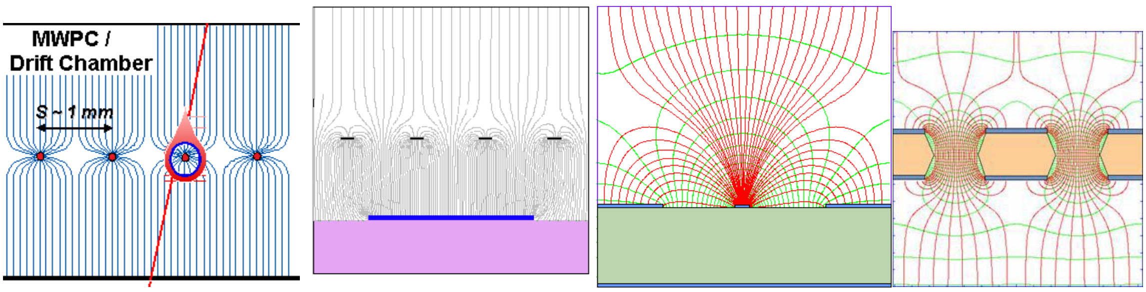

Pic. 2.16 Several configuration of field in multi-wire chamber, MICROMEGAS, MSGC and GEM

The most recent types of detectors aiming at improving spatial and time resolution, capable of economically covering large detection volume with low mass budget are MICROMEGAS and gas electron multiplier (GEM), which both have already demonstrated to behave reliably for long time even in an experimental environment where there is a high rate of particles to detect.

As a remark, the main advantage in MICROMEGAS and GEM detector has been decoupling the gain stage from the induction stage, whereas in wire chambers the gain and the induction stage were together within a few free path length from the wire, giving the conditions for highly energetic discharges. Though discharge remains the main limiting phenomenon even in MPGDs.

MICROMEGAS

The MICROMEGAS (Micro-MEsh Gaseous Structure) (33) is a gaseous detector based on a two-stage parallel-plate avalanche operation.

It consists of two gaps delimited by a thin micromesh: a conversion stage and a narrow amplification stage.

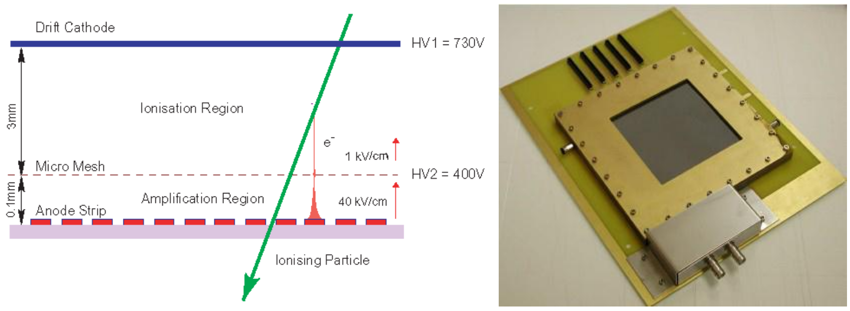

Pic. 2.17 Schematic view and a 10cm x 10cm MICROMEGAS detector in TE-MPE-EM fine pitch workshop

The thin mesh is stretched at a small distance (typically 50–100 μm) above the readout anode (see figure 17). If a high electric field is applied across this gap, and a low electric field is applied to the drift region, electrons will drift towards the mesh, are then focused into the mesh holes and are multiplied in the high field region. Due to the parallel field configuration and the saturation of the Townsend coefficient at high electric fields, the Micromegas have demonstrated excellent gain stability and high rate capability.

The anode plane is a simple Printed Circuit Board on which have been printed, by standard lithography, strips and epoxy pillars ensuring the parallelism between the two planes. The mesh is a metallic grid, made of nickel, obtained by electroforming technique.

MICROMEGAS detector has already proven to behave reliably even when irradiated with a high rate fluxes (up to hundreds of KHz/mm^2) and or highly ionizing particles; MICROMEGAS detector was developed by the CEA Saclay in order to fit the requirements of COMPASS experiment to stand a flux up to 500 $KHz/cm^2$with a spatial resolution better than 100μm and low material budget (34).

The salient feature of this technique is that is accounted to be spark resistant thanks to a resistive layer which protects the read out pads. The method used to render the MICROMEGAS chambers spark resistant while maintaining their ability to measure with excellent precision minimum-ionizing particles in high-rate environments is extensively described in (35). Here we would highlight the structure of such detector, with a cross section; we will come back to it in chapter 4, because this structure inspired a prototype of a ThGEM element.

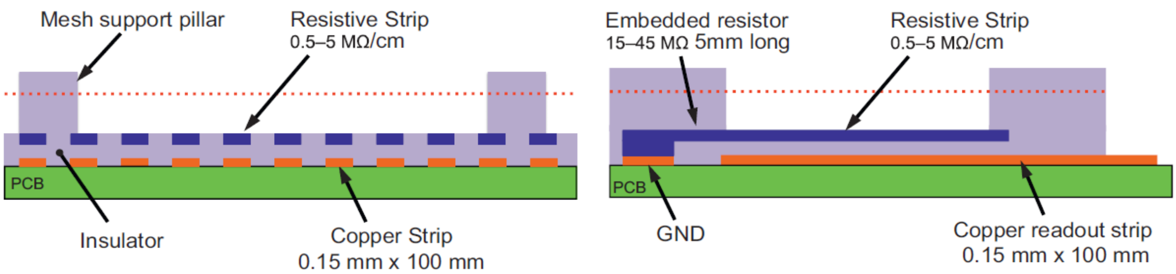

Pic. 2.18 An x and y view of a cross section of MICROMEGAS

GEM

Introduced in 1996 by F. Sauli (36), a Gas Electron Multiplier (GEM) detector consists of a thin-foil copper-insulator-copper sandwich chemically perforated to obtain a high density of holes. The GEM manufacturing method, developed at CERN, is a refinement of the double-side printed circuit technology.

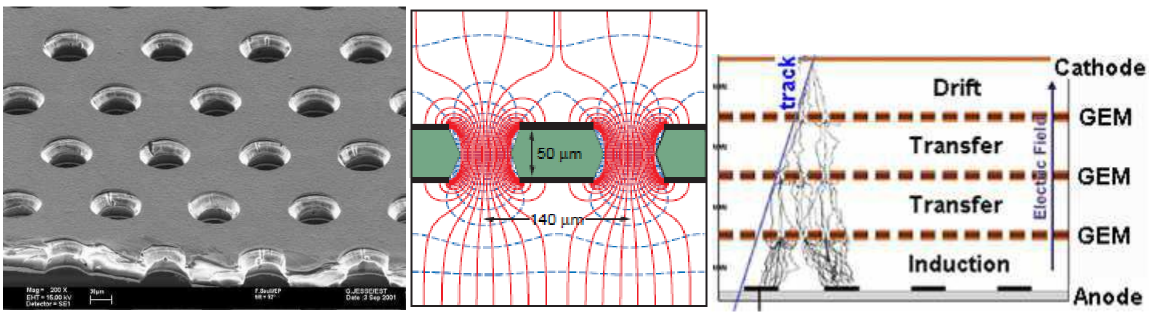

Pic. 2.19 A microscope photo of the dense matrix of holes, the configuration of the field within holes and a three stage configuration (triple-GEM) of a GEM detector

The hole diameter is typically between 25 µm and 150 µm, while the corresponding distance between holes varies between 50 µm and 200 µm. The central insulator is usually the polymer kapton, with a thickness of 50 µm.

Application of a potential difference between the two sides of the GEM generates the electric field indicated in Fig. 19. Each hole acts as an independent proportional counter.

Electrons released by the primary ionization particle in the upper conversion region (above the GEM foil) drift into the holes, where charge multiplication occurs in the high electric field (50 - 70 kV/cm). Most of avalanche electrons are transferred into the gap below the GEM.

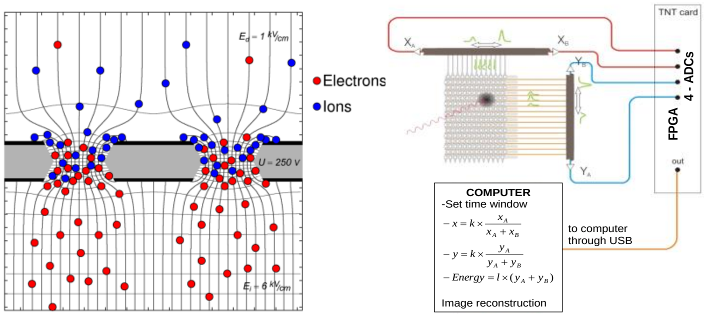

Pic. 2.20 Formation of the signal thanks to a multiplication within the holes and reconstruction of the signal thanks to the x-y anode matrix.

Several GEM foils can be cascaded (see pic 19), allowing the multi-layer GEM detectors to operate at overall gas gain above 10^4 in the presence of highly ionizing particles, while strongly reducing the risk of discharges. This is a major advantage of the GEM technology.

A unique property of GEM detector is a full decoupling of the amplification stage (GEM) and the readout electrode (PCB), which operate at unity gain and serves only as a charge collector.

The GEM community is working on detector applications: Xray Astronomy, Medical Imaging, TPGC, Plasma monitoring, Neutron detector and many other R&D (37).

THGEM

Within the broad family of micro-pattern gas detectors, the THickGEM (THGEM) is one of the most recent developments; it is attracting significant attention due to its simplicity and robustness. The THGEM has a hole-structure similar to the GEM, but with about 5–20-fold expanded dimensions.

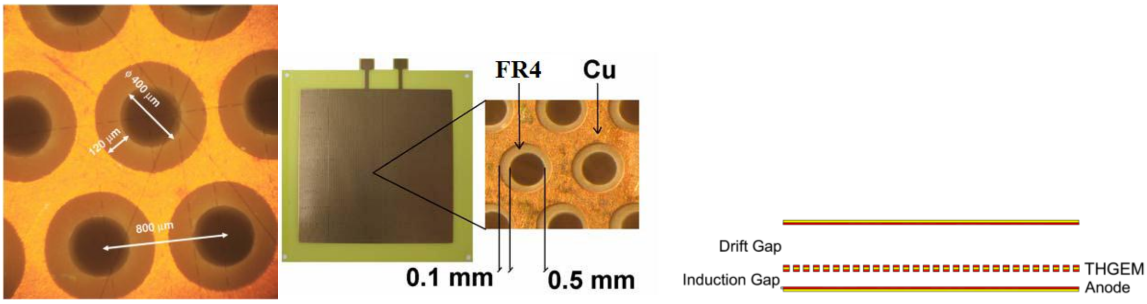

Pic. 2.21 Photo of a THGEM element with rim and one stage configuration THGEM detector

It is manufactured economically by mechanically drilling sub-millimeter diameter(d) holes, spaced by a fraction of a mm(a) in a printed-circuit board(PCB out of various materials e.g. FR-4,G-10, Kevlar, Teflon), followed by Cu-etching of the hole's rim (typically 0.1mm) using photolithographic mask.

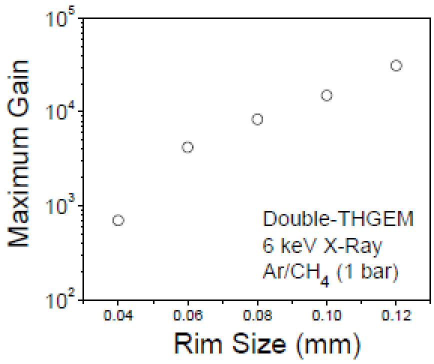

Pic. 2.22 Maximum gain versus rim size

The etched rim reduces edge discharges, resulting in over 10-fold higher gains than without a rim. Two or more THGEM elements can be cascaded, to provide higher gains or increase operation stability. (for a detailed review on the state of the art (38)).

The high gain, sub-millimeter spatial resolution, high counting-rate capability, good timing properties and the possibility of industrial production capability of large-area robust detectors, pave ways towards a broad spectrum of potential applications; some are discussed here in brief.

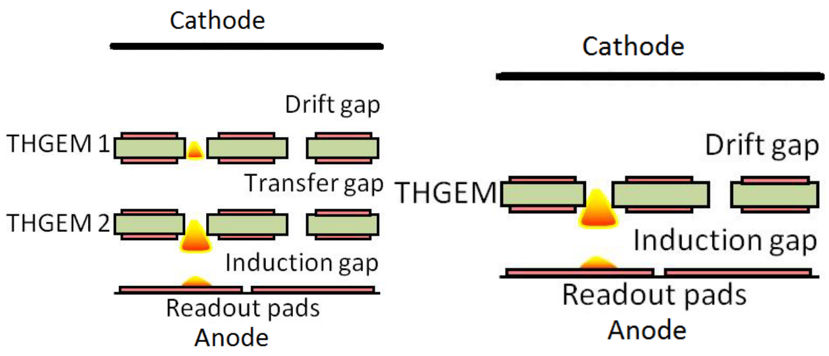

Pic. 2.23Double THGEM with reduced likelihood of discharge and on the right our goal: high gain, single THGEM detector, spark resistant

Moreover the problem of reliability due to discharges limits strongly the wide application of THGEM detector in harsh experimental environment; as said we could stack 2 or 3 THGEM elements reducing the gain of each, as done for GEM detector, but this in turn will increase the material budget, since THGEM is made of standard PCB, up to 2 mm thick.

One of the goal of this work was to prove the feasibility of a single-element THGEM detector, spark resistant.

2.5 Raether's limit

The problem of discharges is the intrinsic limitation of all single-stage micro-pattern detectors in hadronic beams; breakdown in micro pattern gas detectors, including THGEMs, is determined by the Raether limit (39); it occurs when the total charges in the avalanche exceeds a certain limit, Q_{crit}:

$$G_m n_0 = Q_{crit}$$

where G_m is the maximum achievable gas gain, n_0 is the number of primary electrons created by the ionizing radiation. Depending on the detector type and the gas mixture $Q_{crit} \cong 10^8$ electrons. As a result of this condition an enhancement of the electric field in front of and behind the primary avalanche induces the fast growth of a filament-like streamer followed by breakdown.

The equation shown stresses the fact that indeed very high gains may be obtained with single UV photons, under very low ionizing radiation background.

But under intense background, the gain may drop by as much as two orders of magnitude. This effect is of course expected to be more pronounced in "heavier" gas mixtures, e.g. Xe, Kr and Ar, than in Ne-mixtures having lower particle-induced ionization-electron yields.

In addition, *Gm* may also drop with increasing counting rate.

The Raether's limit gas been confirmed under a wide range of operating conditions and multiplying gaps (40). Many authors (41) report detailed studies made over decades on discharges in gaseous detectors for particle physics, since this phenomenon appeared to be the limiting factor even in multi wire chambers.

At the moment V. Peskov (ICN UNAM Mexico, CERN Geneva) and P. Fonte(ISEC and LIP, Coimbra Portugal) are amongst the most active in these studies and in proposing new structures to overcome this big issue (for a detailed overview (42), (43)).

2.6 Discharges in MPGDs

High electric field is present in a large fraction or all gaps between anode and cathode especially on sharp edges. The field is not uniform and it is higher at the metal/dielectric boundaries

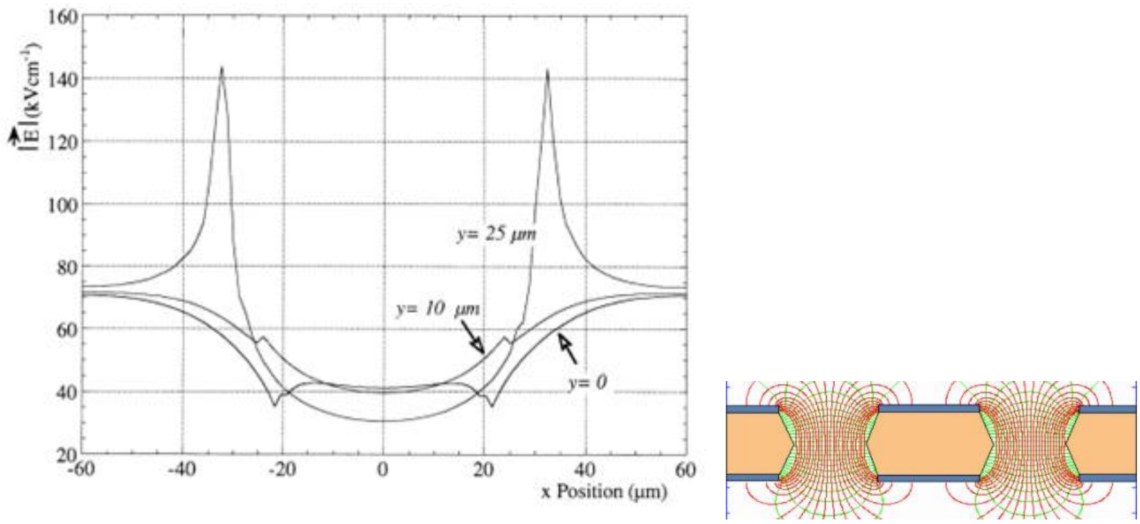

Pic. 2.24 Electric field in a GEM's hole computed along lines parallel to the electrode at different distances from the centre.

Hence in these areas the gain is way more high; high irradiation rate and/or exposure to heavily ionizing tracks can induce transitions from proportional avalanche to streamer probably followed by a discharge (harmful and fatal for the electronics) localized at the edges.

However there are mainly three ways of discharges development in MPGDs:

1. Spontaneous breakdown in absence of radiation: geometry and position-linked (essential role of quality and local defects)
2. Rate-induced breakdown: reduction of the maximum operating voltage
3. Heavily ionizing tracks exposure: considerable decrease of the maximum safe operating voltage

Many studies over years have been lead in order to identify the best geometries which could allow highest gain, here after a chart which summarizes the most remarkable results (44).

Detector	***Gain without α's irradiation*** (Max. Voltage)	***Maximum Gain before disch**** **in presence of α's** (Dischage limit**)
Stand. MSGC	5000 (590)	2000 (550)
Micromegas	$4*10^4$ (470)	3000 (385)
Stand. GEM	5000 (540)	1500 (485)
Conical GEM	**N→W: 2500 (600)** **W→N: 3000 (660)**	**N→W: 1500 (570)** **W→N: 2000 (640)**
Microcat/Well	6000 (540)	1500 (490)
Microdot	10^4 (580)	10^4 (580)
St MSGC+St GEM (ΔV_{GEM} = 400 V)	$2*10^5$ (V_c=625)	10^4 (V_c=450)
Double GEM (ΔV_{GEM2}= 400 V)	10^4 (ΔV_{GEM1}= 460)	10^4 (ΔV_{GEM1}= 460)

*** (**) Gain (Voltage) just below the first non zero discharge probability**

These studies confirmed that differences in max gain reached in a low irradiation environment shown by different single stage devices tends to vanish in presence of heavily ionizing particles.

In this conditions all single stage devices but microdot shown a non-negligible probability of transition from avalanche to streamer at gain between 1000 and 3000. This transition begin to occur when the average avalanche size exceeds 2-3 10^7 electrons (close Raether's limit).

ThGEM detectors despite their simplicity and cheapness have not reached yet the level of reliability required to operate in high rate environment; performance comparable to the more sophisticated GEM detectors can be obtained provided that the devices undergo an intense qualification activity, aimed at fine adjusting the numerous fabrication parameters and adapting the process technology

AGEING

The ageing process of any detector technology (45) must be carefully studied in order to establish the limits of application. Ageing phenomena are usually observed in any detector, but are not always fully understood due to the fact that very subtle processes and many parameters are involved. Many different causes can contribute to gaseous detector ageing:

- Gas: Polymerizing mixtures, pollution, reactive avalanche products, interaction with detector materials etc.
- Material: Outgassing, structural changes due to radiation etc.

Ageing is usually described in terms of integrated charge and tests are normally run at accelerated rates, often on small prototypes, but ageing may depends on:

- Gas mixture and flow
- Irradiation type and irradiated area
- Detector geometry
- Ionization current density

Remind that anyhow the ‘perfect’ test would be the final experiment.

2.7 Applications for THGEM detector

Due to its properties THGEM detector could find many applications in several fields, not only high energy particle physics. As already mentioned in the introduction, THGEM was proposed as an active elements of the end cap hadron calorimeters in the CMS experiment or as a trigger Trigger Detector for ALICE.

The operation of single-, double- and triple-THGEM UV-detectors with reflective

CsI photocathodes (CsI-THGEM) in Ne/CH4 and Ne/CF4 mixtures was investigated in view of their potential applications in a ring-imaging Cherenkov detector (RICH detector) motivated by the ALICE RICH upgrade program (46).

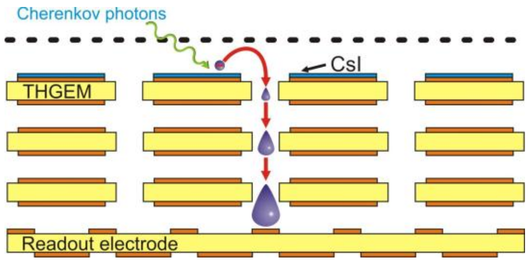

Pic. 2.25 Photo detection with a triple-THGEM detector

THGEM detectors are well suited for photon detection, if the cathode is covered with a photosensitive layer: electrons knocked out of the photocathode by photons will then drift towards the THGEM-stack and will be amplified.

It was demonstrated (47) that the electron collection and amplification is performed with close to 100 % efficiency.

It is, however, crucial to suppress the ions generated during the gas amplification, as far as possible, since ions released into the drift volume can hit the sensitive photocathode with sufficient energy to liberate extra electrons (secondary electron emission and Ions Back Flow problem).

Of particular interest are Cryogenic Two-Phase Detectors (48) with scintillation and/or charge multiplication in the saturated vapor above a noble liquid, for the detection of rare-events (e.g. Dark-Matter searches and neutrino physics)

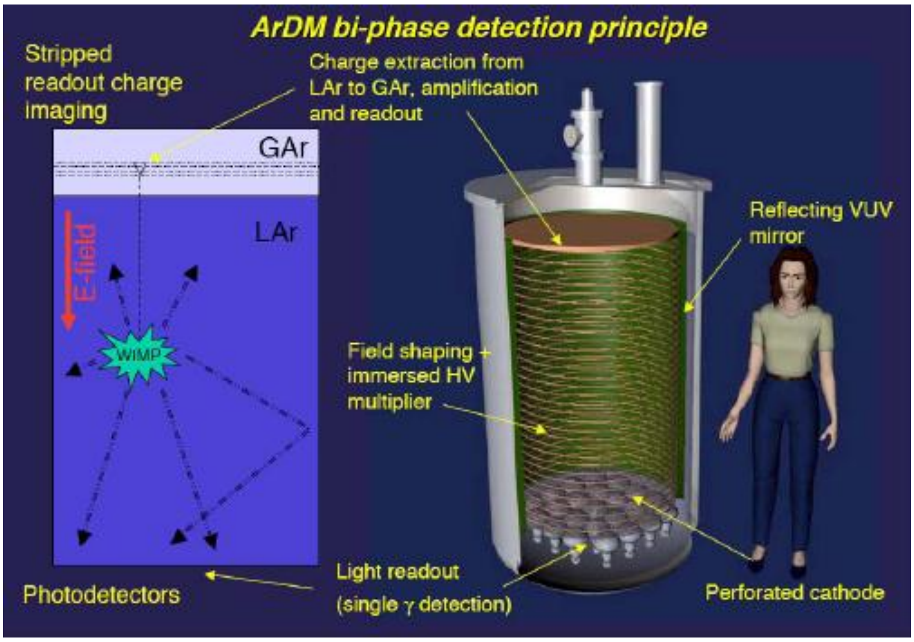

Pic. 2.26 Liquid Argon LEM-TPC with a 1 mm thick segmented LEM.

Recently some groups have reported that Thick GEMs (49), (50), (51) can be also used in these detectors as the gain element in the saturated vapor above liquid Argon for example, in some conditions yielding even higher gas gain than GEMs (52).

2.8 Technology

The strength of MPGDs, beyond their reliability, is that they can be built with a standard, well known photolithographic process in a PCB workshop (53) (54), introducing some dedicated steps where required. CERN has its facility to develop test and deliver to the experiments any micro pattern gaseous detector in building 102, part of Technology department, where I carried out my programme as a technical student from August 2011 and September 2012.

This allows a mass production suitable to cover the large areas of a current high particle physics experiment at a relatively low cost; CMS is about to upgrade its muon chambers, instrumenting them with GEM detectors (55) and the area to be covered is in the order of some hundreds square metres. If the process was not simple, reliable and reproducible, it wouldn’t have been possible to adopt this technology.

Moreover the use of a well-known technology permits transferring the workload to external companies in order to fulfill the requirements of such big experiments. Hence MPGDs production, developed and fine-tuned on the needs of particle physics, perfectly fits with the knowledge transfer, one of the capital CERN’s inspiring concept.

It has been already some years that ELTOS company is contributing largely in the production of high quality boards for particle physics and more recently they are trained by CERN’s experts to make their process suitable for MICROMEGAS production.

On the other hand there are a couple of companies (TechEtch, Newflex) that are starting GEM’s production.

Actually there is a big difference between the process deployed to develop different kind of detector: GEM elements are made with a completely chemical process (a global process, which means that all the holes are created at the same time dipping the samples in a chemical etching bath), instead THGEM and MICROMEGAS are built with a hybrid process, most of it standard PCB technology but with some dedicated steps, especially in the case of MICROMEGAS.

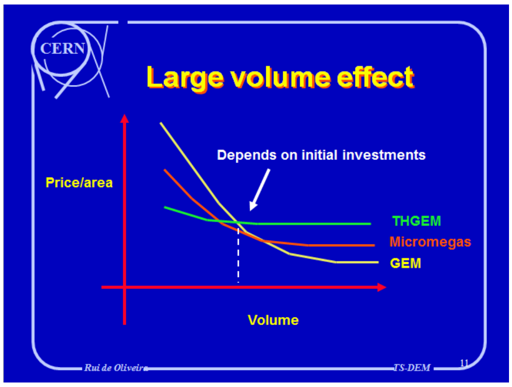

Pic. 2.27 Trend of the cost for large area detectors

2.9 R&D51 – a worldwide collaboration for MPGDs

The RD51 collaboration was founded in April 2008 (56)to coordinate and facilitate efforts for development of micro-pattern gaseous detectors (MPGDs).

The 75 institutes from 25 countries bundle their effort, experience and resources to develop these emerging micro pattern technologies.

MPGDs are already employed in several nuclear and high-energy physics experiments, medical imaging instruments and photo detection applications; many more applications are foreseen. They outperform traditional wire chambers in terms of rate capability, time and position resolution, granularity, stability and radiation hardness. RD51 supports efforts to make MPGDs also suitable for large areas, increase cost-efficiency, develop portable detectors and improve ease-of-use.

Pic. 2.28 Collaboration Meeting in Kobe, 2011

The collaboration is organized in working groups which develop detectors with new geometries, study and simulate their properties, and design optimized electronics. Among the common supported projects are creation of test infrastructure such as beam test and irradiation facilities, and the production workshop.

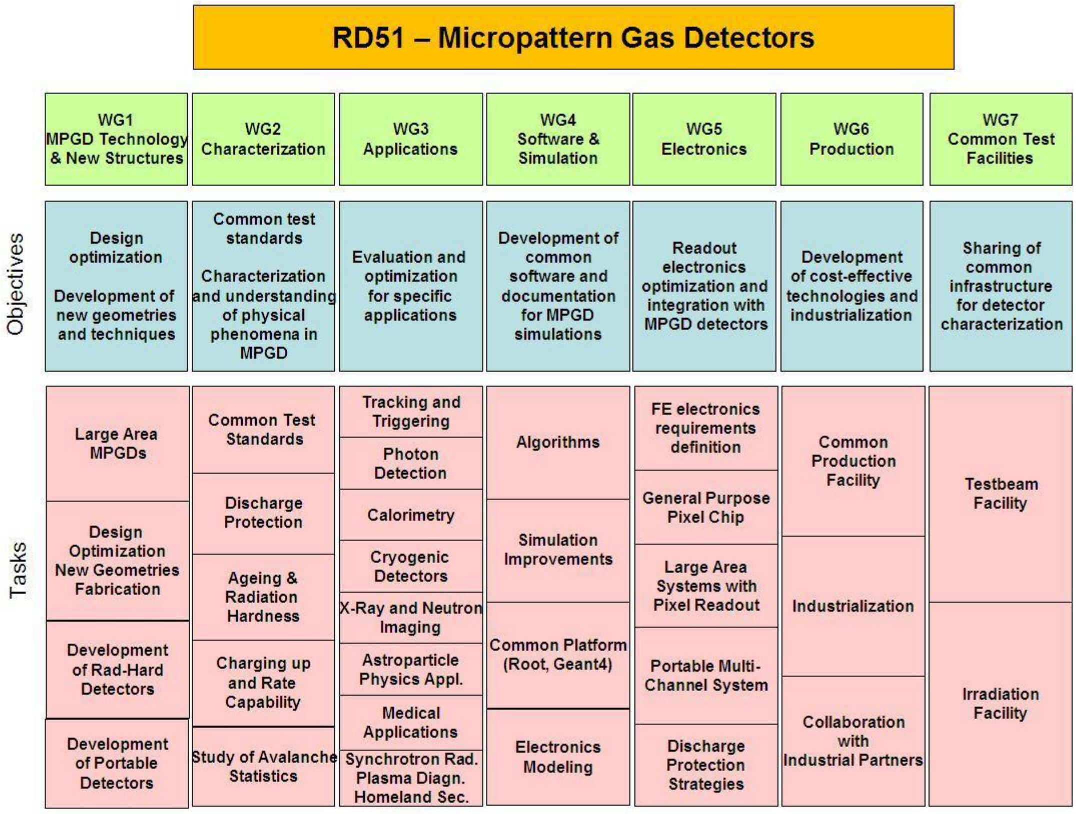

Pic. 2.29: Working groups: TE-MPE-EM workshop is part of WG6.

Chapter 3

3.1 Discharges between two metallic tips in air

In order to gain some feeling about discharges we started with a simple test: we induced discharges to happen between two metallic tips in air, at atmospheric pressure. Indeed a simple and elementary test, though it shed light on several and different aspects which have guided us towards fruitful considerations later on, when we had to understand the reason of the degradation of a THGEM detector.

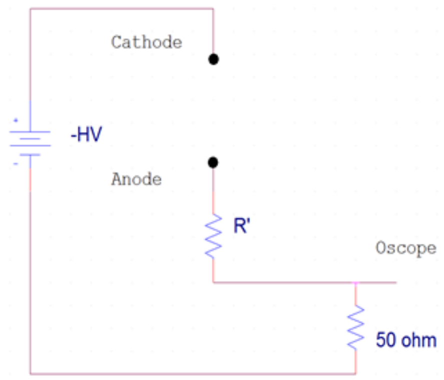

Pic. 3.1 The system: two copper tin coated tips in air at high voltage

The schematic consist only of a resistor with one terminal free and a high voltage power supply (CAEN N471A) able to deliver up to 8 kV at 8 uA; the experiment was ramping up the voltage at fixed distance in between the two tips until the discharge appears; this induces a current through the serial resistors which is detected as a voltage drop by a wide band oscilloscope (Agilent DSO9254A, 2.5 GHz bandwidth, 20 Gsample/s).

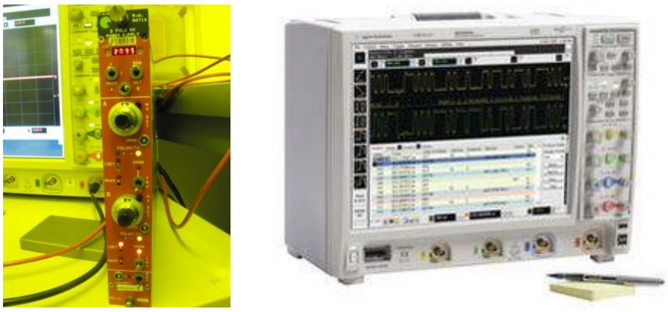

Pic. 3.2 CAEN power supply, Agilent Oscilloscope

The signal induced by the current flow due to the discharge was detected across a shunt 50 ohm serial resistor and ground in order to match the impedance of the input amplifier and the impedance of the cable. Instead $R'$was introduced at first to protect the input of the oscilloscope from the high pulsed signal expected.

It is possible to measure even the average current thanks to a display the power supply has, showing that value drawn by the system.

Both tips are made of tin coated copper leads, the usual material which discrete electrical components' terminals are made of. In order to have a phenomenon not affected by the roughness of the tip's head(that is the enhancement of the field due to needle effect), which may results in a multi-spot discharge, we smoothed the surfaces, previously scraped with fine sandpaper, thanks to a bath in iron chloride. The result is pretty well sharped tips, with a radius in the order of hundreds of um.

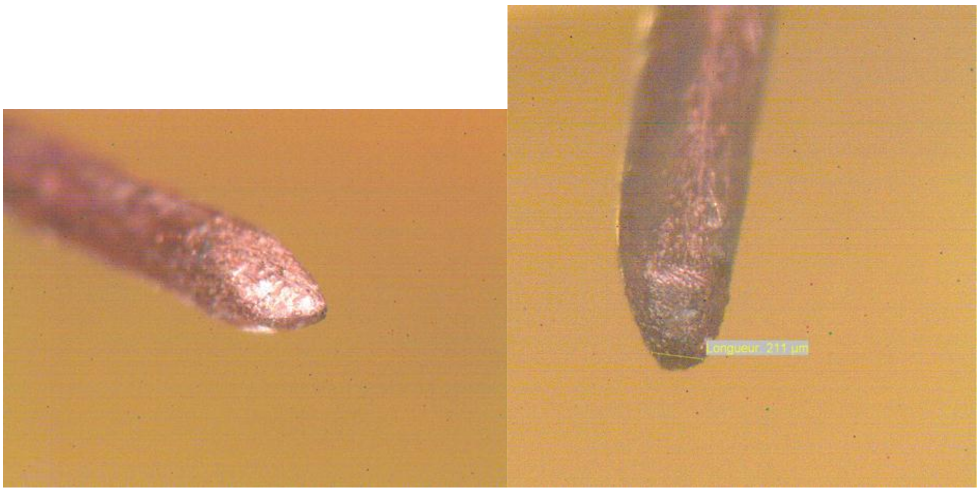

Pic. 3.3 Microscope shots of the tips; on the right a diameter of 211 um is estimated

The power supply delivers the voltage through a SHV connector on the PCB where also the resistors are soldered and the signal is picked up thanks a BNC connector. The BNC coaxial cable is then directly connected to a channel of the oscilloscope.

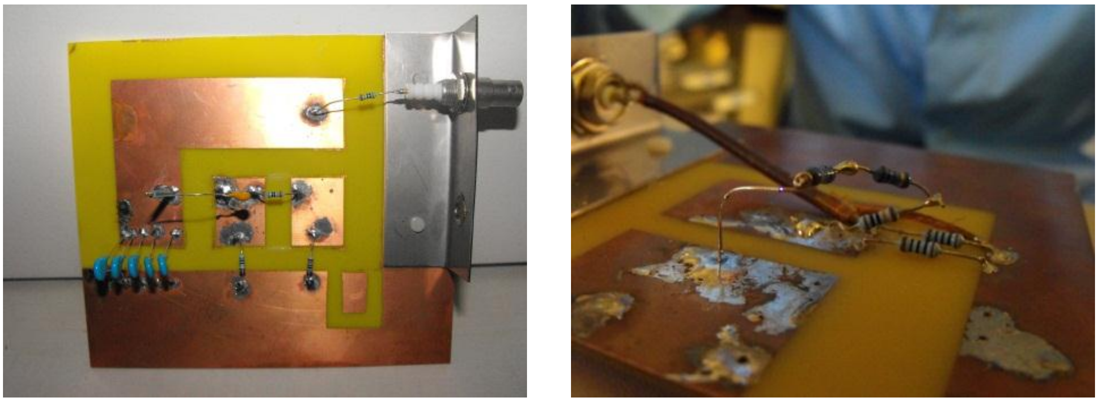

Pic. 3.4 One of the test board; on the left bottom corner, 5 capacitors 1nF to have a big reservoir of charges. On the right is visible even a faint purplish discharge

The main issue has been getting rid of the ringing phenomenon activated by the fast signal of the discharge which at first was hiding the signal we are interested in. In most of the cases was not possible to observe a clear signal, due to the length of the connections, which were introducing a not negligible parasitic inductance.

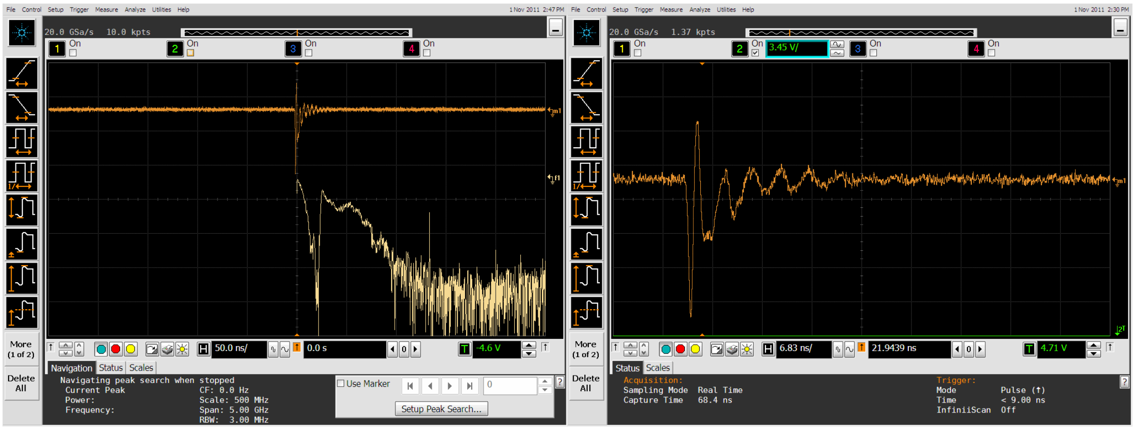

Pic. 3.5A single pulse picked up; on the left screen shot, in white the spectrum of the signal. On the right, an enlargement at 7 ns per division.

All the dimensions of the board and the length of the connections have to be minimized, especially the loop were the discharge happens, in order to reduce as much as possible the parasitic inductance. Last, the ground plane has to be as large as possible to provide a low resistance path for the current to evacuate, hence to avoid any ground shift (57), (58).

Eventually, after some different design of the board, the pulsed was clearly picked, as showed here.

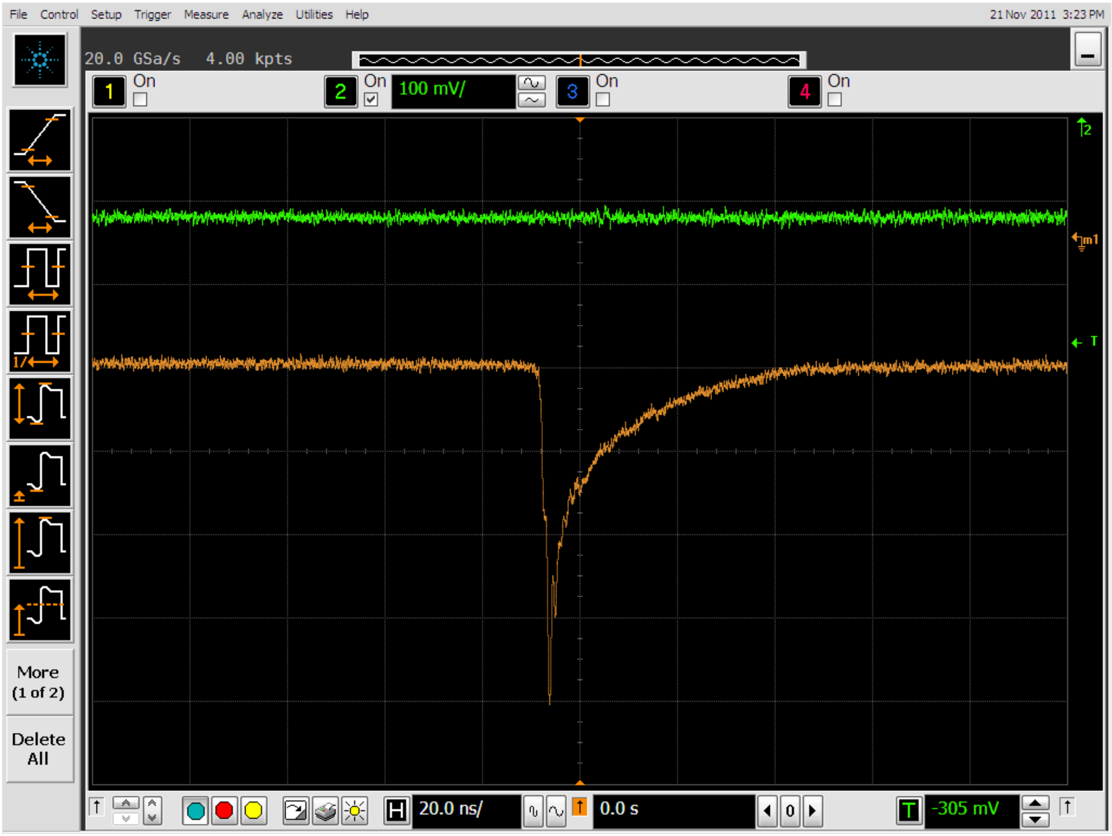

Pic. 3.6 A fast pulsed tip to tip signal, clearly recorded. That is the discharge.

GOALS

Tries have been performed changing the resistor R' and the gap between the tips; the main goals of the test were:

- observe the shape of the induced signal
- understand which are the parameters defining the amplitude of the current
- inspect the behaviour of the system over time

Generally once the voltage has exceeded the breakdown value for that gap the signal is a train of pulses, independently from the serial resistor we put.

Here a plot of the typical signal detected:

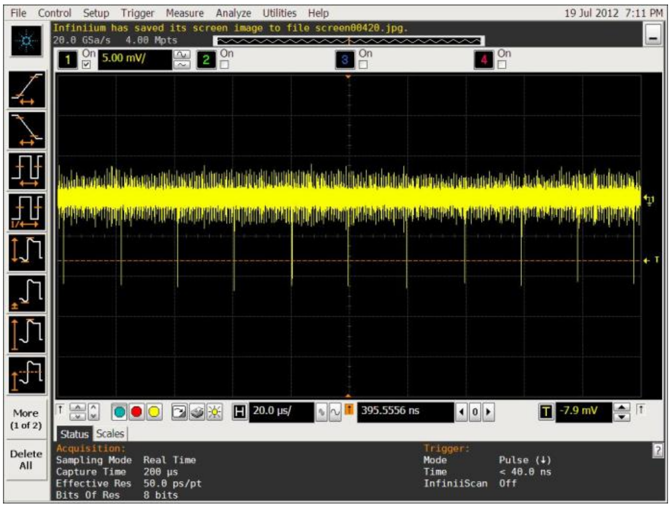

Pic. 3.7 A train of pulses.

The first valuable consideration we observed is that the repetition period is a function of the over breakdown voltage; here we plot two screen-shots, the serial resistor is 700 Mohm and the inter-tips distance is 6 mm in both the configurations.

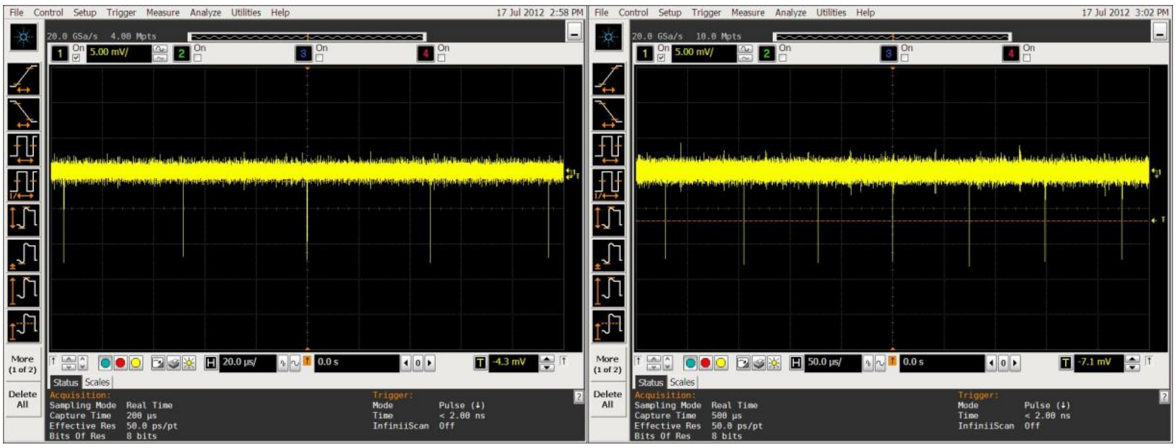

Pic. 3.8 Train repetition period is an increasing function of the voltage. On the right train with a higher voltage imposed by the power supply.

To be noticed also that the amplitude of the peak current is not affected by the voltage. If we enlarge one single peak we can estimate the primary properties of the signal:

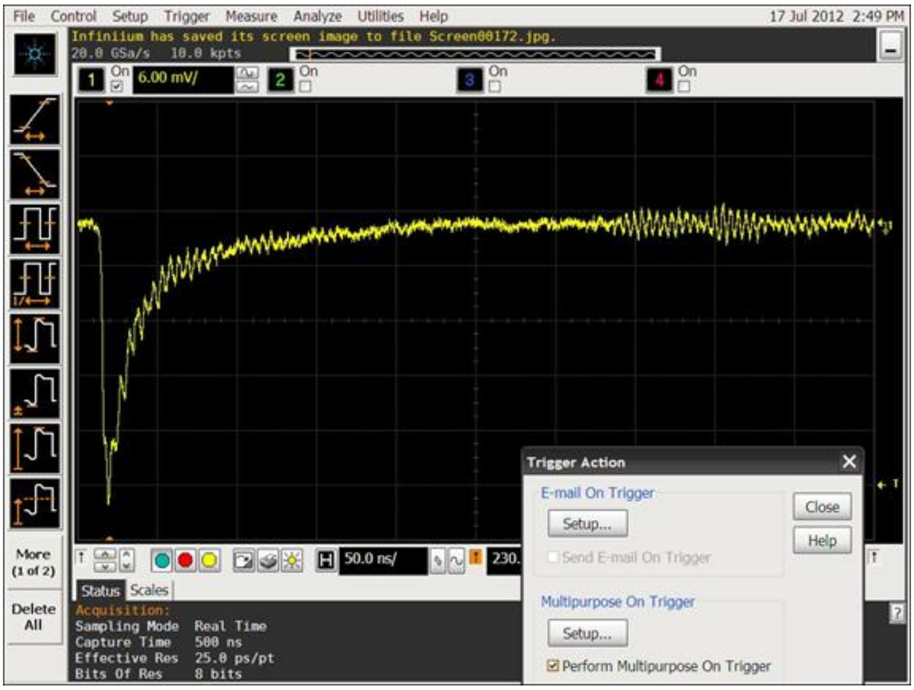

Pic. 3.9 Another pulse.

Mainly at this stage is helpful highlight two properties of the signal:

1. the rise time of the initial fast peak, *tr* (we observed always values between 1 and 2 ns)
2. the subsequent shape, dominated by a certain characteristic time *t*

3.2 A perspective on the system

If we consider the two tips when a discharge has not already happened and we want to describe them with an equivalent electrical component it might not be difficult to see they will be completely described by their capacitance.

The high voltage sets a field with a certain shape depending on the geometries of the tips and the distance in between them; this field, if below the breakdown field of the medium (in this case air), attracts electrons from the terminations on the cathode and push away electrons on the anode sides.

We have all the ingredients to define a capacitance, charges kept away under a certain potential.

Since there is not any analytical expression to calculate the field between two tips, neither ways to measure this tiny capacitance, to perform some estimations we used COMSOL

Multiphysics. Below a plot of the values of capacitance obtained for different inter-electrodes gap.

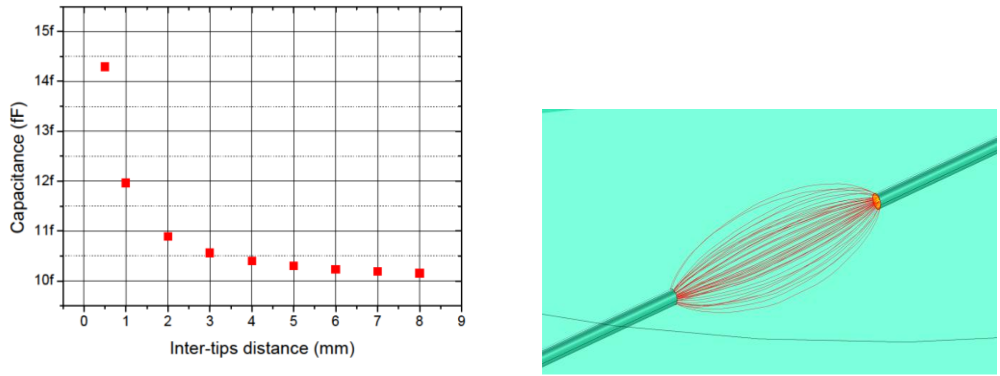

Pic. 3.10 Simulation of the value of the capacitance between two tips in air with COMSOL and on the right the configuration of the field.

In our experiments though there are at least two sources of uncertainty, which make these simulations less close to real case. The first is the exact shape of the tips and moreover the nature of their surfaces which affects strongly the fields, hence the discharge. Second, the distance is not precisely fixed and any misalignment between the needle of the tips changes the capacitance.

So the aim of the simulations in this case was to have an idea of the capacitance we were playing with and to get some feelings on the figures involved.

Then we made tests for several serial resistor (from 100 Kohm to 900 Mohm); once inter-tips distance was fixed, we progressively increased the voltage, taking notes of the DC value of the current showed by the display on the power unit.

We swept the voltage within a range defined by two values, the lowest one being the breakdown voltage of that configuration and the highest the value at which the current drained by the system reached the limit of 8 uA (the highest value the PSU can deliver); at that point we consider that the power supply is affecting the results and limiting the system, so we stopped the test.

3.3 Results

The frequency of the pulses was estimated from the signal displayed on the oscilloscope's screen.

The tests can be grouped into two:

- changing the serial resistor but keeping the same inter tips distance
- changing distance but keeping the resistor

Generally we observed that changing only the serial resistor doesn't affect the current measured; below a plot of the current as a function of the frequency of the repetitive signal for several serial resistors.

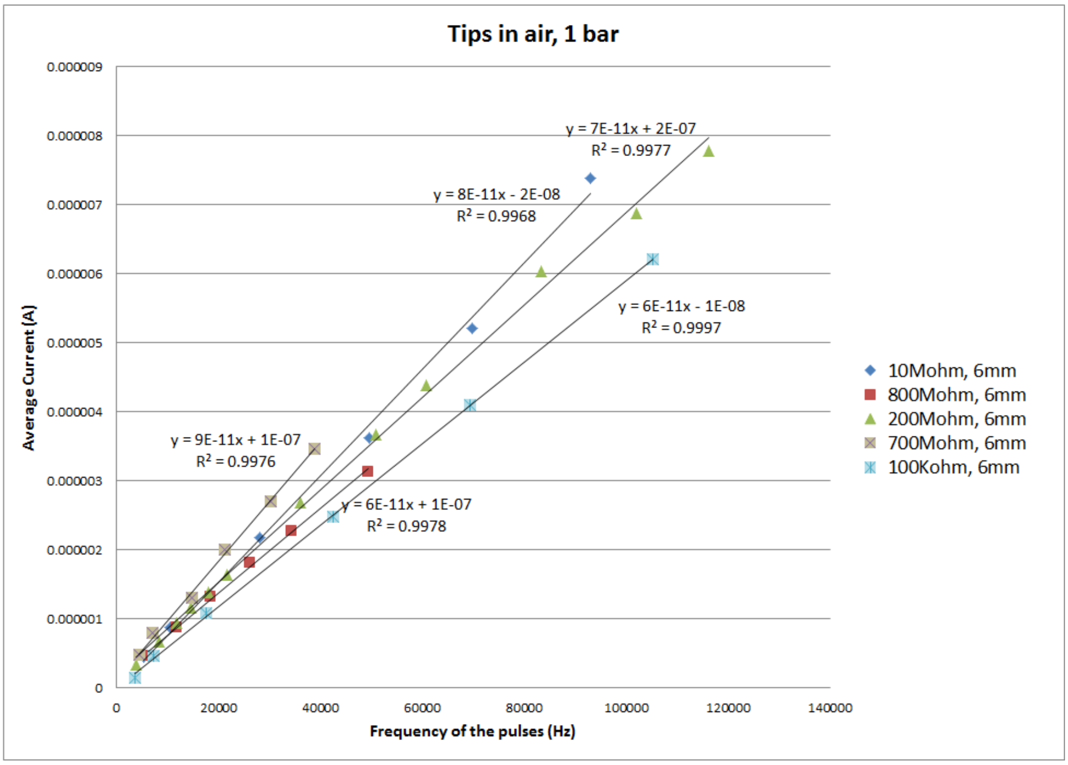

On the other hand, when we changed the distance between the tips keeping the same resistor we observed large changings in the current; below the case with 200 Mohm serial is shown.

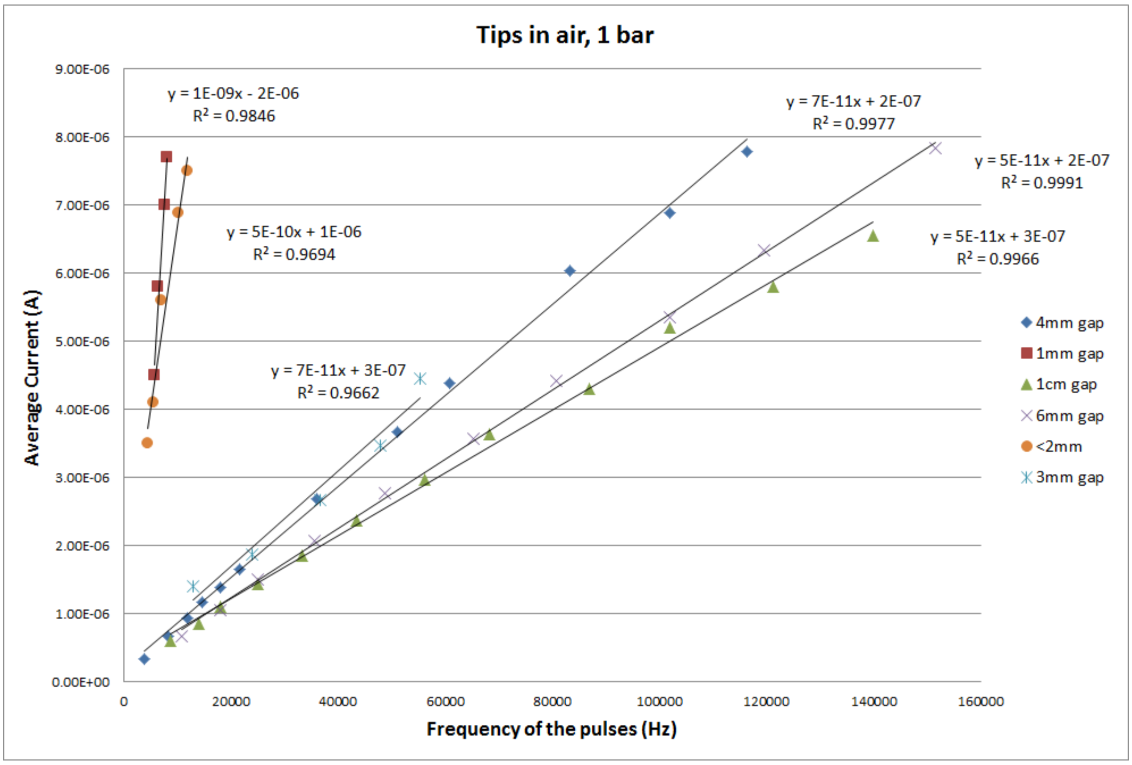

Interpolating the data obtained we saw an almost perfect linear relation between the average current and the frequency and a relation of the frequency of the pulses observed with a squared function of the voltage for any value of serial resistor we put, for any inter tips gap.

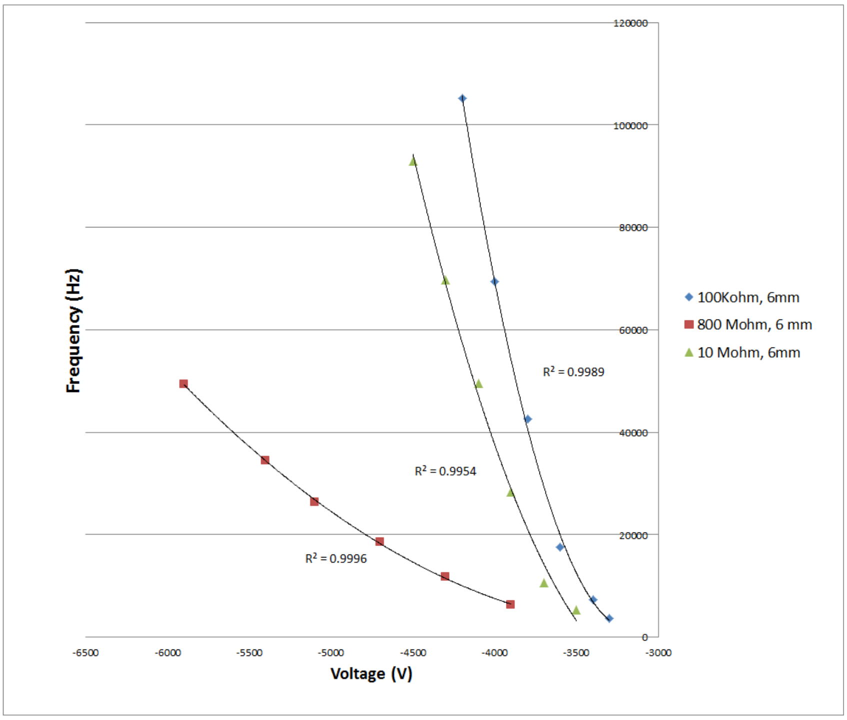

There are studies (59)reporting the same tendencies in a tip-to-plane set up, but no one is considering the tip-to-tip case, maybe because it never raises the attention of the community.

Though, as we will prove in this work, this case becomes important when discharges create defects on the surfaces of the electrodes in gaseous detectors and these defects behave as needles, enhancing locally the field.

3.4 About the discharge of a capacitor

Going back to the results shown in the previous paragraph, it might be interesting to specify the linear relationship we found experimentally through a simple equation.

$$\bar{I} = Q * f$$

where $\bar{I}$is the average current we measure, $f$is the frequency of the pulses estimated and Qdimensionally has to be charges. We did nothing more than putting into a simple formula what we showed in the graphs.

Moreover $Q$is the charge per pulse, assuming that there is no DC current overlapped to the signal; if there was, it would have been so little to under exceed the sensitivity of the input amplifier of the oscilloscope, because no DC component was detectable.

Let's have a look to the pulse, isolating it from the train previously shown. Here after, two pulses: both are taken from a 100 Mohm serial resistor configuration, what changes is the inter-tips distance.

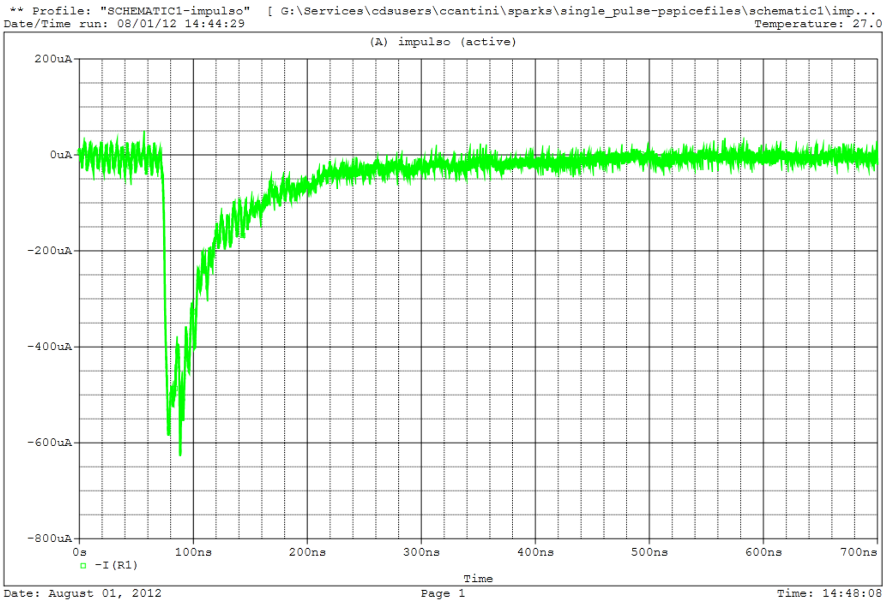

Pic. 3.11 Pulse in a 6 mm gap configuration

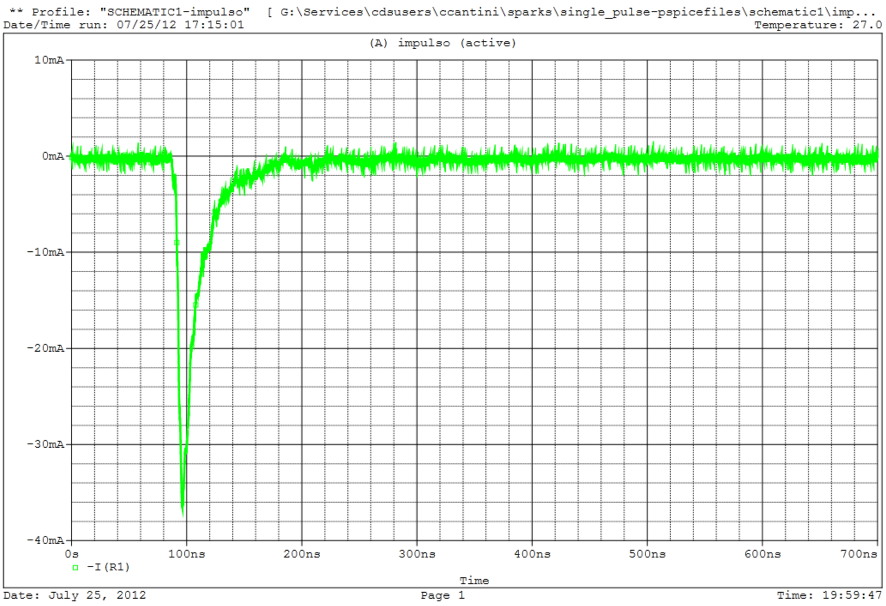

Pic. 3.12 Pulse in a 1 mm gap configuration

In the case of 1mm gap the observed amplitude of the peak is 30-35 mA, two order of magnitude bigger than the 6mm configuration, 600 uA; again, the amplitude of these peaks depends on the distance, that is the capacitance between the tips is changing, being the voltage still well above the breakdown voltage of the air in both cases.

If now we agree on the fact that the tips act like a capacitor we might gain something more about what is happening during a discharge and where the characteristic times - tr and t – come from.

The rise time for a discharge is generally accounted to be in order of the one observed and is determined by the motion of electrons through the gas (60). Instead the fall time could be linked to the value of the equivalent capacitance which is discharging and then sub sequentially recharged by the power supply. More studies should be performed in order to prove or finally refute this hypothesis, which though comes from direct and experimental results.

INTRODUCING THE TRICHEL'S PULSES

Electrical corona is an extremely complex phenomenon which takes many forms under various conditions and involves numerous microscopic mechanisms.

When a negative dc voltage is applied to a needle in an electronegative gas such as air, the corona current to a grounded conducting plane can exhibit a surprising time dependence for some range of conditions. The current at corona threshold consists of irregular pulses in the kilohertz range, with a mean current on the order of a microampere. A small increase in voltage results in the establishment of well-defined pulse frequencies which often extend to the megahertz range. These highly regular current pulses have been studied by Trichel and are known as Trichel's pulses and they are studied usually in a tip-to-plane discharge configuration (61).

Pic. 3.13 Discharge: corona.

Then we think that the phenomenon observed is a "Trichel" like discharge, but in a tip-to-tip configuration, totally not studied yet: this kind of discharge is known to induce defects on tips-like electrodes (62) but we haven't observed valuable changings of the features of the discharges, once that the serial resistor and, more important, the gap was fixed.

3.5 Discharges between copper lines on FR4

Once the test was set up properly and we understood the basics about discharges, we addressed the test to the understanding of the effects of repetitive induced discharges on the materials which a commercial THGEM is made of at the moment, that is copper on a substrate of FR4.

Since we were interested at a first stage in the response of the materials to this kind of phenomenon, we simply used two strips of copper facing with an inter-electrodes gap of hundreds of microns, in the order of millimeter wide, on a FR4 substrate.

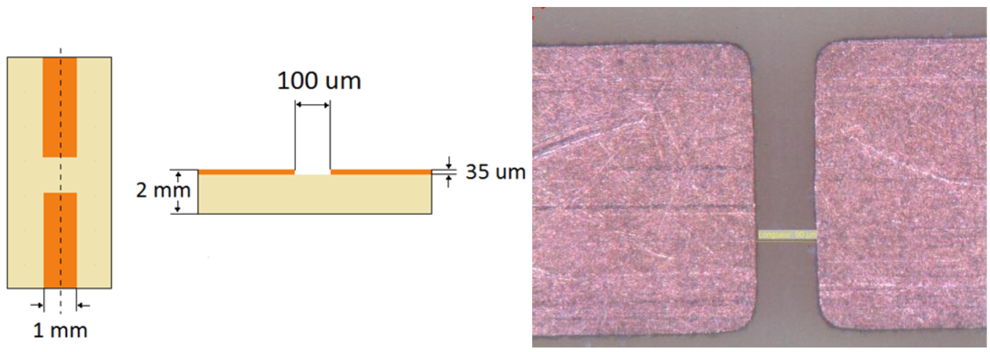

Pic. 3.14 Geometries of the lines used and a photo: the gap in this sample is 90 um.

The samples were obtained from the usual composite raw laminate sheet used for PCBs with the standard process of photo image transfer and copper etching with $FeCl_3$.

The FR4 used is a DE 156 halogen free substrate, provided by Isola; the resin matrix is based on a modified epoxy resin and a conventional glass fabric is used for reinforcement (63).

Actually these two strips are like unfolding on a plane the two electrodes of a THGEM element, reducing the dimensions involved, hence the capacitance.

Differently from the tips' case, here we can define precisely the inter gap distance thanks to the photo transfer image process; so we made several samples with different gap and width of the copper lines, hence different capacitors.

The resulting capacitances were still way too small to be measured by a multi-meter though; therefore we had to rely again on simulations to estimate them.

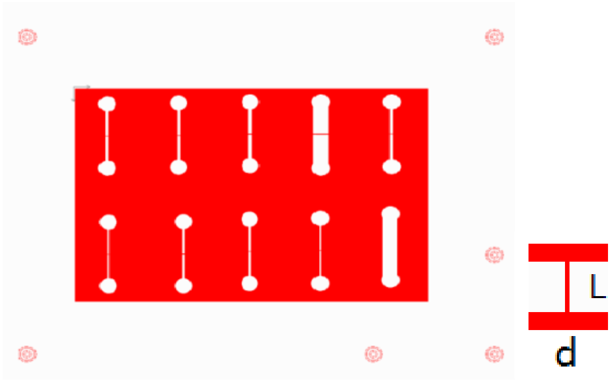

Pic. 3.15 Mask to transfer the copper lines' geometries on copper.

Below a table which shows the values of the capacitors obtained with the mask in pic.(3.15).

L(mm)	d(um)	Capacitance (F)	L(mm)	d(um)	Capacitance (F)
1	168	6.096E-13	0.5	108	6.096E-13
4	116	2.857E-13	1	148	2.857E-13
4	217	3.323E-13	0.5	200	2.952E-13
0.5	180	3.595E-13	1	200	2.945E-13
1	219	3.327E-13	0.5	100	3.144E-13

These simulated values were obtained with COMSOL; here after a shot of the module of the electrical field. To be noticed that the field is extremely dense on the corners of the structure.

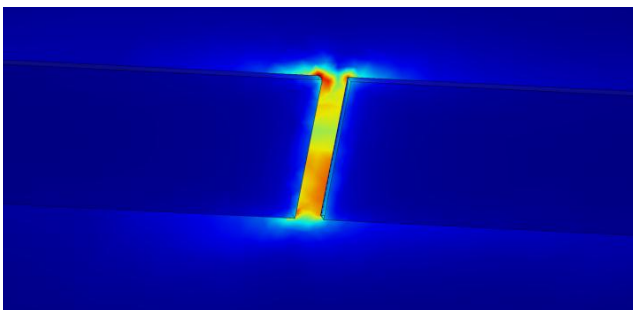

Pic. 3.16 Norm of the field simulated in COMSOL across the gap between two copper strips.

Therefore the test consisted again on powering the two strips with a serial resistor above the breakdown voltage of the gap in air at atmospheric pressure.

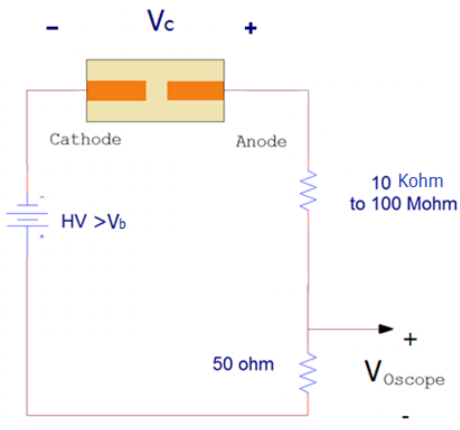

Pic. 3.17 The high voltage test focuses on these copper strips

We made the same tests with a 10 Kohm serial resistor in order to be sure that the system starts working in arch mode, that is the power supply will be not able to deliver the request of current once the discharge is ignited, and also with a 100 Mohm serial resistor in order to verify that the considerations came out from the previous experience with tips were still valid.

AIM OF THE TEST

The aim of the test is twofold:

- Understand the relationship between the estimated capacitance of the two lines and the current during a discharge;
- Figure out which is the effect of long exposure to repetitive discharges on copper and FR4.

Actually the test is still the same for both purposes, but for the first one we had to be sure that the discharges were not affecting the structure limiting their number; hence we were powering only for the time required to take data then switching the power off, raising the voltage and switching it on again, most of the time cleaning the inter-gap as well between one cycle and the next one.

On the other hand, for the second aim, we left the strips discharging for much more time, in some cases also for a day, to perform a kind of a stress test for copper on FR4.

EVOLUTION OVER TIME – SHORT TIME TEST

Unfortunately we didn‘t reach what we expected from it, that is we were not able to link the values of current to the frequencies of repetition of the pulses observed due to the fact that during the test many discharges were going on in different points of the edges and the resulting signals were overlapping.

The system has already became too complex to try any hypothesis on current and on the capacitance.

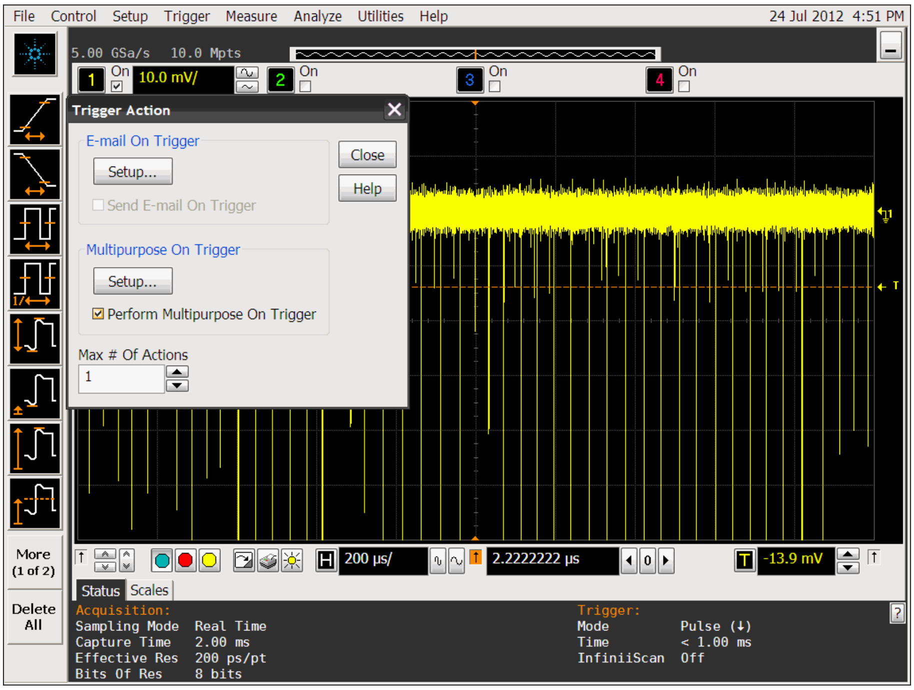

Pic. 3.18 Overlapping of many pulsed trains in the case of two copper strips discharging.

From pic. 3.18 is clear that many trains of pulses are overlapped, each relative to a point of the copper discharging.

Each point has its particular features: the roughness of the surface is not homogenous, hence even the breakdown voltage is not exactly the same everywhere, due to the unavoidable imperfections of the process.

The discharge itself creates locally imperfections in the point where it happens due to the high energy transfered, as explained extensively below.

After tens of seconds we have powered the test above the breakdown voltage, indeed the system was rapidly evolving, the discharges steadily concentrating in only one point of the edges of the copper lines.

But at that point the equivalent capacitance of the two copper strip-lines was not anymore playing a role, being the micro-tip in between predominant in defining the time constant of the train pulse and the shape of the discharge.

A few discharges have then created a system-in-a-system.

EVOLUTION OVER TIME – LONG-TIME EXPOSURE

After some minutes, often already within the first minute of operation, some changings are visible:

- the peaks reduces in amplitude
- the period of repetition decreases

This phenomenon goes on until no peaks are detectable anymore and a current in the order of several uA is drained from the power supply. That value of current is shown from the display included in the power supply and is within the range of current which the power supply itself can deliver, i.e. it is not working in protected mode.

Here some plots showing this behaviour.

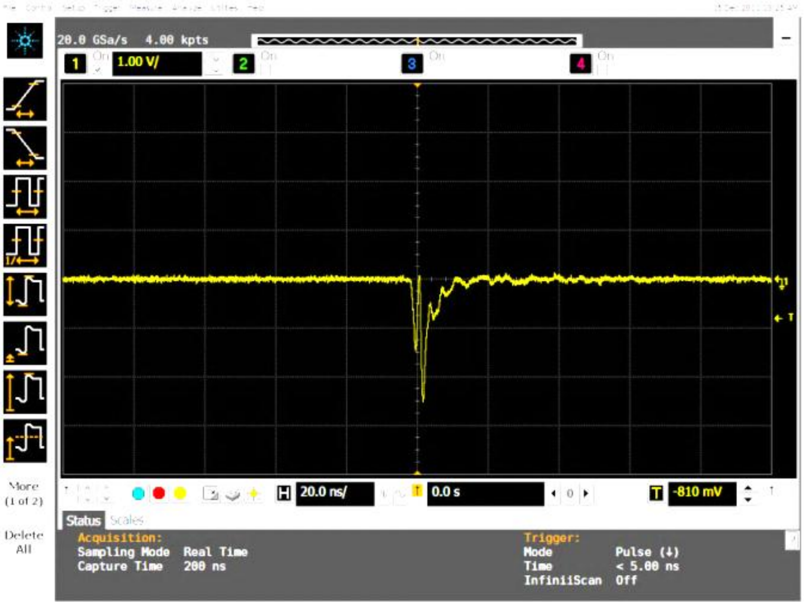

Pic. 3.19 Pulse (a)

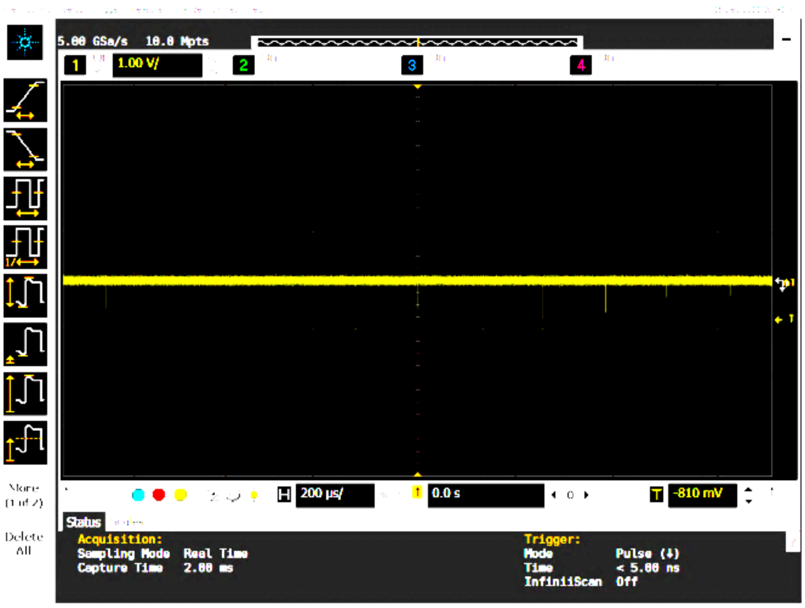

Pic. 3.20 Train (a), from which Pulse (a) was extracted

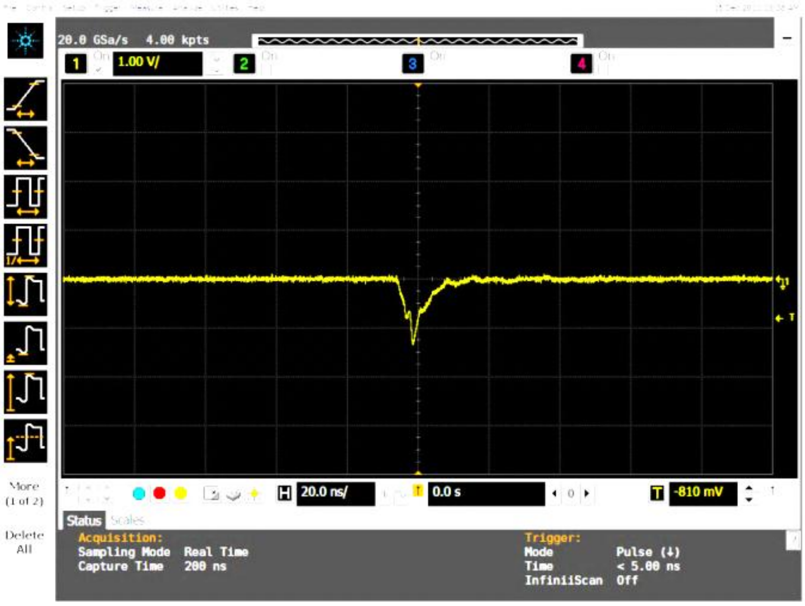

Pic. 3.21 Pulse (b), after some seconds of discharging.

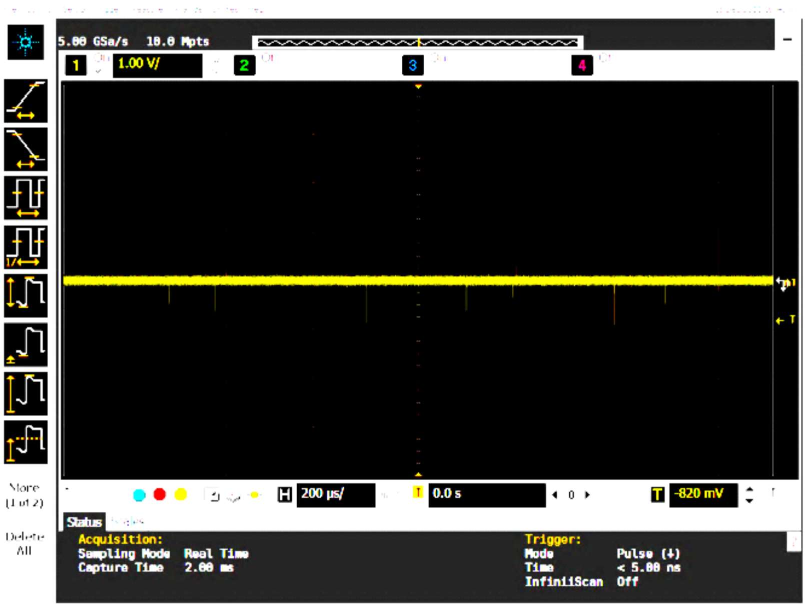

Pic. 3.22 Train (b), the period has reduced.

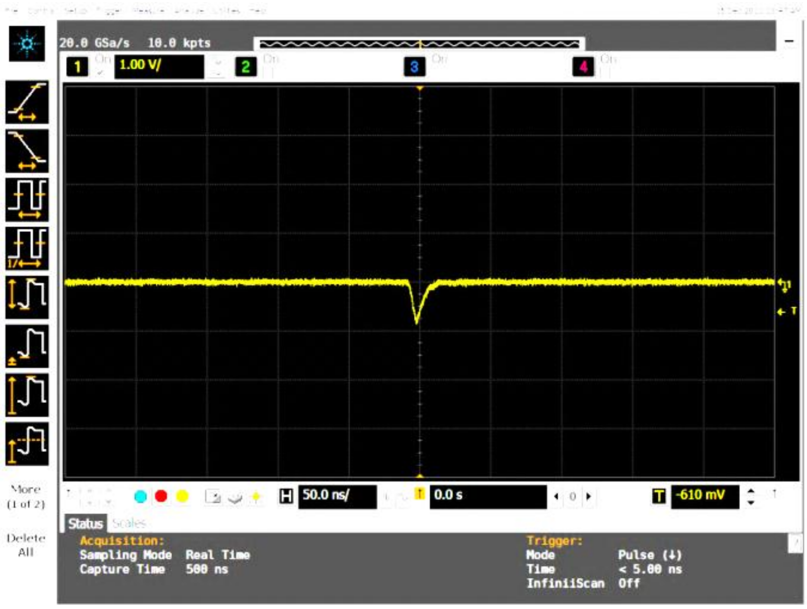

Pic. 3.23 Pulse (c), after some 10s of seconds. The shape has changed, rise time has increased and amplitude decreased.

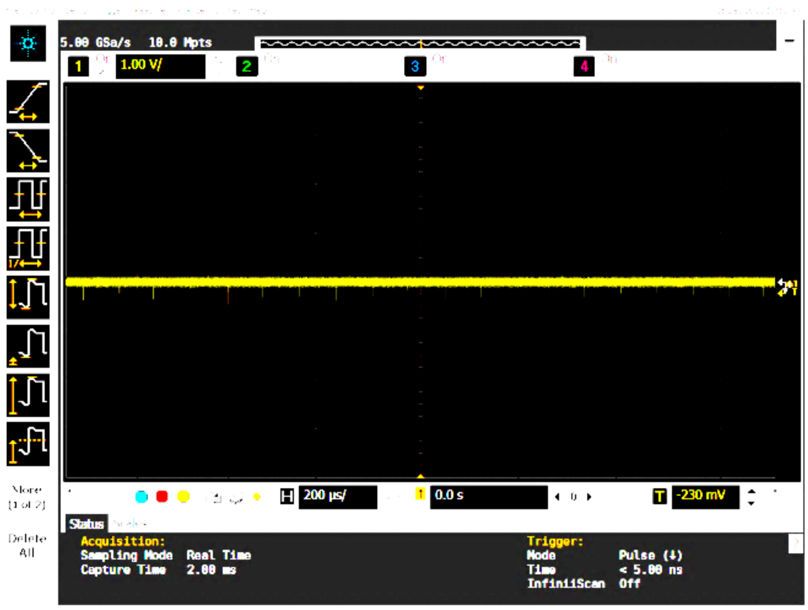

Pic. 3.24 Train C, further decreasing of the period of repetition of the train. In some other 10s of seconds the current will be DC.

To be noticed here that the amplitude of the peaks is changing, but moreover the rise time of the pulse is increasing, from a few ns (1-2 ns) up to ~10 ns.

The effect of degradation observed here in the case of simple copper strip-lines on a plane is totally in agreement with the experience made over time in the *MPE-EM fine pitch workshop* about THGEM detectors: in many cases in the past, experimental set-ups which were using THGEM as gain elements, had demonstrated an abnormal leakage current in the order of μA after some time of functioning which forced to re-open the detector and ask the workshop for a cleaning step of the THGEM element. In these cases a deposition of “brown” material was visible on some holes’ edges, most likely result of discharges (private talks with Rui De Oliveira).

3.6 Effects on materials

Afterwards we took a look again at the edges of the electrodes and we saw that a layer had grown around the area which the discharges were impacting, more evident on the anode but still visible even on cathode.

After a cleaning step the sample showed a clear lack of metal on the cathode side; this effect has been reported as a result of the Trichel, corona-like discharge by several authors (61).

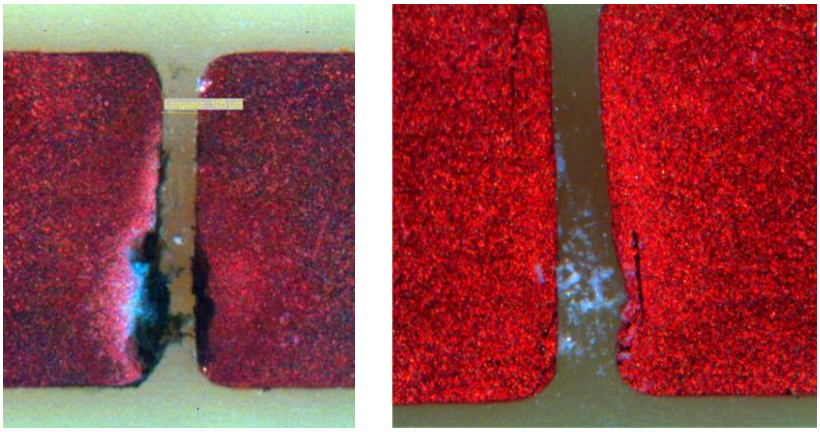

Pic. 3.25 Residual on the edges of the copper lines which undergo the test. After a cleaning step, the copper shows a lack of material, especially on the cathode (on the right picture)

Unfortunately the material deposed is not enough to perform any analysis on it; it might be the result of reactions between the components in the FR4 base material, copper and air. Actually is difficult even to hypothesize which could be the reaction going on during the discharge because FR4 substrates usually contain many different elements (64), being not possible to define the exact composition.

Though seems that this deposition is responsible of the effect of degradation observed.

Let’s consider again the scheme of the gas system we have already introduced in chapter 1; even here there is a capacitor discharging through gas hence that scheme could be useful even in this case in interpreting the observations.

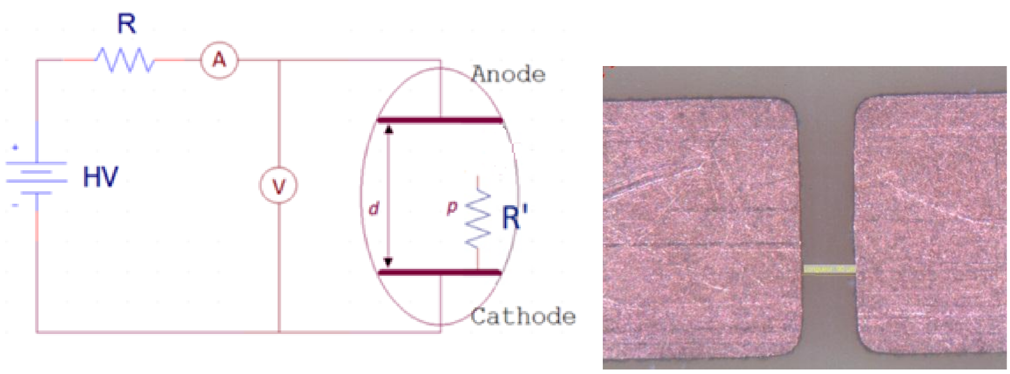

Pic. 3.26 A perspective of the system. The copper lines have an intrinsic capacitance and resistance; when they are perfectly clean the resistance R' is negligible.

To make the scheme a bit more realistic, let's add a resistor on one electrode or on a plate of our capacitor (actually there is one per each electrode, but is enough putting only one) which represents the equivalent distributed resistance of the plate.

At the beginning, when the test has not started yet (or with other words, the detector is brand new) this equivalent resistor has a low value, ideally zero, practically let's say less than 10 Ohms due to imperfections of the surfaces, including the small layer of oxides on them.

Having a look at what we obtained is not difficult to hypothesize that the material on both the electrodes changes the electrical properties of the system and add a new distributed resistance to the external one.

To be noted that we have checked there was not electrical contact between the electrodes, that is the material had not reached the other electrode.

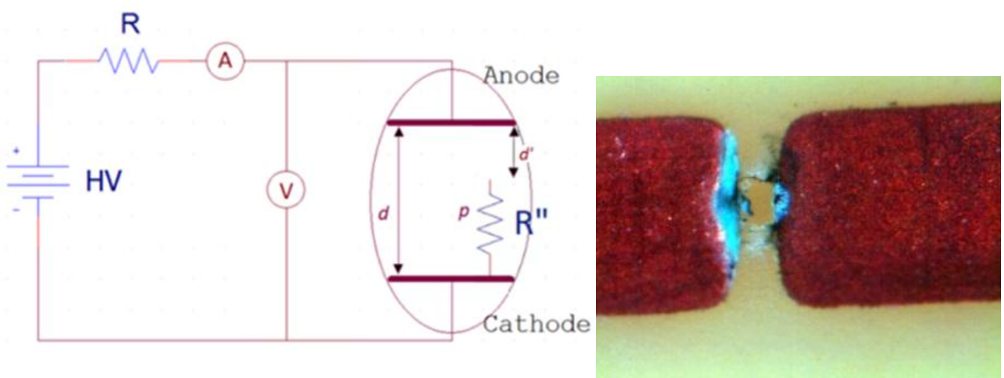

Pic. 3.27 As soon as some material is deposed on them, resistance and capacitance change.

After these considerations, we could add a new resistor at the scheme, whose value is supposed to be higher since likely the process of discharging has created oxides and an irregular surface.

Moreover the irregularities of the surfaces change locally the electrical behaviour of the structure mainly in two ways:

- that outgrowths put physically closer the conductive path between the electrodes, hence the breakdown voltage decreases.
- Having not anymore a flat surface means that the field enhances where the roughness is pronounced, due to the needle effect of these sharp and irregular points.

  The test anyway ends up in a stable mode, which means that the process of growth of resistive material stops some time.

3.7 *V-I* characteristic

If we look back to the *V-I* characteristic of the discharge through gas we might find an explanation: as soon as a resistor is growing the slope of the load line is changing, moving the working point as a result.

For example, we could imagine that when the equivalent resistance of the plates is low (they are “clean”) the crossing point is in the far arch region of the characteristic: the stable point would require currents up to 1 KA DC, values that the power supply cannot sustain.

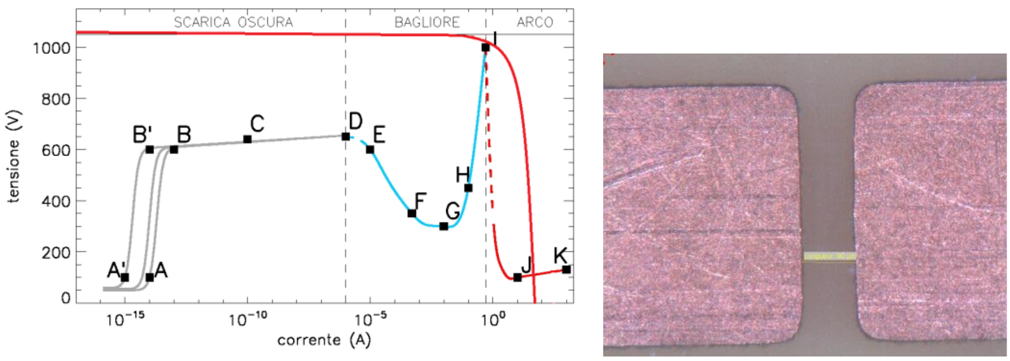

Pic. 3.28 Clean metal-electrodes discharge in arch region .(the load line in semi-log scale assume the shape of an exponential function)

The pulse created by the over breakdown voltage will discharge completely the equivalent capacitor but then the external circuit will be not able to deliver so much current to carry on a DC discharge.

The discharge is self-extinguishing, the highly conductive path created by the breakdown is then quenched by the lack of charges at the right potential; in other words the power supply is not strong enough to deliver charges and maintain the voltage during an arch.

On the other hand if we add to the external serial resistor the internal one created by the discharges, the load line is pushed back:

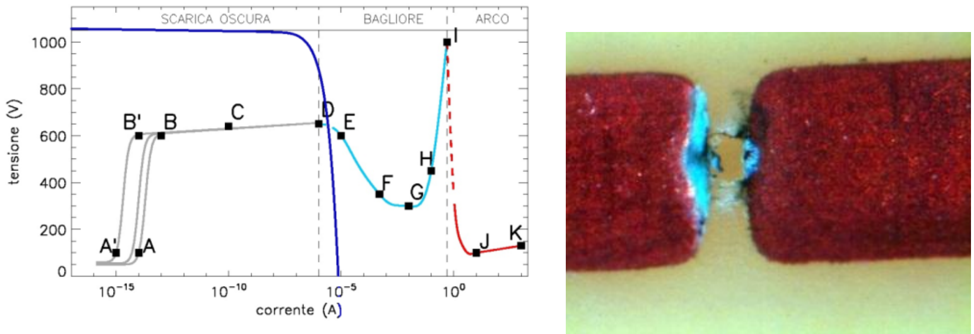

Pic. 3.29 Changing the resistor - here internally - affect the slope of the load line.

The system could reach a point at which the pulses trigger a DC discharge sustainable because the working point now requires a much lower value of current, available from the power supply.

We think that this stress-test simulates well the effect of discharges and explains correctly the degradation observed in THGEM detectors; in order to prove that we designed small samples of THGEM, made of copper on FR4.

3.8 Test on samples

Below the layout of the masks used; is a 4x4 holes, 600 um of diameter, 1 mm pitch. In red and green the contacts to power the two electrodes, here in white. The blue holes in the middle will be used by the software to generate the file read by the CNC drilling machine.

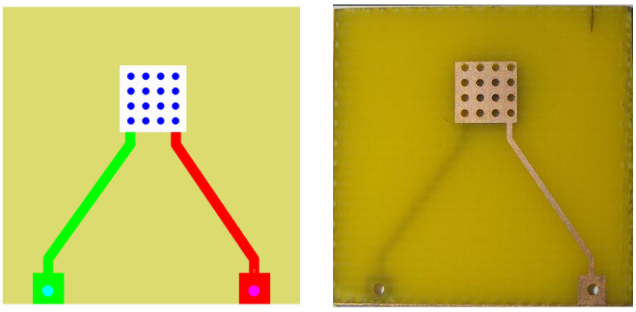

Pic. 3.30 A 4x4 holes THGEM: on the left the layout designed with the aid of the software UCAM. On the right the sample.

These masks have been used to make a stock of samples; below a photo of the two masks unfolded.

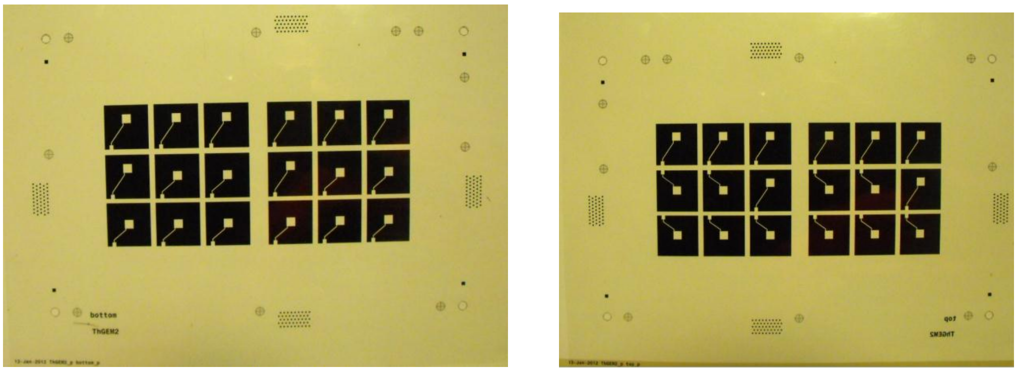

Pic. 3.31 Top mask and bottom mask.

The support is FR4, 1 mm thick; the copper on it instead is 35 um thick. The breakdown voltage was around 4.3 kV, according to the value given by the Paschen's curve in air; this is a sign of good quality of the process.

Then we performed on it the same HV test, letting it run for a long time, up to several hours (8-10 hours); after some tens of seconds though the behaviour was already changing, as explained before in the case of the lines.

We observed a decrease in the amplitude of the peaks but nothing can be said about the period of repetition, since many discharges on different holes were overlapping making impossible to distinguish which discharge on the oscilloscope was related to which hole.

By the way after some minutes the discharge centered on only one hole, staying there for the rest of the test.

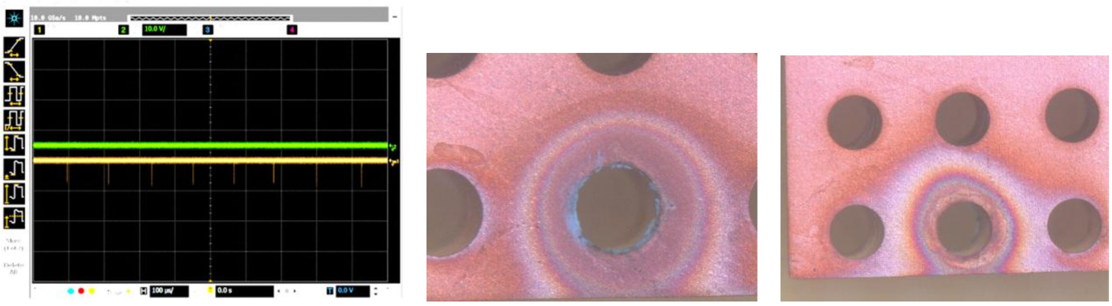

Pic. 3.32 Effects of repetitive discharges on one hole; on the anode - in the central photo - there is more consistent deposit.

A train of pulses with a certain defined period and amplitude was visible on the oscilloscope. The effect of this test on the sample is shown, in a shot of the hole were the discharge mainly stayed.

From picture (3.32) two effects are visible:

- The growth of a material on the edge of the hole
- The result of a not negligible heat transfer, observable in the changings in colour of the copper all around the hole.

The density of the deposed material suggested that it came from some components of the FR4 epoxy glass reinforced substrate while the colour (greenish) suggested that even the copper was contributing possibly going into a process of oxidation.

It was not possible to see any lack of material on the edges of the hole due to the difficult access to these areas, but we could say that the two electrodes are not equally involved in the process since most of the material in general was observed to grow on the anode side.

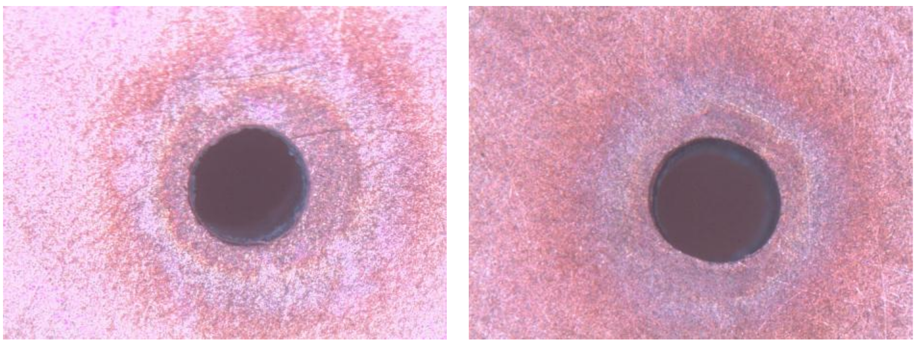

Pic. 3.33 On the left a view of the anode, on the right the cathode.

Below a picture of one hole with irregularities due to the drilling process; this roughness on the edge is responsible for the bad quality of the overall detector since it enhances locally the field, hence the breakdown voltage will be reduced and discharges will appear rather on these points. The THGEM element will not pass the quality HV test.

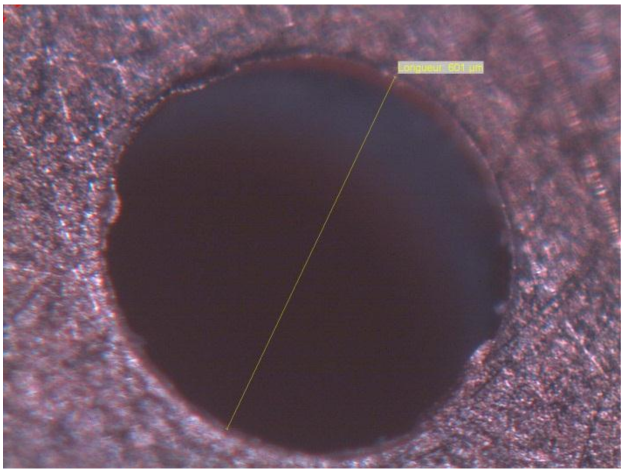

Pic. 3.34 Visible defects on the edge of one hole.

3.9 Conclusions

The test on these small samples of THGEM confirmed then what was seen about copper lines: the growth of some material, not better identified, during repetitive discharges influences strongly the behaviour of the system, lowering the breakdown voltage and in some cases pushing it in a region of the I-V characteristic at lower values of current. In this mode the power supply could be able to deliver the current without going into protection, hence any subsequent discharge could trigger a stable DC current mode.

In case of a real standard detector the problem is not different: if it falls in this mode after some events of discharges, triggered by imperfections, by high rate of particles or highly ionizing events, nothing will bring it back: the leakage current will increase drastically and at the same time the gain will decrease due to the fact that the field has decreased in some holes, hence the strength of attracting primary electrons within.

3.10 Prototypes

At first we thought that to avoid this aging effect due to discharges could have been enough creating free standing electrodes, that is removing the support of the insulator in the nearness of the edge of the holes. In this way we believed to cancel even the opportunity of any material that could be created during discharge to deposit on the electrodes, hence to change the slope of the load line adding a resistor.

Here a cross section of one hole; in orange the copper.

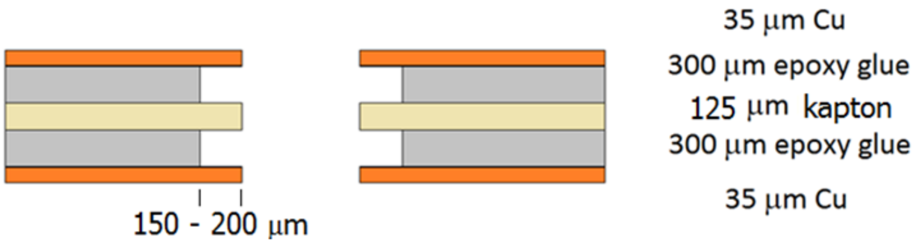

Pic. 3.35 The expected structure – cross section of one hole.

That structure is meant to avoid the deposition of material on the edges of the electrodes; referring to pic.(3.35), R''will not grow anywhere.

This kind of prototype, like all the others in this work, was built stacking different materials, which are available in foils in the workshop and widely used to obtain flexible circuits. After piling up the layers in a clean environment, the resulting stack has to be pressed in a specific machine with a controlled cycle of pressure and temperature, as showed in(3.36).

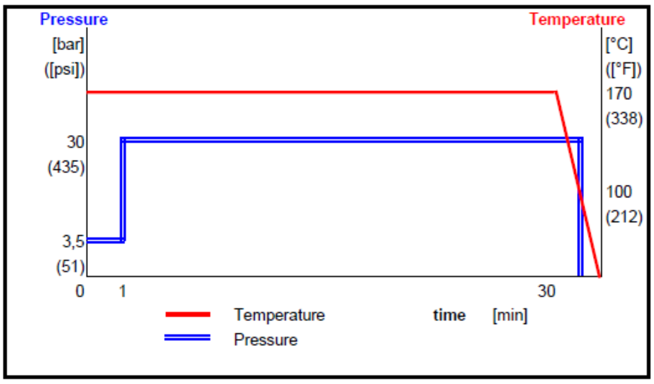

Pic. 3.36 Krempel glue cycle.

To obtain the structure in pic(3.35), we exploited the properties of H_2SO_4 as a selectively wet etchant; briefly, the steps, once the composite board is obtained, are:

- Drill it thanks to a CNC machine; the file containing the footprint is a .sm3 output file generated by the software UCAM, used to design the layout.
- After a deep chemical cleaning step (3 different baths), dip the sample in a 90% solution of H_2SO_4 with the needed cares.

- Rinse the sample with deionized water.
- Etch the copper using the masks (pic 3.31) in order to pattern the electrodes; the process is the standard photo image transfer using a negative type photoresist. The resolution achievable in a workshop like the one in building 102 at CERN is around 10 um.
- Clean again.
- Rinse with pressured water.
- Bake the sample at 180°C, 3h.

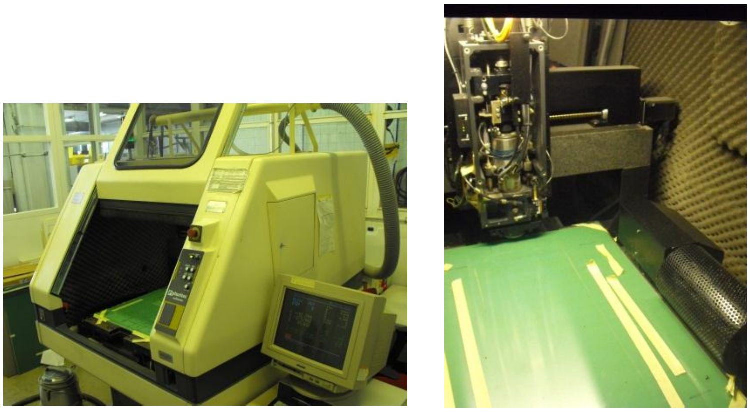

Pic. 3.37 CNC drilling machine.

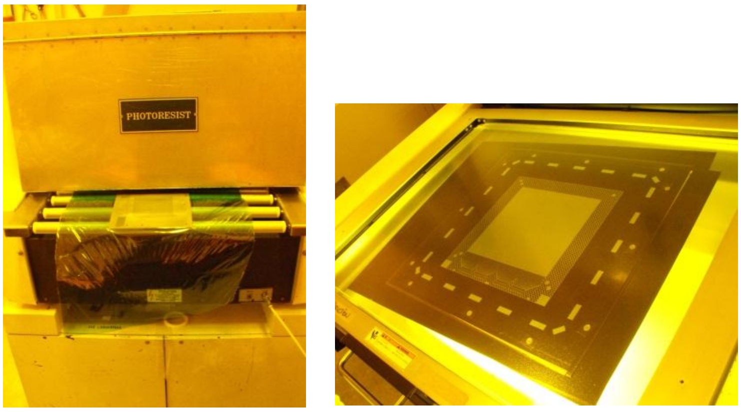

Pic. 3.38 Photoresist laminator and UV photo imprinter.

Pic. 3.39 Chemical baths for the cleaning process.

So the sample will be drilled mechanically and then chemically etched twice (removing the epoxy glue and the copper). To be noted that the first part of the process, the mechanical one, is limited by the time of drilling and the machine has to drill one hole per time, while any chemical etch is effective on all the sample at a time; this is what is called a *global process*.

Regarding this aspect, the technology used to build a THGEM detector, hence its cost, is mainly limited by the time usage of the CNC while for example that is not the case of a GEM detector, entirely build with a *global process*. This means that for large area detectors the costs will scale differently.

The depth of the under-etch obtained in $H_2SO_4$is obviously a function of the etching length while the homogeneity over the all sample is not trivial to obtain; we tried maintaining a good purity of the solution and waving the sample in it. We found that an under-etch in the order of 200 um was achievable within 15 minutes in H_2SO_4.

Here after a cross section of one hole before and after the wet etching in H_2SO_4.

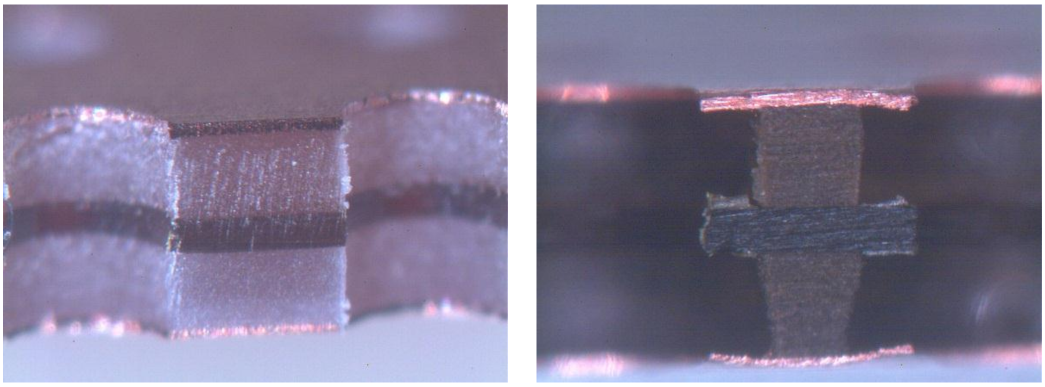

Pic. 3.40 Cross section of one hole. The under-etch is around 200 um.

TEST ON SMALL PROTOTYPES

The same test described previously was performed on these and the following samples; after the test nevertheless we saw that:

- There was a deposition of material anyway, more copious again on the anode (picture 3.41)
- Even the inner part of the free standing electrodes was interested by the discharge, not only the edges as expected.

So, even though we built a sample with free standing electrodes, this was not enough to avoid discharges to happen even in the inner part, moreover depositing materials coming out of the substrate.

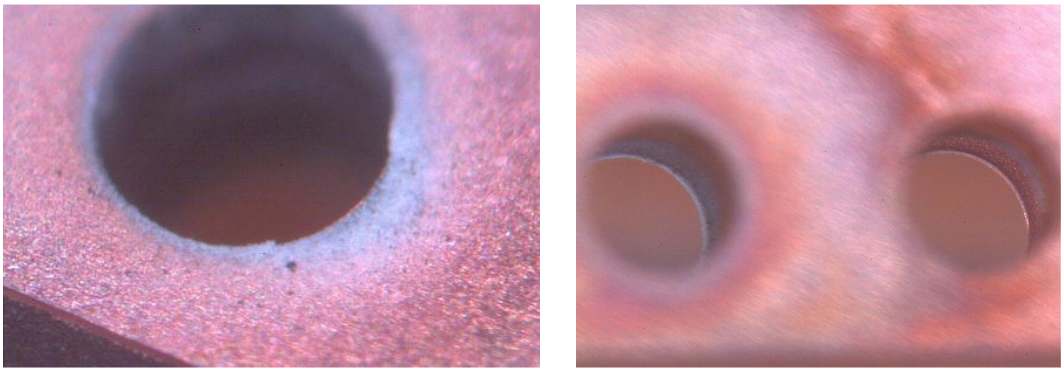

Pic. 3.41 Again deposit of material on the anode and even in the inner surface of the free standing electrode.

Indeed during the test we saw that the discharges were taking place at the same time in the hole and on its edge, each phenomenon characterized by a different colour of emitted light: the edges were discharging in a pulsed way, with a white light, instead there was a bluish light glowing inside, probably interesting the inner part of the electrodes, symptom of a different kind of discharge going on there.

The cavity created by the etch could as well acts like a reservoir for the ionized species of the atoms in the air; in this way a plasma difficult to remove could be created inside it.

The created structure could be, not on purpose, a hollow cathode which is a kind of lamp used in physics and chemistry as a spectral line source and as a frequency tuner for light sources (65).

Unfortunately we could not examine the inner side of the electrodes, but the appearance of the discharge even there could modify in a short time this surface and\or the surface of the edges, giving reason again of the rapid decrease observed in such samples.

Moreover, as already said, Trichel's pulses are accounted to modify the surface, eroding the metal of the cathode (66) as we observed clearly also in the case of the two copper strips. So wherever the discharge appears it modifies almost immediately the surface, changing the system.

The sample not-etched in H_2SO_4 behaved better under the same test, as we will explain later.

TESTING MATERIALS

Since this test started to show a relationship between endurance against discharge and materials, we thought was time to start testing different materials, looking for the right combination for the substrates and electrodes.

Trying to strengthen the electrodes we adopted mainly two solutions:

- Cover the copper with a Ni-Au plating process
- Use stainless steel (INOX 17/8)

These trials were driven by the idea of finding some other metals with a higher melting point, feeling that the repetitive discharges where reaching locally such a high temperature to melt the copper.

Plating with Ni-Au the copper didn't extend the time of correct functioning much: the breakdown voltage decreased as fast as in the case of pure copper's electrodes during the test.

Using INOX and especially drilling it result in a not perfect quality of the holes due to its hardness, hence a lower breakdown voltage, driven by imperfections.

Concerning the insulator, we have used basically two different epoxy glue (Krempel and Nikaflex), both in foils to be piled up, interleaved with a Kapton foil in case we wanted a structure that could have been selectively etched.

Nikaflex® SAFV is an epoxy-based sheet adhesive 40 um thick often used to bond layers in multi-layer and rigid flex circuits. AKAFLEX® CDF (adhesive film) by Krempel is a bonding epoxy adhesive film, 25 um thick.

The two glues, although having the same use, showed different response to H_2SO_4 and precisely was found that Nikaflex is not etched in H_2SO_4 while Akaflex is.

$Kapton$ is a polyimide film developed by DuPont which can remain stable in a wide range of temperatures. These products are all designed for manufacturing flexible printed circuits and are characterized by many outstanding properties (thermal, electrical, mechanical).

At the end we built and tested 9 different structures; out all of them we would compare the results of the test on 5.

After some pictures of samples made with INOX, not etched and etched in H_2SO_4 and other tries with different epoxy glues as substrates.

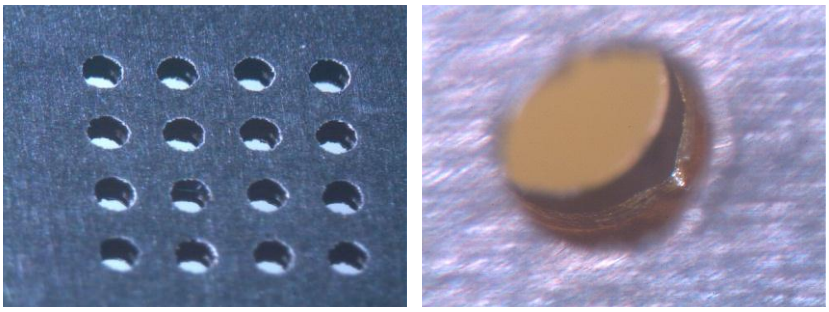

Pic. 3.42 Sample with electrodes in INOX and one hole where the damage induced by the discharges in the inner kapton layer is visible.

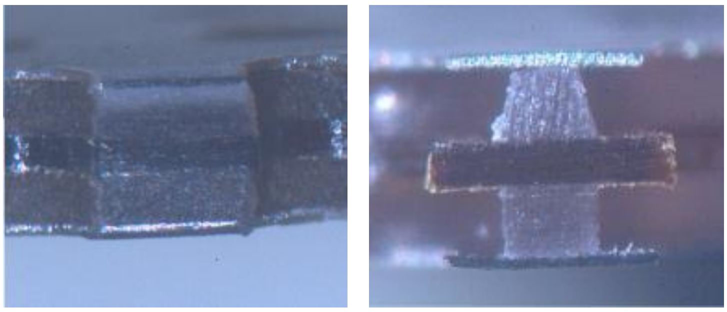

Pic. 3.43Cross section of a sample with inox before and after the etch.

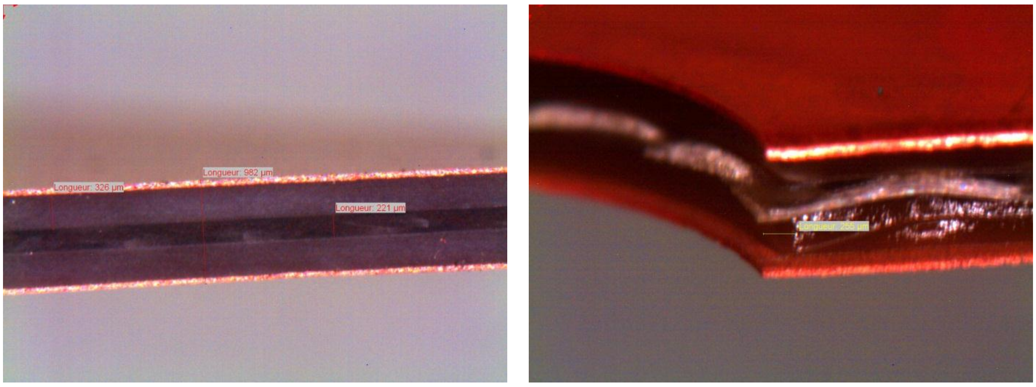

Pic. 3.44 First attempt with a glass-fiber layer in between; after the etch (on the right) even the glass fibers were damaged, providing not a perfect insulation.

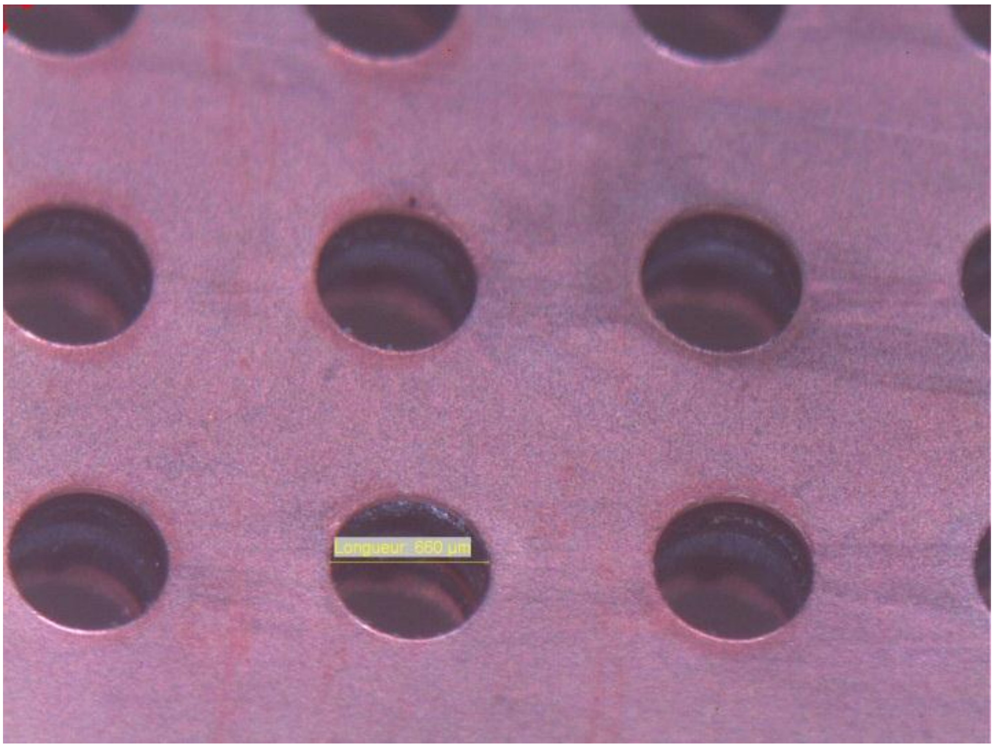

Pic. 3.45A multi-layer sample; diameter of the holes is 660 um.

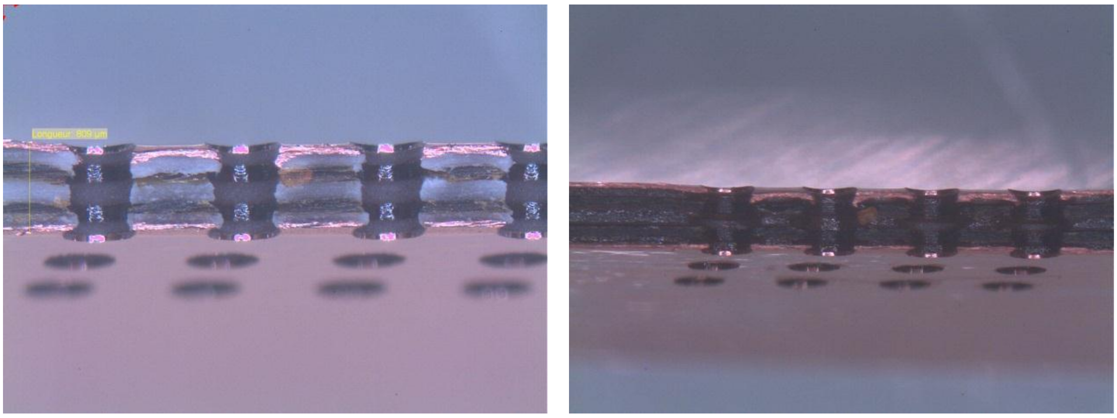

Pic. 3.46 Section of the sample in 3.45; two layers of kapton interleaved with glue and copper as electrodes material. Before(left) and after (right) the etch.

These samples were chosen in accordance with a criterion of quality and even material budget, so we excluded from this analysis samples which:

- Not passed the HV test due to persistent imperfections (the sample in pic 3.46 is difficult to clean properly after the etching in H_2SO_4)
- Behaved bad during the test (e.g. the sample with both electrodes made of resistive kapton showed an unacceptable dead time after each discharge)

We include though the sample with electrodes in stainless steel because we believe that once the whole process has been calibrated on it (basically drilling process and $FeCl_3$etching), INOX could be a good metal as electrodes in gain stages for gaseous detector due to its hardness, poorly interactivity and higher melting point ($1400 - 1500\ °C$, depending on the percentage of the elements in it) compared to copper ($1084\ °C$).

RESULTS ON SOME PROTOTYPES

As a summary, we choose 5 samples 4x4 holes to be tested:

[1] Copper on FR4 material (standard THGEM materials) 

[2] Copper on krempel glue not etched 

[3] Copper on krempel glue etched 

[4] INOX on krempel not etched 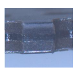

[5] INOX on krempel etched

This test was a bit different compared to the one performed on copper strips: in general in a THGEM detector we are interested in the breakdown voltage and in monitoring it as a function of the damages induced by discharges. So here we powered each sample with a voltage above the breakdown voltage; checking that this was well in accordance with the theoretical one given by Paschen's curve in air, the test could go on, letting discharge continuously the samples. A train of pulses will be established.

After a certain period of time we switched the power supply off and we checked again the breakdown voltage, taken as the voltage at which any kind of discharge started to be visible (as a signal on the oscilloscope or even as a tiny flash light) and\or audible.

Once the period of the pulses was estimated, we knew approximately how many discharges happened during a fixed period of time; meanwhile we were taking note of the value of the breakdown voltage.

Here below a plot of the data acquired.

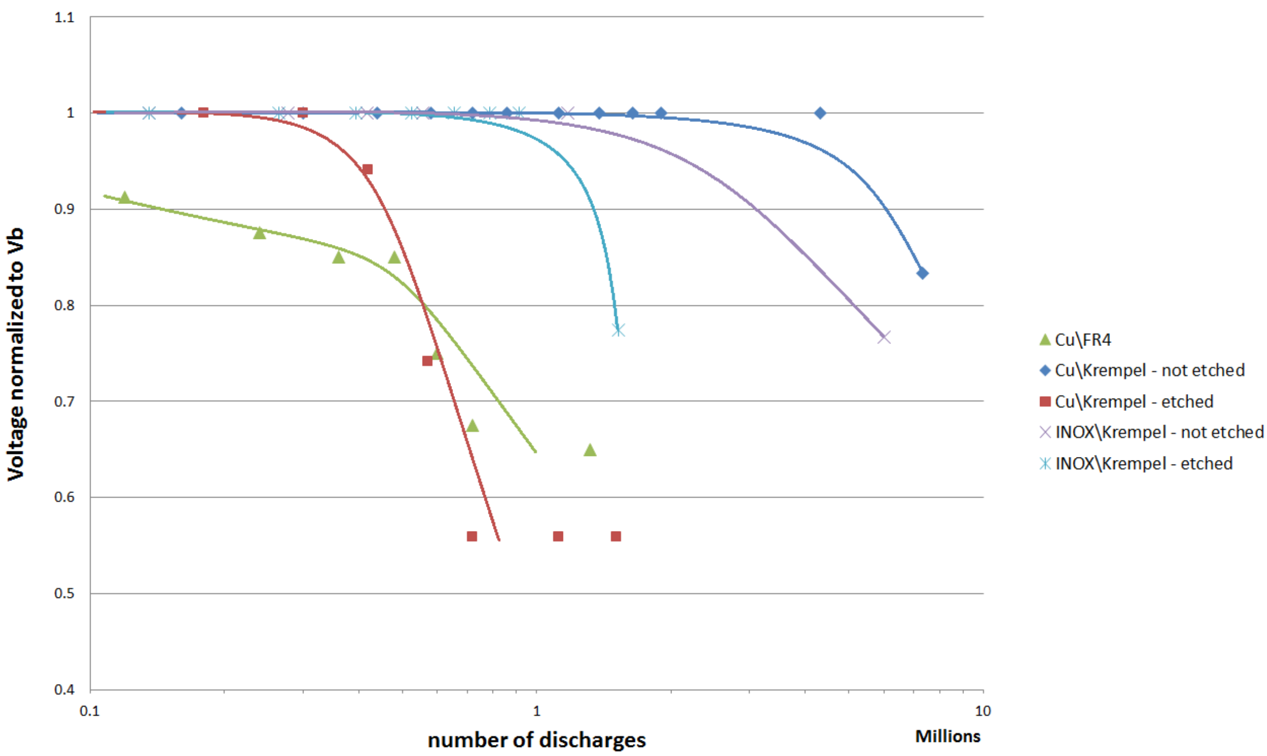

Pic. 3.47 Results of the tests on samples.

A qualitative trend has been drawn for each set of data, in order to display the performances of the samples and compare them.

If we state that $0.9V_b$is a likely threshold below which the degradation of the breakdown voltage is not acceptable any more (because e.g. the leakage current is already too high), then we can estimate how many discharges each sample has handle before reaching that grade of damage.

We see immediately for example that the sample made of copper on FR4 has a fast degradation and its breakdown voltage has already decreased at a level close to $0.9V_b$ just after $\sim 100K$discharges, when the other samples are still good.

The best samples seemed to be the ones with the Krempel epoxy glue as insulator and copper as electrodes, while any samples etched with H_2SO_4 resulted worse than its corresponding not etched.

Now we imagined to put these small sample into a ‘real’ environment that is an environment where a rate of around $200\ \frac{discharges}{s\times m^2}$is induced on the gain element of a gaseous detector by highly ionizing particles or a high rate of particles; this value might have fluctuations due to geometry, gas, aging effects.. Hence has to be taken as a reference point and not necessary as an absolutely figure, even though plausible.

By the way it makes possible a kind of comparison between these samples in terms of lifetime: considering that our samples have an area of $25\ mm^2$, these samples in a highly ionizing environment or high particles’ flux would have had to deal with $5 \times 10^{-3}\ \frac{discharges}{s}$. Using the values obtained experimentally for the numbers of discharges before reaching $0.9V_b$, we can estimate the lifetime of each prototype in such environment.

	Discharges @ $0.9 \times Vb$	**Lifetime (years)**
FR4	$160k$	1.01
Cu + krempel etched	$452k$	2.825
Cu + krempel not etched	$6M$	37.5
INOX + krempel not etched	$3.2M$	20
INOX + krempel etched	$1.2M$	7.5

From this simple comparison, the sample made of copper as electrodes' metal and krempel glue as epoxy base material, interleaved with one foil of kapton, could undergo 37.5 times more discharges than the standard copper on FR4 epoxy reinforced glass fibre, at the moment used in any THGEM detector.

3.11 Test on a $10cm\ X\ 10cm$ THGEM

Then, in order to have a more realistic reference, we performed the same test on a standard $10\ cm\ X\ 10\ cm$ THGEM element, powering it above the breakdown voltage without serial resistor.

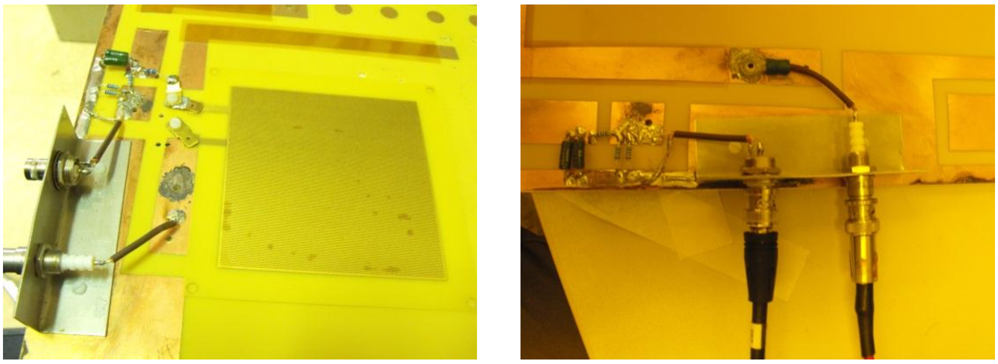

Pic. 3.48 Test board built for large size THGEM elements, like the one shown below; on the right the connectors to power and to pick up the signal.

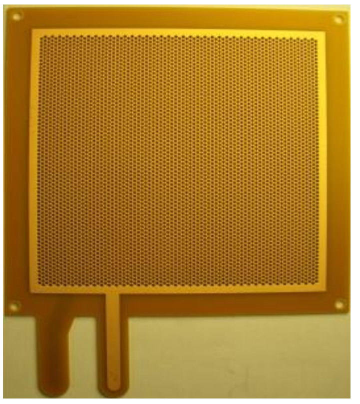

Pic. 3.49A standard dimensions THGEM

A rate of spark of $\sim 2\frac{discharges}{s}$ was observed and the breakdown voltage decreases at $0.9 \times Vb$ within 2 hours, hence it withstood $\sim 14.4\ K\ discharges$; then the small prototype made of copper with Krempel glue as an insulator (sample 2) has handled approximately 400 times more discharges than the standard. Instead the small sample made of copper on FR4 (sample 1) handled roughly 10 times more discharges.

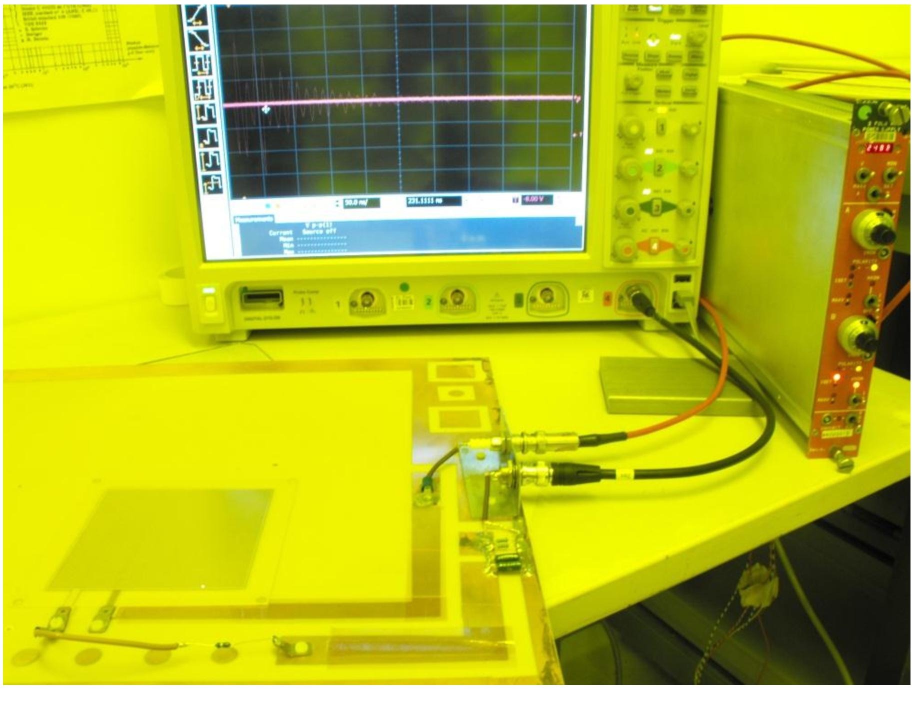

Pic. 3.50 Overall test-bench

The picture is a shot of the overall bench; on the left the sample under test, safely stuck on a bigger board, where some tracks were patterned to power the sample and ground it. On the right edge of this test-board the connectors, one powering the sample (SHV connector in red) and the other to pick up the signal (BNC connector in black, 2 ns of delay). On the right the CAEN power supply, on the bottom the oscilloscope. A trace is visible on the screen, result of a discharge on the sample. Note the oscillation due to the long path between the sample and the point where the signal is picked up which results in a not negligible parasitic inductance. A faint discharge is even visible on the sample itself.

3.12 Conclusions

These results suggests that in order to improve the endurance of a THGEM element against discharges different combinations of material have to be tested, looking for the ones that behave better and do not release compounds during discharges. So far, the best alternative for the insulator to the standard FR4 epoxy glue reinforced fiber glass board – amongst the material available in bldg. 102- seems to be the epoxy glue made by Krempel. Copper still remaining the most common, hence cheapest, metal for electrodes, an intense research on materials could reveal some other conductive elements which may improve more the endurance of the overall detector.

Moreover the last comparison between the standard $10\ cm\ X\ 10\ cm$ and the small sample suggests strongly that already reducing the area of the electrodes results in an appreciable improvement, due to the reduced capacitance.

This drives to a new THGEM element in terms of geometry of the electrodes; introducing some sectors in the design of the electrodes, maintaining though the same overall area, the capacitance of each sector is well smaller than the global. As a consequence, if a discharge occurs it will discharge only one sector and the resulting current will be lower, hence less harmful.

In the next chapter the steps that leaded to a $10\ cm\ X\ 10\ cm$ THGEM element with electrode divided into sectors will be described.

Chapter 4

4.1 Model of a THGEM

Consider now a THGEM element, with the power supply unit connected through a limiting resistor; this is simply the powering scheme adopted generally in any THGEM and GEM detector and is shown in picture 4.1.

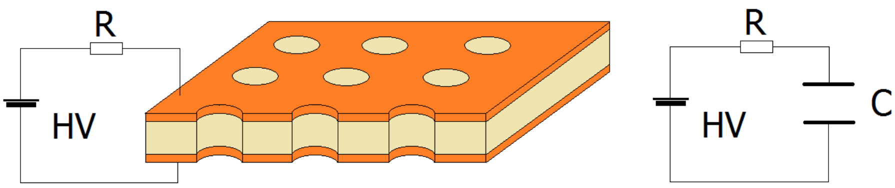

Pic. 4.1 A schematic view of a THGEM; in first approximation we could see it as a capacitor.

Usually the high voltage applied to the electrodes is obtained thanks to a resistive divider from the same low noise, high current power supply unit which provide the voltage for all the THGEM

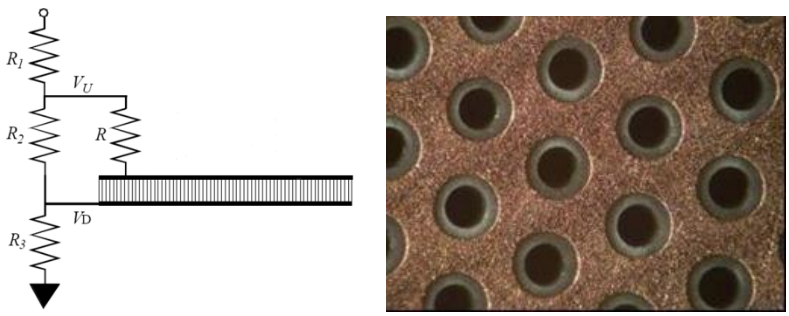

Pic. 4.2 Powering scheme of a THGEM, like the one on the right.

During normal working lifetime, the electrodes of the THGEM are kept at a well separated potential, ensuring the high field within the holes required for an efficient focusing of the electrons and an adequate avalanche. So that high voltage across the plates is guaranteed by the presence of charges on the electrodes themselves, that is electrons on the cathode and a mirrored displacement of electrons on the anode side.

If we abstract from the real structure, we could then reduce our THGEM to a big capacitor; in first approximation we could see it as a parallel plate capacitor with a certain capacitance, given by the charges accumulated on it and the applied voltage, and the gas as the insulator.

The spacing between the electrodes of such a capacitor is the thickness of the THGEM insulator and the gas inside has the same pressure as the gas filling the THGEM chamber. Just as a reminder, the Paschen's curves, already presented in this work, show the breakdown voltage as a function of the pressure by the distance of the electrodes, hence we could consider the gas as an insulator whose electrical properties change depending on its conditions.

This is only a partial and reductive view of the system, the main difference between a real THGEM and this model being the shape of the field, but we will be not speculating on any field related phenomena, using though this scheme to accomplish considerations that drove us in finding a possible relationship between the equivalent value of the capacitance and the properties of the structure during and after a discharge.

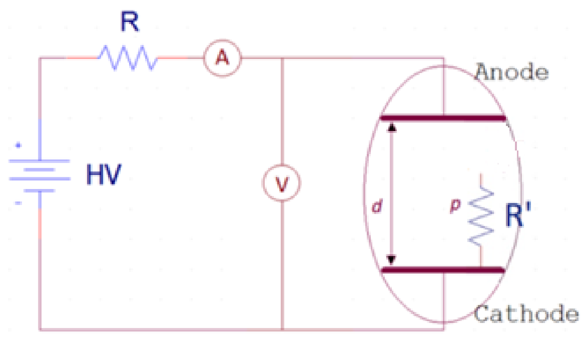

Pic. 4.3 Gas system.

The figure shows even a serial ampere-meter and a voltmeter across the gas system, which permit plotting the V-I characteristic, sweeping the voltage over several decades.

Keeping in mind this interpretation, we can analyze the discharge through the gas in terms of the discharge of a capacitor and its subsequent refill through the serial resistor, that is as a whole a simple RC circuit.

The discharge is a breakdown phenomenon and corresponds to the creation of a highly conducting channel in the gas. Imagine that we raise the voltage provided by the power supply: when the breakdown voltage of the gas is reached, the charges collected on the metallic electrodes then have a path to a lower potential and will tend to nullify their potential following the field through this channel. In other words, the capacitor is completely discharged, all the charges accumulated on its plates being removed.

The following step is affected by the properties of the power supply unit because once the capacitor has been emptied, charges start to be drained from the voltage generator; if it is able to deliver this request of charges and at the same time to maintain the field required by the discharge, the discharge will continue as a DC phenomenon. On the other hand, if one or both of the conditions (current available, field across the electrodes) is missing the discharge will be quenched, the discharge resulting in a pulsed fast signal.

In a standard GEM and THGEM detector serial resistors in the order of tens of MOhm are put in order to limit the current but is not clear or commonly accepted that the peak current of a discharge, which may be destructive or at least damage the electrodes, is given by the charges previously accumulated on the electrodes and only in a second moment the current from the power supply plays a role.

Then the current available from the power supply is set to a value (usually tens of nA) considered not harmful for the structure, in order to limit the DC current in case of discharge, being instead the value of the equivalent capacitance the critical parameter to firstly take care about.

4.2 Current during a discharge in a THGEM element

The value of the equivalent capacitance of a standard $10x10\ cm^2$THGEM element is roughly 1 nF, depending on the thickness of the insulator and the insulator itself.

Pic. 4.4 Measuring the capacitance of a 10 cm x 10 cm, 0.4 mm thick.

In the figure, a $10x10\ cm^2$with a 400 um thick FR4 insulator was measured (parasitic capacitance of the probes is in the order of 0.1 nF). Performing simulations we saw the dependence of the capacitance even on the geometries of disposition of the holes.

Then if we consider 1-2 ns as a plausible value for the rise time of the discharge we can estimate the current of such a capacitor when it discharges, or when the voltage exceeds the breakdown value.

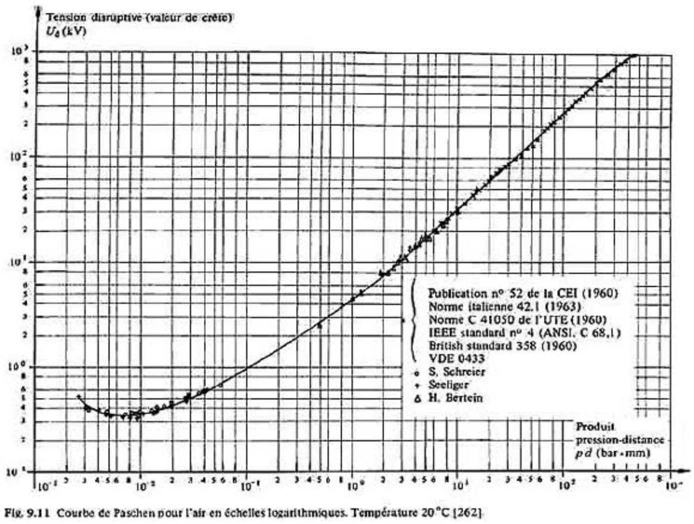

Pic. 4.5 Paschen's curve in air: the chart used as a reference during HV test.

The observed breakdown voltage in air of that sample is 2.1kV, pretty close to the one predicted by Pashen's curve; then

$$Q = C \cdot V_b \cong 2.1\ \mu C$$

When this capacitor discharges, we can estimate the peak value of the resulting current as:

$$I_{peak} = \frac{\Delta Q}{\tau_r} \cong 1kA$$

We believe that these values of peak current are enough to generate immediately local micro damages, modifying the electrodes, hence the gas system.

The endurance of the detector depends at first on the endurance of the material against pulsed transfer of heat and has been already said and proven with stress tests (chapter 3) that there might be better materials to build THGEM elements in comparison with FR4 and copper currently used.

Moreover from what we learnt from the tests, the material growing up during repetitive discharges acts like a resistor, increasing the rise time and shifting the working point towards to lower values of current which might be sustainable by the power supply.

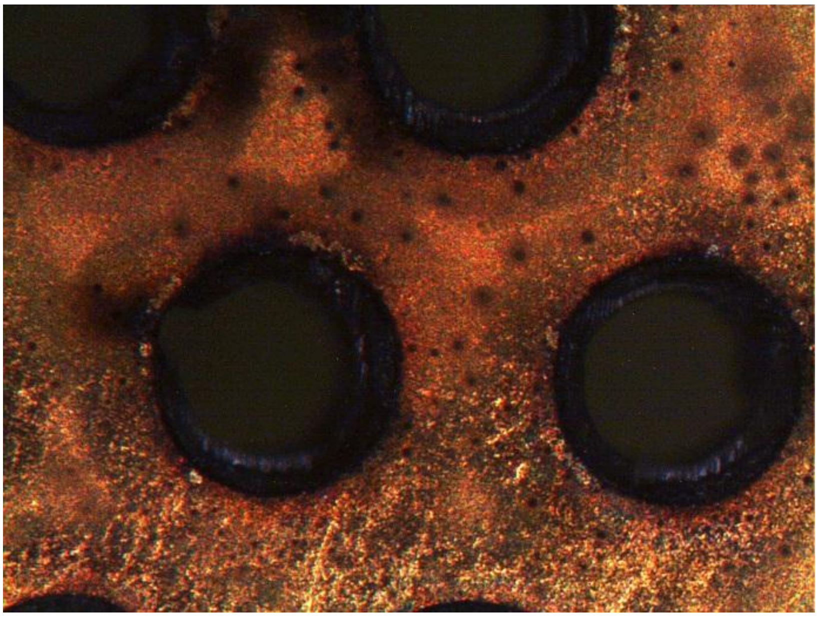

Pic. 4.6 Effect of the HV test with the test bench described in 3.10.

In THGEM with metallic electrodes, the initial resistance of the plates is negligible and the motion of charges during the first discharges is limited only by the gas, giving reason of the rise time observed.

These highly energetic discharges then modify the electrodes; as we largely said, the equivalent effect of these damages is a resistor which is not external but appears inside the gas system, in between the two electrodes. Since then the discharge will imping preferentially on these damaged points, where the field is enhanced by the needle effect and the breakdown voltage is lower due to the reduced inter-electrodes distance.

4.3 Towards a THGEM with sectors

From the experience gained with the test described in chapter 3 we can say that not only looking for new materials could increase the life time, but also dividing the electrodes into sectors, reducing consequently the capacitance of the overall structure, hand in hand with reducing the available charges for a discharge.

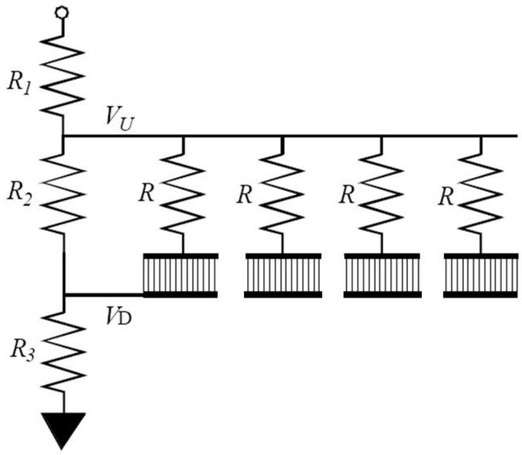

Pic. 4.7 Scheme of the power connection in THGEM with segmented electrodes; each segment has a lower capacitance.

Obviously this would make the technological process a bit more complicated, because every sector has to be connected to the PSU through a serial limiting resistor which cannot be a discrete component, due to the large number of resistors we should solder per THGEM element. The solution is using a resistive paste which obliges in adding a new mask in the process.

We made a prototype of a THGEM of copper and krempel glue in foils piled up as base material 600 um thick with electrode divided in sectors.

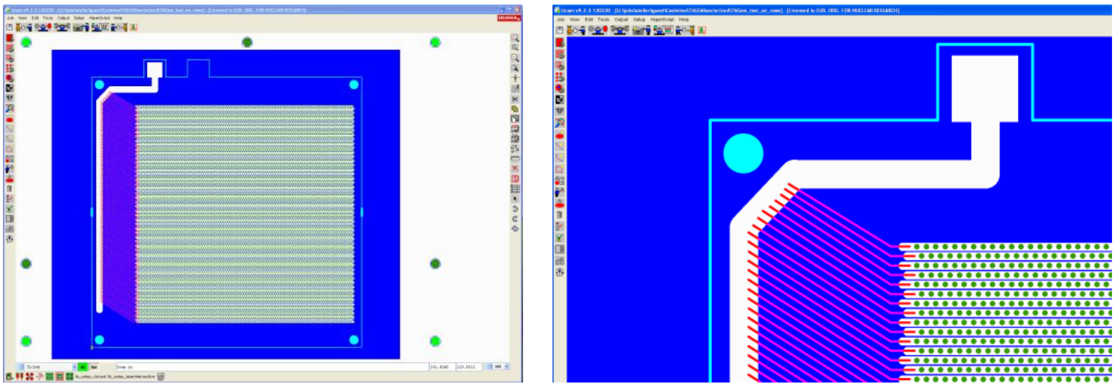

Pic. 4.8 Designing the layout (UCAM) and a detail of the mask which will define the spread resistors(red strips in the picture).

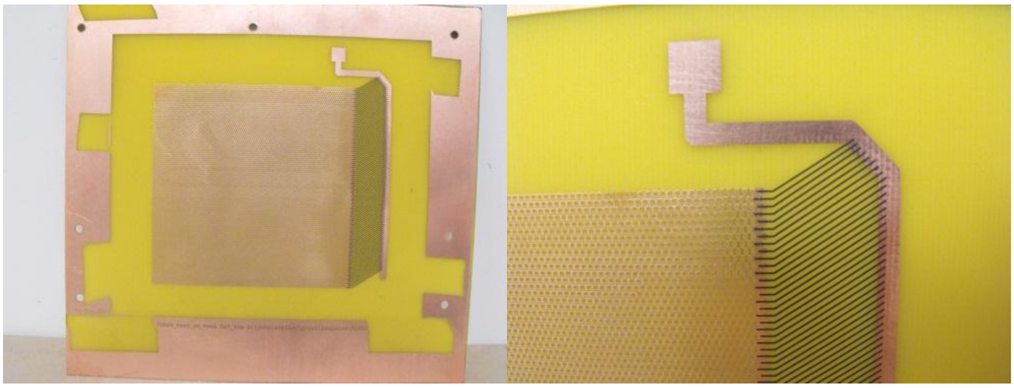

Pic. 4.9 A sample and on the right, enlargement of the resistive strips, one per sector.

This prototype goes into the direction of finding a right value of both R, the resistance of the strip connecting the power supply to the sector (the limiting resistor) and C, the equivalent capacitance of a single sector. We believe that fine-tuning this time constant might allow to define the time response of the detector to a discharge phenomenon. This aspect was already partially figured out in the TE-MPE-EM fine pitch workshop by the former activity of Burnens but introducing the tool of the V-I curve of the gas made it clearer.

4.4 Model of a MICROMEGAS

The salient feature of the MICROMEGAS technique is that is accounted to be spark resistant thanks to the resistive layer;

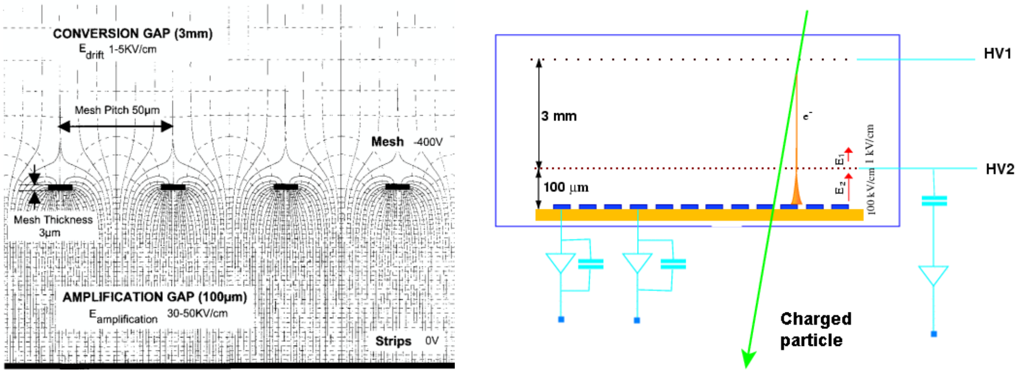

Pic. 4.10 MICROMEGAS: configuration of the field and scheme of the detector, with the amplifiers connected to the anode pads.

The method used to render the MICROMEGAS chambers spark resistant while maintaining their ability to measure with excellent precision minimum-ionizing particles in high-rate environments is extensively described in (67). Here after we will present a schematic section of the element and an equivalent electrical view.

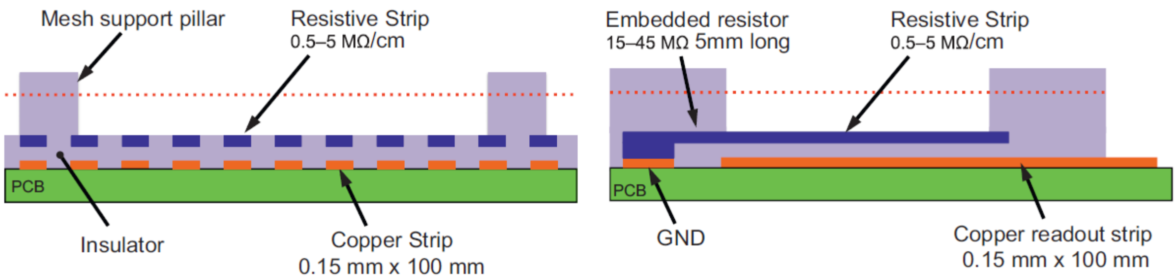

Pic. 4.11 Cross section of a MICROMEGAS with resistive strips.

Before introducing the resistive layer, the most harmful discharges happened between the mesh kept at 600 V and the copper strip, directly connected to the read out amplifier; being the input diodes, present on the input pins of the amplifiers, not always enough to protect the stage against the highly energetic discharges, often even the readout was damaged.

This new technology which makes the most of a further UV transfer image process step allowed to build strong and reliable MICROMEGAS detector, even in large area (panels around 1m x 2m expected soon).

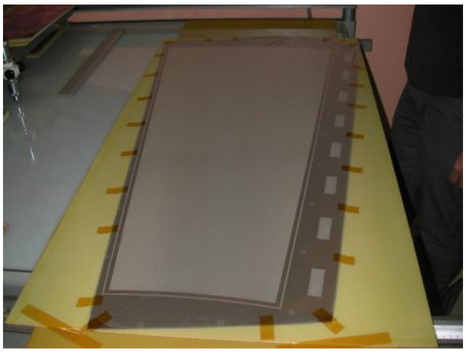

Pic. 4.12 A large MICROMEGAS panel.

The secret of such endurance hence has to rely on this resistive layer protecting the metallic pads and a good understanding and possibility of reproduce this feature even on other detectors could come from an appropriate model of the MICROMEGAS' structure. Many at CERN and in other research centers are leading studies towards this direction (68).

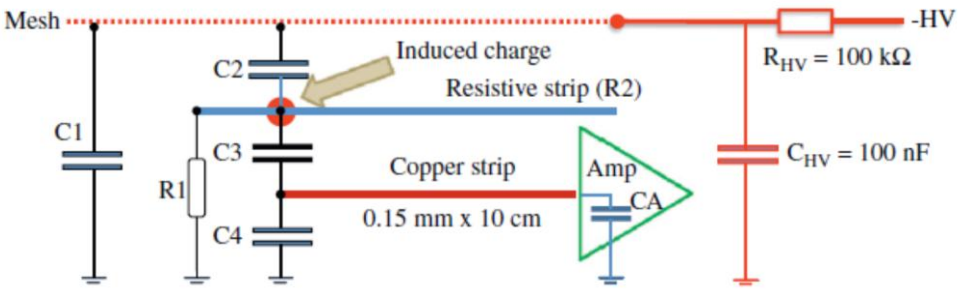

Pic. 4.13 Electrical equivalent scheme(67).

In pic 4.13 is highlighted the impact point of charges which might come from an avalanche developed in the amplification gap; this charge is spread on the resistive strip and then drained towards ground. The signal is induced through a distributed capacitance due to the resistive layer kept isolated from the copper strip thanks to an insulating gap and picked up by the underlying copper strip.

In case of a discharge the process of signal's generation is roughly the same, only the number of charges available is way more. Below a discharge picked up directly from an anode pad of a resistive MICROMEGAS, terminated on a 50 ohm resistor without any electronics plugged.

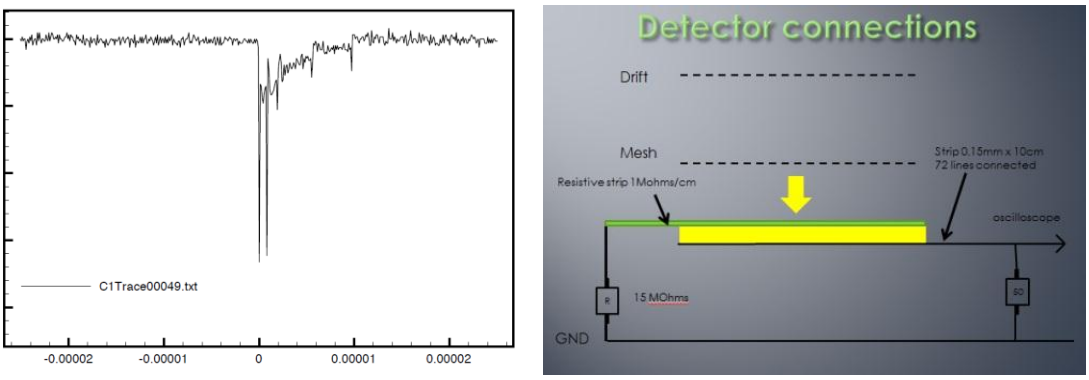

Pic. 4.14A discharge detected in a resistive MICROMEGAS with a configuration shown on the right; no amplification stage connected (68).

Looking closely to the point where the charges impinge, we could focus on the process of the generation of the signal in the metallic strips, hence understand which are the parameters shaping the signal in terms of its amplitude, characteristic rise and fall time and propagation time through the composite layers between the surface of the resistive strip and the readout electronics.

So, as soon as charges are reaching the surface a signal is induced through the resistive paste, that is the avalanche doesn't reach directly the electrodes, like happens instead in the case of a discharge in a THGEM, but the electrons travel in a resistive medium, or a distributed resistance. Observing this schematic we thought to transfer the same structure on a THGEM, to possibly acquire the same endurance against discharge as a MICROMEGAS.

A SPARK RESISTANT THGEM INSPIRED BY MICROMEGAS

We tried in building some structures with both electrodes entirely made of a resistive material (resistive Kapton 1$Mohm/_\blacksquare$), but all of them were already in a DC low current mode after the first discharges

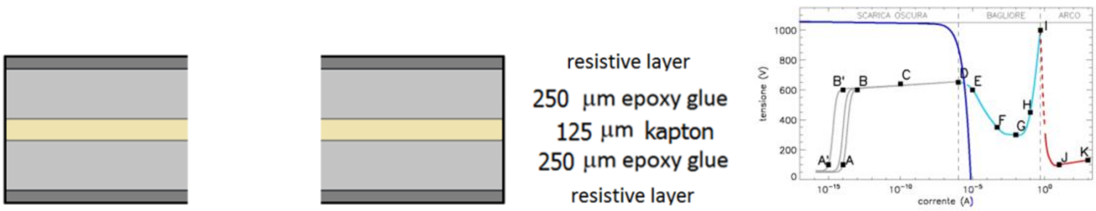

Pic. 4.15 A THGEM with all resistive electrodes might be already in glow discharge.

From experience on the other hand with entirely metallic electrodes, too energetic discharges were created, because when the impedance is negligible the load line cross the V-I curve of the gas in the arch region.

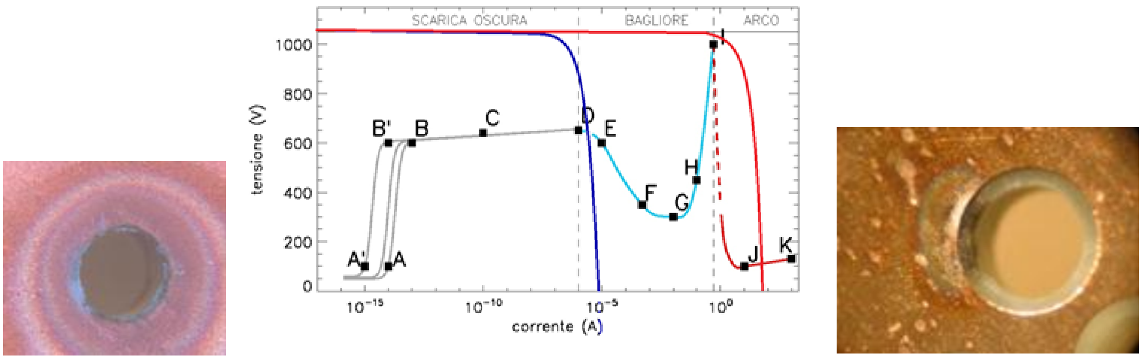

Pic. 4.16 From glow to arch: on the left effect of a glow continuous discharge on one hole, on the right effect of highly energetic pulse.

So we are dealing with two opposite structures, the one with metallic electrodes discharges in arch mode with high current able to damage immediately the electrodes, instead the one with resistive layers as electrodes has a so high value of impedance (depending on the position of the hole, could be even tens of GOhm) that once it discharges is already in a glow mode (low DC current, sustainable by the power supply). Can we stay in the middle? Is there a way to shape the structure in order to have a certain impedance which is in series with the flow of current during a discharge?

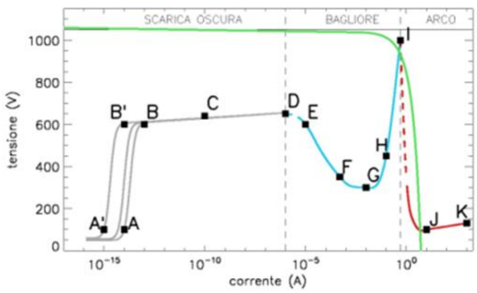

Pic. 4.17 Is there any not-harmful value of current in between the two extremes?

The idea is putting a metallic electrode sunk in the insulator and to have a resistive electrodes upon it, protecting the metal exactly in the same way the resistive paste is protecting the copper pads in MICROMEGAS. Moreover changing geometrical dimensions, we could regulate the impedance, hence the working point in a region where the current is not so high to damage the electrodes but neither too low to be sustainable by the power supply as a DC current.

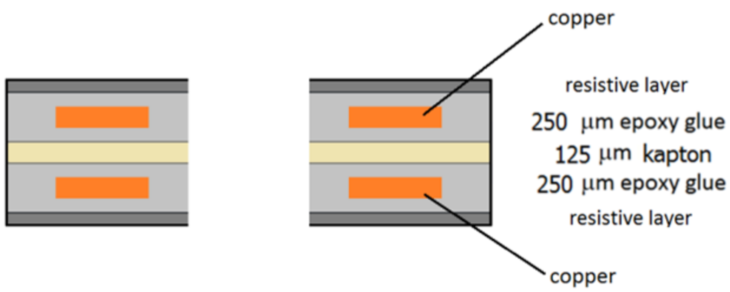

Pic. 4.18 A structure to shape the impedance during a discharge, hence the current.

Hopefully when the discharge appears in this structure, it will for sure discharge the equivalent capacitor (but not with such a high current to damage the electrodes) and then will be quenched because the power supply will be not able to provide the DC current of the working point.

Actually this structure could be compared to the MICROMEGAS'; going back to its structure and enlarge a sub section:

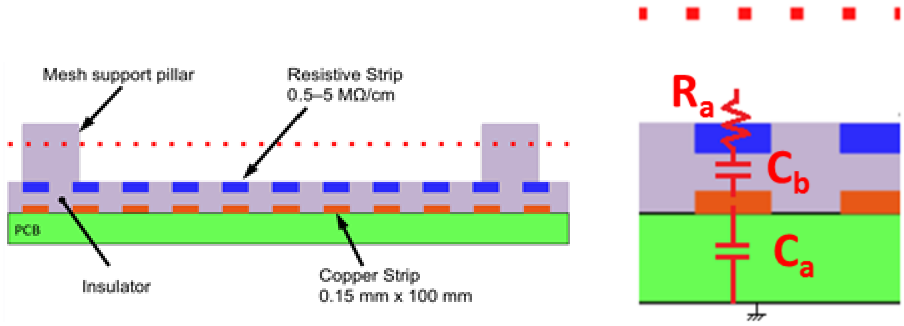

Pic. 4.19 Structure of MICROMEGAS; on the right, the equivalent electrical parameters are stressed. Actually they are distributed values.

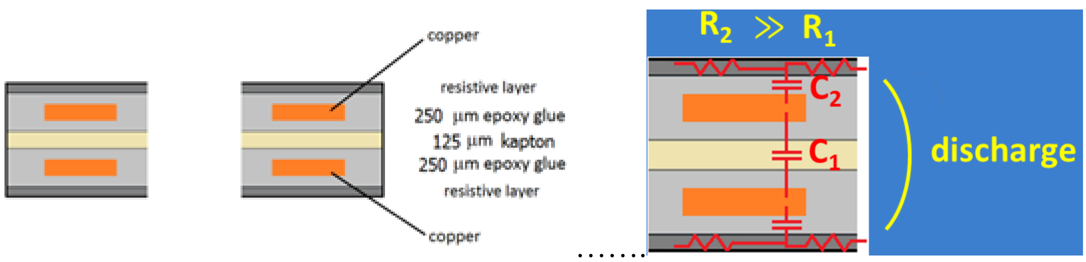

Pic. 4.20 Our proposal; on the right the analogy is highlighted: the discharge still interests a distributed resistor and capacitor.

An enlargement of the edge of one hole in the THGEM element proposed, enlighten the analogy. In case of a discharge between the upper and the lower electrodes, the same distributed elements would play a role as a MICROMEGAS. If we are able to shape the geometries thanks to a really fine process in order to have:

- C1 large value
- C2 ≅ Cb
- R1 ≅ Ra

Then we could expect the same behaviour from both the structures during a discharge.

In order to build the structure exposed the technological process became more complex; we have been trying to build a structure with only one floating copper electrodes but the result was not good , showing a lower breakdown voltage during the HV test compared to the one given by Paschen's curve.

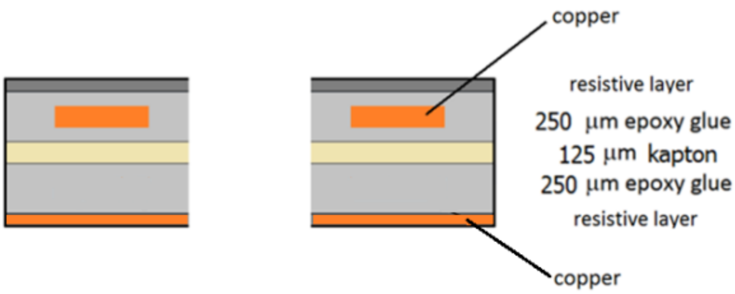

Pic. 4.21 The structure effectively built.

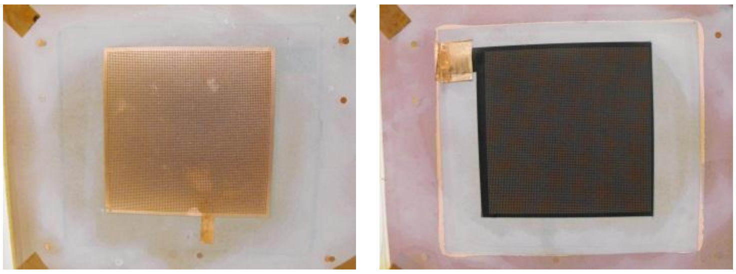

Pic. 4.22 Views of the two electrodes' sides: one metallic (copper) the other resistive (resistive Kapton).

However we believe that a validation period focused in tuning the process for this structure would have good result.

4.5 A proposal on simulation

In order to understand how different materials in MICROMEGAS (basically, different resistive material as electrodes with different thickness and different thickness of the insulator between the resistive layer and the copper anode pads) could behave in presence of a discharge, or even during normal operation, when an avalanche is approaching the surface, we proposed and started to set up a simulation environment comprehensive of all the variables.

This task was carried out thanks to the activity of an intern, John Oulagam Fortaillier which has developed most of the simulation environment in COMSOL multi-physics.

There are even more complete simulation environment for gaseous detector (GEANT 4, Garfield, MagBoltz) but none of them is oriented towards the extraction of electrical equivalent parameters depending on geometries (R and C) or generally towards materials.

The first big step was simulating the distribution of the charges inside the resistive layer induced by the incoming avalanche, showed in picture; unfortunately COMSOL still suffers of a lack of libraries regarding resistive materials.

We didn’t have time enough to perform complete simulations about the avalanche approaching the surface (a really complex task that actually was not even our purpose), but we think that even simulation on materials used in micro pattern gaseous detectors, could reveal many aspect at the moment underestimate (thickness and composition of the different layers).

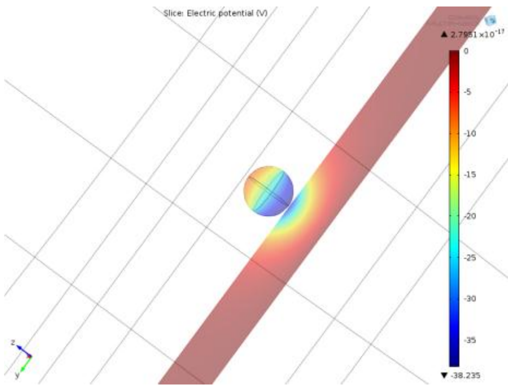

Pic. 4.23 A very preliminary simulation of a Raether's limit bunch of charges approaching a resistive layer Note the induced field on the resistive layer.

Moreover COMSOL could be used efficiently, as already mentioned, to perform simulation on the capacitance of composite structures and this could be of interest during the design of micro pattern gaseous detector where the capacitance, and this work proves it, is an essential parameter in defining the life time of the detector.

4.6 A thicker GEM

The last try was proposing a THGEM made with a global process; actually is a thicker GEM, obtained piling up some foils of Krempel epoxy glue with the two electrodes in copper to reach the global thickness 300 um. Then patterning the copper with the standard etching in iron chloride and using a bath in sulfuric acid to etch the glue and eventually open the holes.

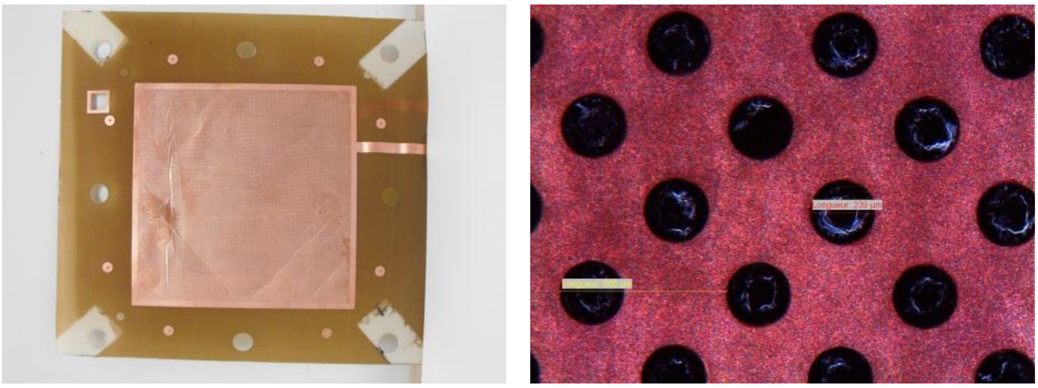

Pic. 4.24 A 10 cm x 10 cm of a THGEM made with a global process; on the right photo at the microscope of the matrix of holes – 239 um of diameter, 600um of pitch.

This method beyond the advantage of being completely chemical, so global and the quality of the sample not suffering from the imperfections due to a mechanical drilling process, would provide a sturdier gain element which might raise interest as a UV converter, since the cathode of the first element in this kind of detector has to be covered with *CsI* hence preferably more mechanically resistant.

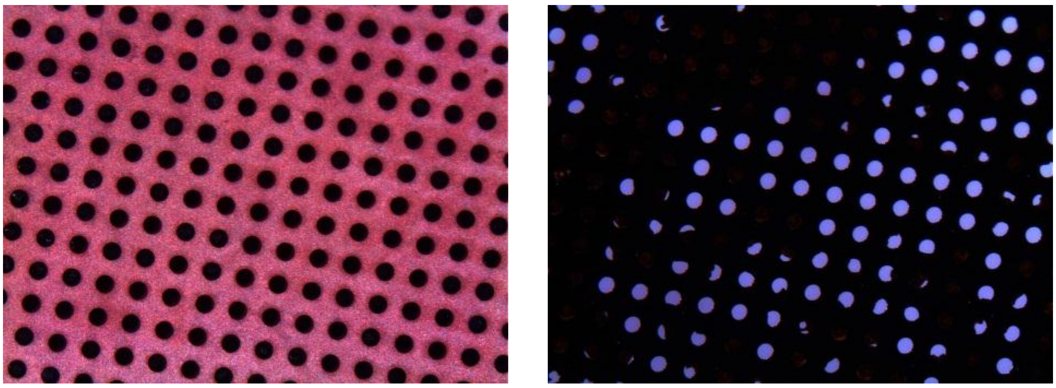

Pic. 4.25 A test on the transmitted light of the sample, shows clearly that most of the holes are still sealed with glue. A different process is needed – spray etch.

Dipping the sample in H_2SO_4 didn't give good results, most of the holes being still partially sealed with the epoxy glue not removed by the acid, having this a direct impact on the transparency of the structure in terms of electrons; unfortunately a precise control of any etch in H_2SO_4 is critical because the etch rate depends on temperature which is not easy to stabilize over a surface 10cm x10 cm in a simple bath. A spray-etch with the same etchant would be better recommended.

Conclusions

In this thesis work we have focused on the mechanism of discharge in simple structures which are the electrical equivalent of some MPGDs, especially THGEM, GEM and MICROMEGAS; anyhow the conclusions can be extended to any detector whose working principle is based on ionization of a gas.

A test bench has been developed which allow the stress test of these structures under repetitive discharges and picking up the fast (1-2 ns rise time) signal of the discharge thanks to an oscilloscope. This possibility could allow some more deeper studies on the features of the discharge, in terms of charges transferred and relationship between them and the equivalent capacitance of the structure.

We have introduced the *I-V* characteristic of the gas as a valid interpretation tool of the degradation induced by discharges observed in THGEM detectors; the load line method puts evidence even on the external powering circuitry of the detector, suggesting that the system has to be considered in its whole complexity. The limiting resistor and the maximum current available from the power supply are some of the electrical parameters that have to be carefully chosen and completely customized depending on the detector connected, in order to not fall into the glow discharge of the gas (or in a low DC current mode) after some events of discharge.

Tests of repetitive discharges were performed on a variety of samples of THGEMs, designed and made in the workshop, implementing the findings of the previous tests on said structures; the aim is extending the life time of the gain element of the detector in harsh environment of highly ionizing particles or even high flux of particles to detect.

We found that the solution could be twofold: use new substrate materials and design new structures.

In the first case we found that simply using a new epoxy glue by Krempel Group extended the life time of a prototype of a factor 37 in comparison with the same structure made with standard FR4 used at the moment as the base material for THGEM detectors. This is a promising preliminary results which will be likely implemented soon in standard dimensions THGEMs. This study suggests even that looking for different electrodes' material could improve further on the life time; anyhow we have to deal with the standard metals available in a common PCB workshop and to keep in mind that specializing too much the process results in higher costs.

Concerning new structures, we proved that reducing the area of the electrodes brings to an extended lifetime, hence possibly the next THGEM detector's gain elements will be segmented in order to reduce the capacity of the discharging structure.

Then we tried transferring the scheme of an already spark-protected detector (MICROMEGAS with resistive layer) to a THGEM, in order to make it spark protected as well: the technological process has not been tuned perfectly yet but the idea below could be valid and is worth more deepening, with prototypes and even simulations.

Finally a "thicker-GEM" which is not properly a THGEM has been proposed: the advantages of such device are the process (entirely chemical, which guarantees higher quality and homogeneity of the holes and moreover a cost which is decreasing with volume faster than THGEM) and its stiffness, a way in between a GEM and THGEM.

Bibliography

1. **Operation of a Thick Gas Electron Multiplier (THGEM) in Ar, Xe and Ar-Xe, R. Alon et al.**

2. **Stable operation with gain of a double phase Liquid Argon LEM-TPC with a 1 mm thick segmented LEM, F. Resnati et al.**

3. **THGEM-based detectors for sampling elements in DHCAL: laboratory and beam evaluation, L. Arazi et al.**

4. **Thick GEM-like (THGEM) Detectors and Their Possible Applications, R. Chechik, M. Cortesi, A. Breskin, SNIC Symposium, Stanford, California.**

5. **Mobility of Electrons in the Noble Gases, Joszpl C. Bowe, Physical review.**

6. **Mobilities of electrons in pure gases, Focken.**

7. **Performance of a triple-GEM detector for high rate charged particle triggering, G Benciveni, NIM A 494 (2002) 156-162.**

8. **The mean free path of an electron in a gas and its minimum ionizing potential, Karl Compton PhysRev 8 386.**

9. **DRIFT AND DIFFUSION OF ELECTRONS IN ARGON/CO, MIXTURES D.M. BINNIE, Nuclear Instruments and Methods in Physics Research A234 (1985) 54-60.**

10. **Gas Discharge Physics, Yuri P. Raizer.**

11. **Measurements of contact potential difference (work functions) of metals and semiconductors surface by the static ionized capacitor method, Sergey Nikolaevich Novikov, Advances in Colloid and Interface Science 105 (2003) 329–339.**

12. **Experimental study of breakdown voltage and effective secondary electron emission coefficient for a micro-plasma device, D. Mariotti et al, Plasma Sources Sci. Technol. 13 (2004) 207–212.**

13. **J. S. Townsend, Nature 62, 340 (1900) e Phil. Mag. 1, 198 (1901).**

14. **Calculation of the Townsend Discharge Coefficients and the Paschen Curve Coefficients, K.T. A. L. Burm, Contrib. Plasma Phys. 47, No. 3, 177 – 182 (2007).**

15. **Electrical breakdown limits for MEMS, hand out University of Rochester.**

16. **Electrical breakdown and ESD phenomena for devices with nanometre-to-micron gaps, Al Wallash and Larry Levit.**

17. **Electric field breakdown at micrometre separations in air and nitrogen at atmospheric pressure, R.S.Dhariwal, J.-M.Torres and M.P.Y. Desmulliez, IEE Proc-Sci. Mens. Technol., Vol. 147, No. 5, September 2000.**

18. **Wikipedia.**

19. **DC pulse-powered micro-discharges on planar electrodes, Yogesh B. Gianchandani.**

20. **http://www.stratford.gov.uk.**

21. **http://www.ifa.hawaii.edu/~barnes/ASTR110L_F05/spectralab.html.**

22. **http://public.web.cern.ch/public/en/Research/Detector-en.html.**

23. **http://www.unibas.it/utenti/cavallo/cms.htm.**

24. **Muon tracking and triggering with gaseous detectors and some applications Archana Sharma, Nuclear Instruments and Methods in Physics Research A 666 (2012) 98–129.**

25. **Principles of operation of multiwire proportional and drift chambers, F. Sauli, CERN 77-09.**

26. **Techniques for Nuclear and Particle Physics Experiments: A How-To Approach, Di William R. Leo.**

27. **Study of a self-quenching streamer mode in pure gases of DME and isobutane, Yu.I.Davydov.**

28. **http://www4.nau.edu/microanalysis/Microprobe-SEM/Signal_Detection.html.**

29. **http://www.ergotelescope.org/.**

30. **MICRO-PATTERN GASEOUS DETECTORS, CERN-EP/99-69, Fabio Sauli, Archana Sharma.**

31. **Gaseous Detectors: recent developments and applications, Maxim Titov, arXiv: 1008.3736.**

32. **Micropattern Gas Detectors, Jochen Kaminski.**

33. **MICROMEGAS: a high-granularity position-sensitive gaseous detector for high particle-flux environments Y. Giomataris, Ph. Rebourgeard, J.P. Robert, G. Charpak, NIM A 376 (1996) 29-35.**

34. **D. Thers et al., Micromegas as a large microstrip detector for the COMPASS experiment, Nucl. Instr. and Meth. A 469 (2001) 133.**

35. **A spark-resistant bulk-micromegas chamber for high-rate applications, J.Burnens, Nuclear Instruments and Methods in Physics Research A 640 (2011) 110–118.**

36. **F. Sauli, “GEM: A new concept for electron amplification in gas detectors,” Nucl. Instrum. Meth. A 396 (1997) 531.**

37. **Development of a gaseous detector based on Gas Electron Multiplier (GEM) Technology, F.Murtas.**

38. **A concise review on THGEM detectors A. Breskin et al. / Nuclear Instruments and Methods in Physics Research A 598 (2009).**

39. **H. Raether, Electron avalanches and breakdown in gases, London, 1964.**

40. **High rate behavior and discharge limits in micro-pattern detectors, A. Bressan, Nuclear Instruments and Methods in Physics Research A 424 (1999) 321-342.**

41. **Paulo Fonte "The physics of streamer and electrical discharges", 2008, 2nd RD51 Collaboration meeting Paris 13-15 October.**

42. **Research on discharges in micro pattern and small gap gaseous detectors V. Peskov, P. Fonte ICN UNAM, Mexico CERN, Geneva ISEC and LIP, Coimbra Portugal.**

43. **New micro pattern spark-protected gaseous detectors and their applications to High Energy Physics and Medicine, Peskov.**

44. **HIGH RATE BEHAVIOUR AND DISCHARGE LIMITS IN MICRO-PATTERN DETECTORS, Nuclear Instruments and Methods in Physics Research A 424 (1999) 321- 342 A. Bressan, et all.**

45. **CERN, Aging of Gaseous Detectors: assembly materials and procedures M. Capeans.**

46. **Peskov, Further evaluation of a THGEM UV-photon detector for RICH – comparison with MWPC V.**

47. **Detection of single photons with THickGEM-based counters, M. Alexeev, Nuclear Instruments and Methods in Physics Research A.**

48. **B.A. Dolgoshein et al., New method of registration of ionizing-particle trackers in condensed matter, JETP Lett. 11 (1970) 513.**

49. **L. Periale et al., Photosensitive gaseous detectors for cryogenic temperature applications, Nucl. Instrum. Meth. A 573 (2007).**

50. **P. Otiougova, Development of a Large Electron Multiplier (LEM) based charge readout system for the ArDM experiment, Diss. ETH No.17704.**

51. **Stable operation with gain of a double phase Liquid Argon LEM-TPC with a 1 mm thick segmented LEM, F. Resnati, A. Badertscher, A. Curioni, S. Horikawa, L. Knecht, D. Lussi, A. Marchionni, G. Natterer, A. Rubbia, T. Viant ETH Zurich.**

52. **A. Bondar et al., Thick GEM versus thin GEM in two-phase argon avalanche detectors, 2008 JINST 3 P07001.**

53. **Rui de Oliveira, "MPGD technologies" e Workshop on Micropattern Gas Detectors, CERN, 10-11 September 2007.**

54. **Micropattern gas detector technologies and applications The work of the RD51 collaboration, Serge Duarte Pinto, on behalf of the collaboration.**

55. **A High Eta Forward Muon Trigger & Tracking detector for CMS STATUS – UPDATE for Large Size Prototype Archana Sharma For CMS High Eta Upgrade Team (CMS, GDD and RD51).**

56. **R & D Proposal Development of Micro-Pattern Gas Detectors Technologies, RD51 2008-001 28 July 2008.**

57. **Electro-magnetic Compatibility Handbook, Kaiser.**

58. **Dispense di Compatibilità Elettromagnetica, Agostino Monorchio.**

59. **Systematic study of the electrical characteristics of the ”Trichel" current pulses from negative needle-to-plane coronas, W. L. Lama and C. F. Gallo, J. Appl. Phys. 45, 103 (1974).**

60. **Michael Jonker, private conversation.**

61. **Trichel pulse characteristics—negative corona discharge in air, Sattari, Gallo et al, 2011 J. Phys. D: Appl. Phys. 44 155502.**

62. **On the Nature of Copper Cathode Erosion in Negative Corona Discharge, Alexey A. Petrov, IEEE TRANSACTIONS ON PLASMA SCIENCE, VOL. 37, NO. 7, JULY 2009.**

63. **http://www.westak.com/downloads/P_DE156.pdf.**

64. **CHARACTERIZATION OF FR-4 PRINTED CIRCUIT BOARD LAMINATES BEFORE AND AFTER EXPOSURE TO LEAD-FREE SOLDERING CONDITIONS, Ravikumar Sanapala, Master of Science, 2008.**

65. **Direct current glow discharges in atmospheric air, Robert H. Stark, Appl. Phys. Lett. 74, 3770 (1999).**

66. **On the Nature of Copper Cathode Erosion in Negative Corona Discharge, Alexey A. Petrov, IEEE TRANSACTIONS ON PLASMA SCIENCE, VOL. 37, NO. 7, JULY 2009.**

67. **A spark-resistant bulk-micromegas chamber for high-rate applications, J.Burnens, Nuclear Instruments and Methods in Physics Research A 640 (2011) 110–118.**

68. **Resistive protections for Bulk Micromegas, Rui de oliveira, Joerg Wotschack, Venetios Polychronakos, Freiburg collaboration meeting.**